

UTILIZING SUPERCRITICAL CO<sub>2</sub> AND IONIC LIQUIDS FOR THE  
EXTRACTION OF ACTINIDES AND LANTHANIDES:  
APPLICATIONS OF NON-CONVENTIONAL SOLVENTS FOR  
NUCLEAR WASTE MANAGEMENT

A Dissertation

Presented in Partial Fulfillment of the Requirements for the  
Degree of Doctorate of Philosophy

with a

Major in Chemistry

in the

College of Graduate Studies

University of Idaho

by

Donna Ly Quach Baek

July 2014

Major Professor: Chien M. Wai, Ph.D.

## Authorization to Submit Dissertation

This dissertation of Donna Ly Quach Baek, submitted for the degree of Ph. D. and titled "Utilizing Supercritical CO<sub>2</sub> and Ionic Liquids for the Extraction of Actinides and Lanthanides: Applications of Non-Conventional Solvents for Nuclear Waste Management," has been reviewed in final form. Permission, as indicated by the signatures and dates given below, is now granted to submit final copies to the College of Graduate Studies for approval.

Major Professor \_\_\_\_\_ Date \_\_\_\_\_  
Dr. Chien M. Wai

Committee  
Members \_\_\_\_\_ Date \_\_\_\_\_  
Dr. Bruce J. Mincher

\_\_\_\_\_ Date \_\_\_\_\_  
Dr. Sofie P. Pasilis

\_\_\_\_\_ Date \_\_\_\_\_  
Dr. Patricia D. Paviet

Department  
Administrator \_\_\_\_\_ Date \_\_\_\_\_  
Dr. Ray von Wandruszka

Discipline's  
College Dean \_\_\_\_\_ Date \_\_\_\_\_  
Dr. Paul Joyce

Final Approval and Acceptance by the College of Graduate Studies:

\_\_\_\_\_ Date \_\_\_\_\_  
Dr. Jie Chen

## Abstract

Supercritical carbon dioxide (sc-CO<sub>2</sub>) and room temperature ionic liquids (RTILs) were used as non-conventional solvents for the investigation of actinide and lanthanide extraction and separation in this dissertation. Nuclear waste management is traditionally facilitated by the Plutonium Uranium Reduction EXtraction process, better known as the PUREX process. The drawback to this important process is the production of hazardous organic and aqueous waste. RTILs and sc-CO<sub>2</sub> have inherent benefits over using hydrocarbon solvents, such as low volatility and minimizing secondary liquid waste generation.

A brief review of actinide and lanthanide extraction and separation using traditional solvents, sc-CO<sub>2</sub>, and RTILs is presented. To be able to optimize extraction efficiencies, the understanding of solvation, speciation, and complexation behavior of lanthanides and actinides in RTILs, sc-CO<sub>2</sub> and RTIL/sc-CO<sub>2</sub> mixtures are important. Thus, the coordination of U(VI) with nitrate and TBP dissolved in 1-butyl-3-methylimidazolium bis(trifluoromethylsulfonyl)imide ([C<sub>4</sub>MIM][Tf<sub>2</sub>N]) containing tetrabutylammonium nitrate (TBAN), nitric acid, or TBAN and TBP via ATR-FTIR and UV-Vis spectroscopy was studied.

Tristructural isotropic (TRISO) fuel particles are used in very high temperature reactors to achieve higher burnup levels; however, recycling techniques have not been fully developed. Included in this dissertation is an investigation using sc-CO<sub>2</sub> with TBP to extract U(VI) from TRISO fuel particles, which have been exposed to gamma irradiation. Also, mechanical crushing of TRISO fuel particles is currently the only method to expose the

uranium for extraction; thus radioactive contamination is an issue. Ultrasound was applied to TRISO fuel particles in an enclosed pressure vessel in the attempt to fracture the fuel in liquid CO<sub>2</sub> and extract U(VI).

Furthermore, various actinides and lanthanides are present in used nuclear fuel that need to be extracted and separated from each other to recover uranium as the product and reduce the radiotoxicity of the waste requiring storage. The extraction and separation of uranium from the actinides neptunium, plutonium and americium and the lanthanide series were studied. These species were extracted from a range of nitric acid concentrations, in the absence of, or in the presence of, a number of traditional reducing and/or complexing agents by sc-CO<sub>2</sub> modified with TBP to demonstrate the separation of these metals from uranium under sc-CO<sub>2</sub> conditions.

## Acknowledgments

I would like to graciously thank my major professor Dr. Chien Wai for his academic and financial support during my entire graduate studies and endless efforts helping me with my research. Without his support I would not have the opportunity to grow as a chemist nor become the person I am today.

I sincerely thank my committee members Dr. Bruce Mincher, Dr. Sofie Pasilis, and Dr. Patricia Paviet for their comments and suggestions which improved my dissertation. Extra thanks go to Dr. Bruce Mincher for all the effort he put forth arranging all my necessary paperwork during my time at the INL. I would like to thank Dr. Sofie Pasilis for her guidance during my first year as a graduate student and her time in helping me improve my literature seminar. Also, thanks go to Dr. Patricia Paviet for taking the time to organize a class to teach me the ins and outs of the nuclear fuel cycle.

I would like to thank my research colleagues Dr. Horng-Bin Pan, Dr. Wei-Chun Hung, Dr. Yu-Jung Liao, Dr. Anirban Das, Dr. Naomi Miyamoto, Dr. Weisheng Liao, Andrew Markelonis, Wen-Lung Chang, and Mary Mincher for their research discussions and advice. In addition, I would like to thank the Department of Chemistry staff - Cindy, Terry, Laila, and Deb for everything they have helped me with.

Many thanks go to my family who has supported me and my decisions throughout my graduate studies. In addition, thanks to my roommates and friends who have kept me sane during my academic career.

## **Dedication**

TO MY HUSBAND AND SON

## Table of Contents

<b>Authorization to Submit Dissertation .....</b>	<b>ii</b>
<b>Abstract.....</b>	<b>iii</b>
<b>Acknowledgments .....</b>	<b>v</b>
<b>Dedication .....</b>	<b>vi</b>
<b>Table of Contents.....</b>	<b>vii</b>
<b>List of Figures.....</b>	<b>xi</b>
<b>List of Tables.....</b>	<b>xv</b>
<b>List of Abbreviations .....</b>	<b>xvi</b>
<b>Chapter 1 Introduction.....</b>	<b>1</b>
1.1 Objective .....	1
1.2 Nuclear Energy and Waste Management.....	1
1.2.1 Nuclear Fission of $^{235}\text{U}$ and Decay of $^{239}\text{U}$ .....	3
1.2.2 Nuclear Waste .....	8
1.2.3 Recycling Used Nuclear Fuel .....	9
1.3 Traditional Solvent Extraction .....	10
1.3.1 PUREX Process .....	12
1.4 Novel Non-Conventional Extraction Techniques.....	19
1.4.1 Supercritical Fluid.....	19
1.4.2 Room Temperature Ionic Liquids .....	21
1.5 Overview of Dissertation .....	23
1.6 References .....	26

<b>Chapter 2 Literature Review.....</b>	<b>30</b>
2.1 Introduction.....	30
2.1.1 <i>Supercritical Carbon Dioxide.....</i>	<i>30</i>
2.1.2 <i>sc-CO<sub>2</sub> as a Solvent for Actinide and Lanthanide Extraction .....</i>	<i>32</i>
2.1.3 <i>Room Temperature Ionic Liquids .....</i>	<i>36</i>
2.1.4 <i>Room Temperature Ionic Liquids as a Solvent for Actinide and Lanthanide Extraction.....</i>	<i>36</i>
2.1.5 <i>Supercritical Fluid-Ionic Liquid Coupled Extraction.....</i>	<i>41</i>
2.2 Conclusions.....	42
2.3 References.....	43
<b>Chapter 3 Attenuated Total Reflection-Fourier Transform Infrared and Ultraviolet-Visible Spectrometry Studies of Uranyl Coordination with Nitrate and Tri-n-butyl Phosphate in a Room Temperature Ionic Liquid .....</b>	<b>46</b>
3.1 Introduction.....	46
3.2 Experimental.....	52
3.2.1 <i>Chemicals and reagents.....</i>	<i>52</i>
3.2.2 <i>Instruments.....</i>	<i>53</i>
3.2.3 <i>Synthesis of 1-butyl-3-methylimidazolium bis(trifluoromethylsulfonyl)imide [C<sub>4</sub>MIM][Tf<sub>2</sub>N].....</i>	<i>53</i>
3.2.4 <i>Synthesis of uranyl bis(trifluoromethylsulfonyl)imide [UO<sub>2</sub>(Tf<sub>2</sub>N)<sub>2</sub>] .....</i>	<i>53</i>
3.2.5 <i>Sample preparation .....</i>	<i>54</i>
3.3 Results and Discussion.....	55
3.3.1 <i>Coordination study of uranyl nitrate complexes formed in [C<sub>4</sub>MIM][Tf<sub>2</sub>N].....</i>	<i>55</i>



3.3.2	<i>Coordination study of uranyl-nitrate TBP complexes formed in [C<sub>4</sub>MIM][Tf<sub>2</sub>N]</i>	65
3.4	Conclusion.....	70
3.5	Acknowledgement.....	71
3.6	References .....	71
<b>Chapter 4 Recycling Uranyl from TRISO Fuel Particles using Supercritical CO<sub>2</sub> .....</b>		<b>74</b>
4.1	Introduction.....	74
4.2	Experimental.....	78
4.2.1	<i>Chemicals and Reagents</i> .....	78
4.2.2	<i>Experimental Setup and Instruments</i> .....	79
4.3	Results and Discussion.....	82
4.3.1	<i>sc-CO<sub>2</sub> Extraction of U(VI) from Non-Irradiated and <math>\gamma</math>-Irradiated TRISO Fuel Particles.....</i>	82
4.3.2	<i>The Effect of TRISO Exposed to Ultrasound in Liquid CO<sub>2</sub>.....</i>	83
4.4	Conclusions .....	84
4.5	Acknowledgement.....	85
4.6	References .....	85
<b>Chapter 5 Supercritical Fluid Extraction and Separation of Uranium from Other Actinides and Lanthanides .....</b>		<b>87</b>
5.1	Introduction.....	87
5.2	Experimental.....	90
5.2.1	<i>Chemicals and reagents</i> .....	90
5.2.2	<i>Experimental setup and instruments</i> .....	91
5.2.3	<i>sc-CO<sub>2</sub> extraction procedure</i> .....	93

5.3 Results and Discussion.....	95
5.3.1 <i>Liquid liquid extraction of U(VI), Np(VI), and Pu(IV) from nitric acid solution...</i>	95
5.3.2 <i>sc-CO<sub>2</sub> extraction of U(VI), Np(VI), and Pu(IV) from nitric acid solution.....</i>	96
5.3.3 <i>sc-CO<sub>2</sub> extraction of Pu and Np from nitric acid solution in the presence of     reducing/complexing agents .....</i>	99
5.3.4 <i>sc-CO<sub>2</sub> extraction and separation process .....</i>	105
5.4 Conclusion and future studies.....	108
5.5 Acknowledgement.....	109
5.6 References .....	109
<b>Chapter 6 Conclusion .....</b>	<b>113</b>
<b>Appendix A.....</b>	<b>117</b>

## List of Figures

Figure 1-1 Fission product yields for the thermal neutron fission of $^{235}\text{U}$ (according to AECI – 1054). <sup>8</sup> .....	4
Figure 1-2 Decay chain from nuclear reaction of $^{238}\text{U}$ by neutron absorption. (Reproduced with permission from ref 8. Copyright Wiley-VCH Verlag GmbH & Co. KGaA.) See Appendix A for documentation of permission to republish this material. ....	7
Figure 1-3 Chemical structure of tri-n-butyl phosphate.....	12
Figure 1-4 Plot of different oxidation states for actinide elements.....	13
Figure 1-5 Distribution of actinides extracted from HLW by kerosene modified with 50% TBP (Reprinted with permission from ref 31. Copyright (1979), with permission from Elsevier .....	15
Figure 1-6 Distribution ratio of U(VI) extracted from $\text{HNO}_3$ solutions by, kerosene modified with 4.8% TBP (lower curve) and 19% TBP (upper curve) (Reprinted with permission from ref 29. Copyright (1958), with permission from Elsevier. See Appendix A for documentation of permission to republish this material. ....	16
Figure 1-7 Flowsheet of the PUREX process.....	17
Figure 2-1 Phase diagram for carbon dioxide.....	31
Figure 2-2 Schematic of the general chemical structure of diglycolamide (DGA). ....	40
Figure 3-1 UV-Vis spectra of 0.02 M $\text{UO}_2(\text{NO}_3)_2 \cdot 6\text{H}_2\text{O}$ dissolved in ketonic solvents. The less intense spectra acquired contain 0.02 M $\text{UO}_2(\text{NO}_3)_2 \cdot 6\text{H}_2\text{O}$ dissolved in acetone (solid line), methyl isobutyl ketone (dashed line), and cyclohexanone (dashed-dotted line). The spectrum having the most intense peaks was acquired from a solution containing 0.02 M $\text{UO}_2(\text{NO}_3)_2 \cdot 6\text{H}_2\text{O}$ and 0.02 M TBAN in acetone (dotted line). (Reprinted with permission from ref 13. Copyright (1956), with permission from Elsevier) See Appendix A for documentation of permission to republish this material. ....	49
Figure 3-2 ATR-FTIR spectra showing the $\nu_{\text{as}}(\text{UO}_2^{2+})$ region for solutions of 0.1 M $\text{UO}_2(\text{Tf}_2\text{N})_2$ in $[\text{C}_4\text{MIM}][\text{Tf}_2\text{N}]$ containing a) no $\text{HNO}_3$ , b) 0.1 M $\text{HNO}_3$ , c) 0.2 M $\text{HNO}_3$ , and d) 0.3 M $\text{HNO}_3$ . (*Reprinted with permission).....	56

Figure 3-3 ATR-FTIR spectra showing the $\nu(\text{NO})$ region for solutions of 0.1 M $\text{UO}_2(\text{Tf}_2\text{N})_2$ in $[\text{C}_4\text{MIM}][\text{Tf}_2\text{N}]$ containing a) no $\text{HNO}_3$ , b) 0.1 M $\text{HNO}_3$ , c) 0.2 M $\text{HNO}_3$ , and d) 0.3 M $\text{HNO}_3$ . (*Reprinted with permission).....	58
Figure 3-4 UV/visible absorption spectra of solutions of 0.1 M $\text{UO}_2(\text{Tf}_2\text{N})_2$ in $[\text{C}_4\text{MIM}][\text{Tf}_2\text{N}]$ containing a) no $\text{HNO}_3$ , b) 0.2 M $\text{HNO}_3$ , c) 0.3 M $\text{HNO}_3$ , and d) 0.4 M $\text{HNO}_3$ . (*Reprinted with permission).....	59
Figure 3-5 ATR-FTIR spectra showing the $\nu_{\text{as}}(\text{UO}_2^{2+})$ region for solutions of 0.1 M $\text{UO}_2(\text{Tf}_2\text{N})_2$ in $[\text{C}_4\text{MIM}][\text{Tf}_2\text{N}]$ containing a) no TBAN, b) 0.1 M TBAN, c) 0.2 M TBAN, and d) 0.3 M TBAN. (*Reprinted with permission).....	62
Figure 3-6 ATR-FTIR spectra showing the $\nu(\text{NO})$ region for solutions of 0.1 M $\text{UO}_2(\text{Tf}_2\text{N})_2$ in $[\text{C}_4\text{MIM}][\text{Tf}_2\text{N}]$ containing a) no TBAN, b) 0.1 M TBAN, c) 0.2 M TBAN, and d) 0.3 M TBAN. (*Reprinted with permission).....	63
Figure 3-7 UV/visible absorption spectra of solutions of 0.1 M $[\text{UO}_2(\text{Tf}_2\text{N})_2]$ in $[\text{C}_4\text{MIM}][\text{Tf}_2\text{N}]$ containing a) no TBAN, b) 0.2 M TBAN, c) 0.3 M TBAN, and d) 0.4 M TBAN. (*Reprinted with permission).....	64
Figure 3-8 Graph showing the shift in $\nu_{\text{as}}(\text{UO}_2^{2+})$ mode for solutions of 0.1 M $\text{UO}_2(\text{Tf}_2\text{N})_2$ in $[\text{C}_4\text{MIM}][\text{Tf}_2\text{N}]$ containing 0.2 M TBAN or 0.3 M TBAN upon the addition of 0.1 M TBP, 0.2 M TBP, and 0.3 M TBP. ....	66
Figure 3-9 ATR-FTIR spectra showing the $\nu(\text{NO})$ region for solutions of 0.1 M $\text{UO}_2(\text{Tf}_2\text{N})_2$ and 0.3 M TBAN in $[\text{C}_4\text{MIM}][\text{Tf}_2\text{N}]$ containing a) no TBP, b) 0.1 M TBP, c) 0.2 M TBP, and d) 0.3 M TBP. ....	68
Figure 3-10 UV/visible absorption spectra of solutions of 0.1 M $\text{UO}_2(\text{Tf}_2\text{N})_2$ in $[\text{C}_4\text{MIM}][\text{Tf}_2\text{N}]$ containing a) no TBAN or TBP, b) no TBAN and 0.1 M TBP, c) 0.3 M TBAN and no TBP, d) 0.3 M TBAN and 0.1 M TBP, e) 0.3 M TBAN and 0.2 M TBP, and f) 0.3 M TBAN and 0.3 M TBP. ....	69
Figure 4-1 Schematic diagram showing the five different layers of a TRISO particle. (Slightly modified version from: <a href="http://aris.iaea.org/ARIS/reactors.cgi?requested_doc=report&amp;doc_id=70&amp;type_of_output=html">http://aris.iaea.org/ARIS/reactors.cgi?requested_doc=report&amp;doc_id=70&amp;type_of_output=html</a> ). ....	74

- Figure 4-2 Illustration of TRISO fuel particles being processed into a fuel element for a nuclear reactor. See Appendix A for documentation that this material is in the public domain.<sup>2</sup> ..... 75
- Figure 4-3 Several point defects are shown on a 2D crystal lattice. 1. monovacancy, 2. self-interstitial, 3. interstitial impurity atom, 4. undersize substitutional atom, and 5. oversize substitutional atom. (Reprinted with permission from ref 7. Copyright Wiley-VCH Verlag GmbH & Co. KGaA.). See Appendix A for documentation of permission to republish this material. .... 78
- Figure 4-4 Schematic of the ultrasound pressure vessel. Details: A. SCF extraction chamber, B. Stainless steel cell body, C. Langevin horn, D. Piezoelectric transducer, E. Counter mass, F. Endplate G. Endplate with o-ring seal H. Tensioning threaded rod, I. Tensioning nut, J. Fluid outlet port, and K. Fluid inlet port. .... 81
- Figure 4-5 SEM images of the surface of TRISO fuel particles. A. Untreated TRISO fuel particle; B. Exposure to ultrasound; C. HF treatment and then exposure to ultrasound. .... 84
- Figure 5-1 sc-CO<sub>2</sub> apparatus showing extractant and sample cells, and trap solution in the collection vial..... 92
- Figure 5-2 Extraction efficiency of U(VI), Np(VI), and Pu(IV) from nitric acid solution. (a) 6 mol % TBP liquid-liquid extraction (b) 1 mol % TBP SCF extraction at 40°C and 20 MPa. The lines connecting the data points are meant merely to guide the eye. (\*Reprinted with permission)..... 98
- Figure 5-3 Extraction of Pu(IV) from nitric acid solutions into sc-CO<sub>2</sub> phase containing 1 mole % TBP in the presence and absence of reducing and/or complexing agents. AHA is acetohydroxamic acid, OA is oxalic acid. The lines connecting the data points are meant merely to guide the eye. (\*Reprinted with permission)..... 101
- Figure 5-4 UV-Vis absorption spectra of Np species. Black- Np dissolved in 3M nitric acid showing mainly Np(VI) from 350-450 nm. Gray- Np and 0.1 M NaNO<sub>2</sub> dissolved in 3 M nitric acid showing mainly Np(V) at 980 nm. (\*Reprinted with permission). .... 103

Figure 5-5 Extraction of nominally Np(VI) from nitric acid solutions into sc-CO <sub>2</sub> phase containing 1 mol % TBP in the presence and absence of reducing and/or complexing agents. AHA is acetohydroxamic acid, OA is oxalic acid. The lines connecting the data points are meant merely to guide the eye. (*Reprinted with permission). .....	104
Figure 5-6 sc-CO <sub>2</sub> schematic containing two stripping columns in addition to an extractant and sample cell.....	106
Figure 6-1 Schematic diagram illustrating the concept of recycling uranium from used fuel by using sc-CO <sub>2</sub> and counter-current stripping columns. ....	116

## List of Tables

Table 1-1 Fission products mainly responsible for neutron absorption. (Reproduced with permission from ref 8. Copyright Wiley-VCH Verlag GmbH & Co. KGaA.) See Appendix A for documentation of permission to republish this material. ....	5
Table 1-2 D values of actinides extracted with kerosene modified with 19% v/v TBP from 5 M HNO <sub>3</sub> . <sup>29, 30</sup> .....	14
Table 1-3 Critical constants of common molecules used as SCF solvents. <sup>36</sup> .....	19
Table 1-4 Physical properties of gases, supercritical fluids, and liquids. ....	20
Table 1-5 Generic structures of common RTILs. See Appendix A for documentation that this material is in the public domain. <sup>41</sup> .....	21
Table 1-6 Select physical properties of two alkyimidazolium cations with three anions. See Appendix A for documentation that this material is in the public domain. <sup>41</sup> .....	23
Table 4-1 Comparison of the extraction yield of uranium from different particle sizes of TRISO fuel particles either not $\gamma$ irradiated or $\gamma$ irradiated at 691 or 1047 kGy. ....	82
Table 5-1 Extraction efficiencies of U and Pu in the absence and presence of 0.1 M acetohydroxamic acid (AHA) or oxalic acid (OA) in 3 M nitric acid. NE = no extraction. (*Reprinted with permission).....	102
Table 5-2 Extraction efficiency of U(VI) and Np(VI) in the absence and presence of 0.1 M NO <sub>2</sub> <sup>-</sup> in 1 M nitric acid. NE = no extraction. (*Reprinted with permission). ....	105
Table 5-3 The percent extraction of uranium, neptunium, plutonium, americium, and the lanthanide series from 1 M nitric acid solution by sc-CO <sub>2</sub> modified with 1 % TBP at 40°C and 200 atm. Lanthanide series: La, Ce, Pr, Nd, Sm, Eu, Gd, Tb, Dy, Ho, Tm, Yb, and Lu. ....	107
Table 5-4 The percent extraction of uranium, neptunium, plutonium, americium, and the lanthanide series from 1 M nitric acid solution with 0.1 M sodium nitrite by sc-CO <sub>2</sub> modified with 1 % TBP at 40°C and 200 atm. Lanthanide series: La, Ce, Pr, Nd, Sm, Eu, Gd, Tb, Dy, Ho, Tm, Yb, and Lu. ....	108

## List of Abbreviations

%E	% Extracted
[C <sub>4</sub> MIM][Tf <sub>2</sub> N]	1-butyl-3-methylimidazolium bis(trifluoromethylsulfonyl)imide
[C <sub>4</sub> MIM][Cl]	1-butyl-3-methylimidazolium chloride
[C <sub>4</sub> MIM][PF <sub>6</sub> ]	1-butyl-3-methylimidazolium hexafluorophosphate
[C <sub>4</sub> MIM][BF <sub>4</sub> ]	1-butyl-3-methylimidazolium tetrafluoroborate
[C <sub>6</sub> MIM][Cl]	1-hexyl-3-methylimidazolium chloride
[C <sub>6</sub> MIM][PF <sub>6</sub> ]	1-hexyl-3-methylimidazolium hexafluorophosphate
[C <sub>6</sub> MIM][BF <sub>4</sub> ]	1-hexyl-3-methylimidazolium tetrafluoroborate
AHA	acetohydroxamic acid
amu	Atomic mass unit
ATR-FTIR	Attenuated Total Reflection-Fourier Transform Infrared
CCD	Charge Coupled Device
CE	crown ether
CMPO	octyl(phenyl)-N,N-diisobutylcarbonoylmethyl-phosphine oxide
CO <sub>2</sub>	carbon dioxide
D	Distribution Ratio
DGA	Diglycolamide
EBR-1	Experimental Breeder Reactor-1
EXAFS	Extended X-ray Absorption Fine Structure
FOD	2,2-dimethyl-6,6,7,7,8,8,8-heptafluoro-3,5 octanedione
HFA	Hexafluoroacetylacetone
HLW	High Level Waste
HNO <sub>3</sub>	nitric acid
HPGE	High-Purity Germanium
IAEA	International Atomic Energy Agency
ICP-MS	Inductively Coupled Plasma Mass Spectrometry
INL	Idaho National Laboratory



IPyC	inner pyrolytic carbon
KW <sub>h</sub>	Kilowatt Hour
LiFDDC	lithium bis(trifluoroethyl) dithiocarbamate
LLW	Low Level Waste
MA	Minor Actinide
MOX	Mixed Oxide
NAA	Neutron Activation Analysis
NMR	Nuclear Magnetic Resonance
NRC	Nuclear Regulatory Commission
OA	oxalic acid
OPyC	outer pyrolytic carbon
PPE	Personal Protective Equipment
PUREX	Plutonium Uranium Reduction Extraction
PWR	Pressurized Water Reactor
REDOX	Reduction-Oxidation
RRE	Rare Earth Elements
RTIL	Room Temperature Ionic Liquid
Sc-CO <sub>2</sub>	Supercritical Carbon Dioxide
SCF	Supercritical Fluid
SEM	Scanning Electron Microscopy
SFC	Supercritical Fluid Chromatography
TALSPEAK	Trivalent Actinide - Lanthanide Separation by Phosphorus reagent Extraction from Aqueous Komplexes
TBAN	tetrabutylammonium nitrate
TBP	tri-n-butyl phosphate
TBPO	tri-n-butyl phosphine oxide
TODGA	N,N,N',N'-tetra(n-octyl)diglycolamide
TOPO	tri-n-octyl phosphine oxide
TPPO	triphenyl phosphine oxide

TRISO	Tristructual Isotopic
TRU	Transuranic
TRUEX	Trans-Uranium Extraction
TTA	Thienoyltrifluoroacetylacetone
TW <sub>h</sub>	Terawatt Hour
UC	uranium carbide
UCO	uranium oxycarbide
UNF	Used Nuclear Fuel
UREX+	Uranium Extraction+
UV-Vis	Ultraviolet-visible
VHTR	very high temperature reactor
VOC	Volatile Organic Compound
WIR	Waste Incidental to Reprocessing

# Chapter 1

## Introduction

### 1.1 Objective

My thesis work is focused on the use of non-conventional solvents such as room temperature ionic liquids (RTILs) and supercritical carbon dioxide (sc-CO<sub>2</sub>) for the development of a more sustainable separation technique for recycling used nuclear fuel (UNF). Uranium is the main element making up the fuel used in a nuclear power reactor and is important in nuclear waste management. Fission products, other actinides, and lanthanides are also present in the used nuclear fuel and should be separated to mitigate the radiotoxicity and heat present in the waste.

In this introduction, I will briefly discuss nuclear energy and the waste produced and then how the waste is managed. Traditional solvent and novel non-conventional solvent extraction techniques are presented. Lastly, I will summarize the contents of this dissertation.

### 1.2 Nuclear Energy and Waste Management

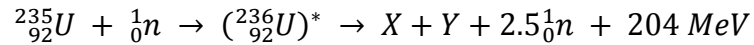
Throughout the world one of the greatest challenges today is accommodating the strong growth in energy demand while still trying to lower greenhouse gas production.<sup>1,2</sup> Coal and natural gas are the top two sources of electricity in the United States and also the highest carbon dioxide (CO<sub>2</sub>) emitters.<sup>3,4</sup> Some alternative energy sources such as wind,

solar, and nuclear power, which do not emit CO<sub>2</sub>, have the potential to alleviate the power struggles faced today.<sup>5</sup> However, the harvesting of wind and solar energy varies depending on the location, season, and time of day, so they are not reliable sources of electricity. Also, the equipment required to generate and harvest wind and solar energy are expensive and take up a large amount of space. Generating nuclear energy is independent of season and time of day and is capable of converting and storing the electricity produced.<sup>2</sup> For these reasons nuclear energy may be the best alternative source of electricity in the US.

Electricity was generated for the first time in the world by a nuclear reactor on December 20, 1951, at the Experimental Breeder Reactor-1 (EBR-I) experimental station near Arco, Idaho, which was enough to light up four light bulbs. It was confirmed in 1953 that the reactor could breed more fuel than it consumed, making nuclear energy a potential source of electricity.<sup>6</sup> Nuclear energy begins at the nucleus of an atom of certain isotopic elements capable of fission. Fission is often induced by neutron absorption which causes the splitting of the unstable nuclei, releasing energy in the form of heat and smaller atoms (fission products) and neutrons. The released neutrons can then cause a chain reaction to release more neutrons thus producing more heat and nuclear energy. The heat produced from nuclear fission boils water and creates steam to turn a turbine. As the turbine spins, the generator turns and produces electricity. As of 2012, the US has 100 nuclear power reactors in operation, producing nearly 770 Terawatt hour (TWh) of energy as reported by International Atomic Energy Agency (IAEA).<sup>7</sup> This represents about 20% of the electricity produced in the US, whereas about 80% of the electricity generated in France is produced by nuclear power plants.

### 1.2.1 Nuclear Fission of $^{235}\text{U}$ and Decay of $^{239}\text{U}$

Fission of  $^{235}\text{U}$  is illustrated by the following reaction



Where  $X$  and  $Y$  are fission products produced with a mass number in the range between about 70 and 160, the number of neutrons emitted is between 2-3, and the total amount of nuclear energy released by the fission is about 204 MeV.<sup>8</sup> The total energy is split in the following way:

▪ Kinetic energy of the fission products	167 MeV
▪ Kinetic energy of the neutrons	5 MeV
▪ Prompt $\gamma$ rays	6 MeV
▪ $\beta$ decay of the fission products	8 MeV
▪ $\gamma$ from transmutation of the fission products	6 MeV
▪ Neutrinos	12 MeV

A neutrino's interaction with matter is negligible, thus their energy is disregarded. If the neutrino's energy is omitted from the total usable energy, the sum of the energies listed above is reduced to 192 MeV. This amount of usable nuclear energy correlates 1 kg of  $^{235}\text{U}$  to a maximum value of  $1.85 \times 10^7$  kWh (kilo watt hour) of energy produced. The amount of usable energy produced by burning 1 kg of coal is 9.4 kWh, so if the energy produced by nuclear fission and by the burning of coal are compared, the ratio of the energies producible from 1 kg of  $^{235}\text{U}$  and coal is  $2 \times 10^6$ .<sup>8</sup> This comparison of how much energy is produced by using  $^{235}\text{U}$  and coal illustrates how inefficient coal is and is another reason to use nuclear energy.

During the fission of  $^{235}\text{U}$ , fission products are also formed. In Figure 1-1, the plot shown is of the fission yield as a function of the mass number of the fission products. The most abundant fission products produced have mass numbers between 90 – 100 amu (atomic mass unit) and between 133 – 143 amu. As can be seen in the mass distribution curve, the peaks are at 100 and 134. This phenomenon is explained by the fact that the nuclei of the fission product is more stable when there is an even number of protons and/or neutrons produced from the splitting of the nuclei,  $^{236}_{92}\text{U}$ .<sup>8,9</sup>

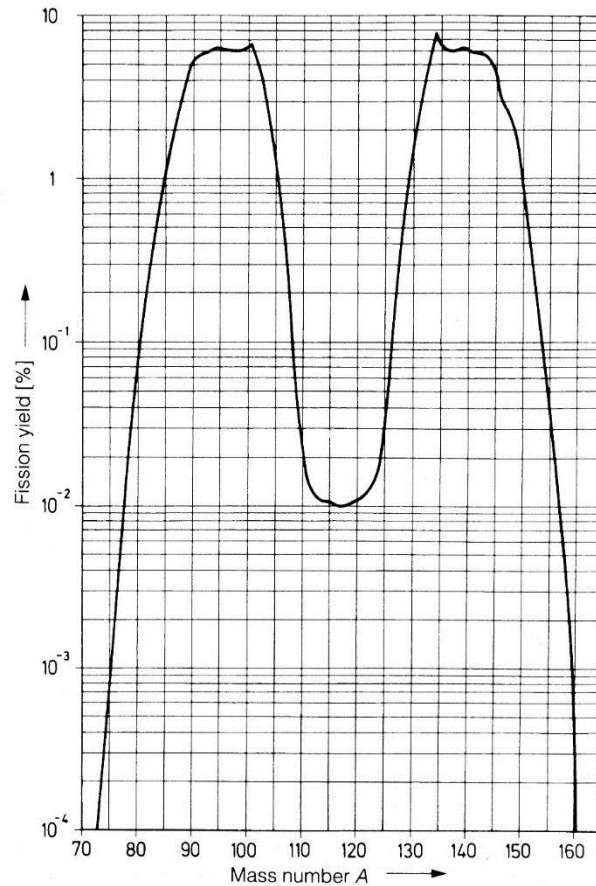


Figure 1-1 Fission product yields for the thermal neutron fission of  $^{235}\text{U}$  (according to AECI – 1054).<sup>8</sup>

The presence of fission products in used nuclear fuel causes poisoning of the reactor by neutron absorbing fission products. The neutron absorption of  $^{135}\text{Xe}$  is extremely high, as can be seen in Table 1-1.<sup>8</sup> The neutron capture cross section of  $^{235}\text{U}$  is 582 barns and for  $^{135}\text{Xe}$  is  $2.65 \times 10^6$  barns, which means  $^{135}\text{Xe}$  neutron capture cross section is about 5000 times larger than  $^{235}\text{U}$  and  $^{135}\text{Xe}$  is able to absorb that many more neutrons. With  $^{135}\text{Xe}$  absorbing the majority of neutrons, nuclear fission of  $^{235}\text{U}$  is unable to proceed to produce nuclear energy. This is why  $^{135}\text{Xe}$  is such a problem. Lanthanide fission products are also neutron absorbing fission products. In fact, the second most neutron absorbing fission product are the lanthanides (Table 1-1). The main problem is that they are stable products, meaning they do not decay like  $^{135}\text{Xe}$ . Lanthanides remain in the nuclear fuel forever unless the used nuclear fuel undergoes recycling.

Table 1-1 Fission products mainly responsible for neutron absorption. (Reproduced with permission from ref 8. Copyright Wiley-VCH Verlag GmbH & Co. KGaA.) See Appendix A for documentation of permission to republish this material.

Element	Relative abundance in the fission products (%)	Relative neutron absorption (%)
Noble gases	7	72
Lanthanides	70	24
Technetium	10	1
Cesium	4	0.5
Molybdenum	1	0.2
Other elements	8	1.3

Transuranic elements are also produced in the process of nuclear fission; however, this occurs through neutron capture by  $^{238}\text{U}$  and not by  $^{235}\text{U}$ , unlike what has been discussed earlier. The nuclear reactor fuel is enriched with about 4% of  $^{235}\text{U}$  and the remaining 96% is  $^{238}\text{U}$ , so it is natural that  $^{238}\text{U}$  undergoes neutron absorption to form  $^{239}\text{U}$ . The nuclear reaction and decay chain of  $^{238}\text{U}$  by neutron absorption is summarized in Figure 1-2.<sup>8</sup> The main product is the long-lived nuclide  $^{239}\text{Pu}$ ; however through the process of neutron capture coupled with radioactive decay,  $^{238}\text{U}$  produces other isotopes of Pu and Am. The relative amount of these radionuclides is determined by the amount of time  $^{238}\text{U}$  undergoes irradiation.



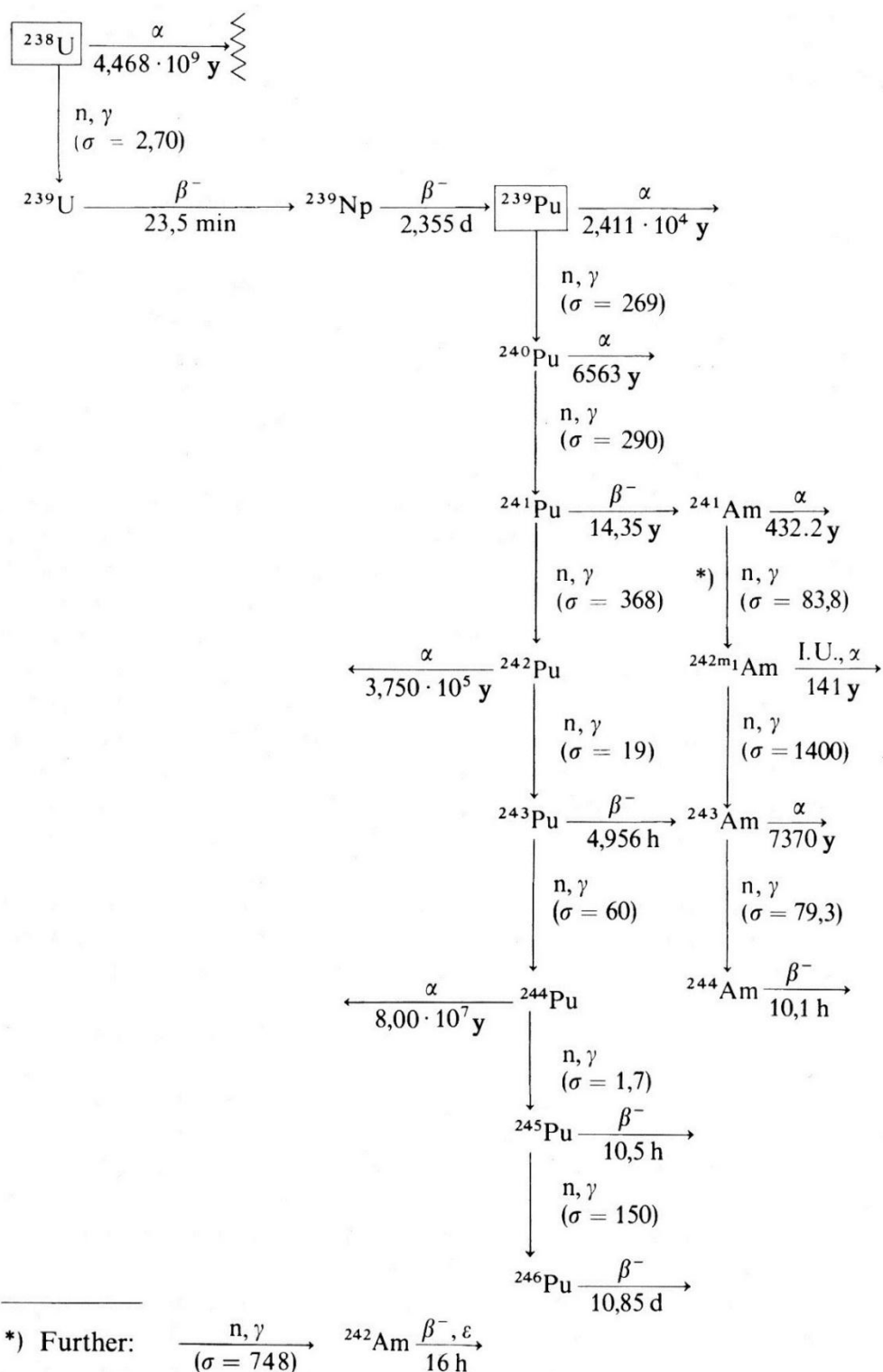


Figure 1-2 Decay chain from nuclear reaction of  $^{238}\text{U}$  by neutron absorption. (Reproduced with permission from ref 8. Copyright Wiley-VCH Verlag GmbH & Co. KGaA.) See Appendix A for documentation of permission to republish this material.

### 1.2.2 Nuclear Waste

Radioactive waste is produced with varying degrees of contamination from the nuclear reactors and must be handled accordingly. The United States Nuclear Regulatory Commission (US NRC) regulates the radioactive waste produced and can be split into essentially two main categories depending on its toxicity:<sup>10</sup>

1. Low Level Waste (LLW): LLW is produced when workers are interacting with radioactive materials. This includes the following items that have been contaminated with radioactive material: personal protective equipment (PPE), pipet tips, glassware, paper towels, filters, etc. The waste cannot be disposed with ordinary refuse due to its high radioactivity levels. LLW must be stored in a safe interim location to allow the short-lived radionuclides to decay to benign levels.
2. High Level Waste (HLW): HLW comes mostly from the core of nuclear reactors, from nuclear weapon processing, and UNF reprocessing. It is highly radioactive and requires shielding to reduce exposure from high levels of radiation. Spent nuclear fuel is stored in swimming pools at the reactor sites or in a dry cask made of metal or concrete.
  - i. Waste Incidental to Reprocessing (WIR): During the reprocessing/recycling of UNF, radioactive liquid waste is produced. This is considered WIR and is considered high-level due to where it originated.
  - ii. Uranium Mill Tailings: During the milling of ores to extract uranium, the waste produced is called uranium mill tailings. The majority of the waste produced is of high levels of radioactivity; however, the volume is small. This waste includes fine

grains of radium, thorium, and residual uranium and gaseous radon produced during the processing of the ore.

The highest concern is for the UNF or spent fuel generated in the reactor core, because fission products and transuranic elements are highly radioactive and hot. There are essentially two options for handling UNF or spent fuel: recycling and direct disposal.<sup>11</sup> Since there is still quite a large amount of uranium within the UNF (95%), the most resourceful choice is to recover the fuel by recycling it. Also, by recycling UNF, radiotoxic and heat generating products may be separated from those that are less harmful and don't require special disposal conditions or facilities. Since it is important to recycle UNF, the main goal of my research is to develop new and innovative sustainable techniques to recycle UNF without generating a large amount of wastes. Therefore recycling UNF will be discussed further in section 1.2.3.

### 1.2.3 Recycling Used Nuclear Fuel

In the US, recycling UNF is not practiced, but it may be considered in the future because of the lack of space for storing the used fuel and to replenish the uranium inventory.<sup>12</sup> Even though the US does not recycle UNF, research in the separation of actinides is very active.<sup>2, 13</sup> For a recycling technique to be successful, the oxidation state of the actinides must be manipulated to allow selective extraction and separation of actinides from each other. The majority of UNF, in the US, contains about 95% of uranium, which can be recycled and reused in pressurized water reactors (PWRs). Another actinide recovered from UNF, is plutonium (1%). The remaining 4% is comprised of fission products and

transuranic elements and is separated from uranium and plutonium to decrease the heat generated and the radiotoxicity present in the aqueous waste.<sup>14</sup>

The separation techniques for recycling UNF include pyroprocessing,<sup>15</sup> precipitation,<sup>16, 17</sup> ion exchange,<sup>17</sup> solvent extraction,<sup>2, 13, 14, 17, 18</sup> and novel non-conventional extraction techniques.<sup>2, 19-21</sup> Solvent extraction possesses several advantages over other recycling techniques such as continuous operation, high throughput, high purity and selectivity, and solvent recycling, all of which are essential to recycle UNF.<sup>14</sup> However, with environmental concerns growing, novel non-conventional solvents have emerged into the field of recycling UNF. RTILs<sup>19</sup> and supercritical fluid (SCF)<sup>22</sup> have become an attractive alternative to organic solvents because of their ability to minimize liquid waste production and non-volatility. Traditional solvent and novel non-conventional extraction techniques will be discussed in more detail in the next section.

### **1.3 Traditional Solvent Extraction**

Aqueous reprocessing began during the Manhattan project in the 1940s to recover <sup>239</sup>Pu. Glenn Seaborg was able to extract microgram quantities of <sup>239</sup>Pu using the bismuth phosphate precipitation process, which was later scaled up at Hanford to kilogram amounts.<sup>13, 23</sup> This was the beginning of the solvent extraction of actinides for weapons use, but later transitioned to the recycling of UNF from commercial nuclear power plants. Several solvent extraction techniques were developed such as the bismuth phosphate process, reduction-oxidation chemistry process (REDOX), and the extraction based on the solvent dibutoxy diethylene glycol (BUTEX). Each had their share of advantages and

disadvantages, which led to the current process used in the industry worldwide, i.e. PUREX process.<sup>12, 24, 25</sup> The original meaning of the acronym PUREX is **P**lутonium **U**ranium **R**eduction **E**xtraction.<sup>26</sup> Thus far, the PUREX process has proven to be an effective method for recycling UNF. The process focuses on the separation of uranium nitrate from plutonium nitrate which is then recycled and reused in PWRs and as mixed oxide (MOX) (U, Pu)O<sub>2</sub> fuels.<sup>12</sup> The PUREX process will be discussed in more detail in the next section (1.3.1). Researchers have been working on developing new flow sheets to further separate other fission products, actinides, and lanthanides. This new process is called the uranium extraction + process (UREX+) and was investigated until 2010. It was comprised of four basic variations: UREX +1, +2, +3, and +4; therefore, the partitioning of actinides from each other to a certain degree may be achieved.<sup>27</sup> The UREX + process begins similarly to the PUREX process, where the fuel is dissolved in nitric acid and mixed with tri-n-butyl phosphate (TBP) diluted in a paraffinic diluent. However, a key difference is the addition of the reducing agent acetohydroxamic acid (AHA). Simple hydrophilic hydroxamic ligands such as AHA were used for the stripping of tetravalent actinides in the UREX process flowsheet. This approach is based on the high coordinating ability of hydroxamic acids with tetravalent actinides, Np<sup>4+</sup> and Pu<sup>4+</sup> compared with hexavalent uranium, UO<sub>2</sub><sup>2+</sup>. A stream of U(VI) and Tc(VII) are separated while Np(IV) and Pu(IV) are complexed by AHA and remain in the aqueous phase. This is followed by the removal of fission products via the FPEX process, such as <sup>90</sup>Sr (t<sub>1/2</sub>=30 yrs), <sup>137</sup>Cs (t<sub>1/2</sub>=30 yrs) and <sup>135</sup>Cs (t<sub>1/2</sub>=3x10<sup>6</sup> yrs) because they generate a lot of heat, and then the isolation of other actinides and lanthanides. Lastly, the actinides and lanthanides are separated from each other. Drawbacks to these solvent

techniques included the production of too many different waste streams, no immiscibility, organic solvent waste with high disposal costs and environmental contamination issues.<sup>13,</sup>

<sup>25</sup> Thus, non-conventional separation processes are being developed to safely and effectively separate the useful and desired components of spent fuel from the UNF, while dramatically reducing the volume and toxicity of the liquid wastes. Novel non-conventional extraction techniques will be discussed in sections 1.4.1 and 1.4.2. Since my research is based on the basic principles of the PUREX process, it will be discussed more in detail in the next section (1.3.1).

### 1.3.1 PUREX Process

Before discussing the PUREX process, there are several basic principles which need to be considered. There are several parameters which affect the extraction efficiency of metal species in solution, but only the following three will be discussed: first is the oxidation state of the metal ion species of interest, another is the concentration of nitrate, and last is the concentration of TBP (Figure 1-3). By knowing how these parameters affect the extraction efficiency, design of a separation scheme is possible.

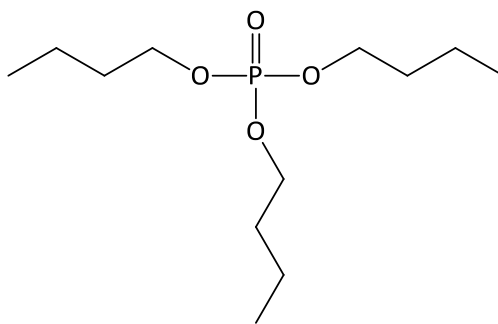


Figure 1-3 Chemical structure of tri-n-butyl phosphate.

Actinides have multiple oxidation states in aqueous solution, as can be seen in Figure 1-4. Some oxidation states are more stable for a certain actinide than others. Researchers take advantage of this fact to develop separation schemes by manipulating their oxidation states.

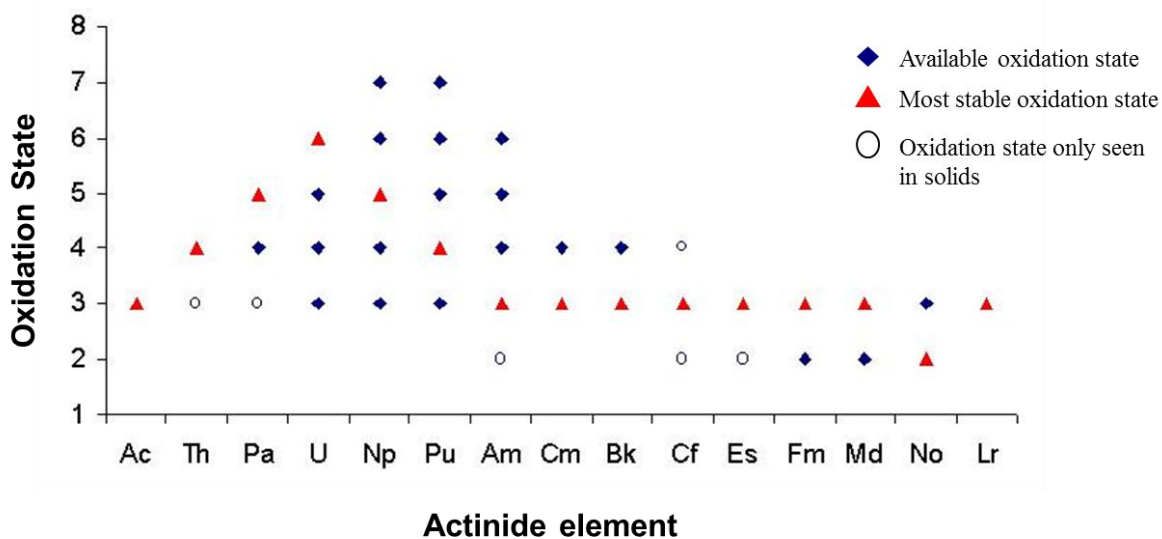
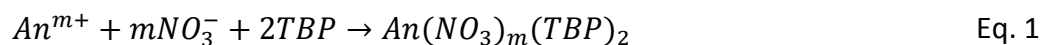


Figure 1-4 Plot of different oxidation states for actinide elements.

To be able to perform extraction of actinide ions there are charge neutralization and ligand solvation requirements. The phase transfer equilibrium for the extraction of neutral actinide ions with TBP is shown in Eq. 1. It is known, tetra- and hexavalent metal ions are capable of being extracted by TBP and tri- and pentavalent metal ions present are not extracted.<sup>28</sup>



To know how well the extraction of the desired species from aqueous solution is, the distribution ratio may be calculated. The distribution ratio represents the amount of

metal extracted quantified by the ratio of the analytical concentration of metal species in the organic phase to its analytical concentration in the aqueous phase at equilibrium as described in Eq. 2. If  $D \geq 1$ , 50% or more of the desired species is extracted and if  $D \leq 1$ , 50% or less of the desired species is extracted.

$$D = \frac{[(An^{x+})(NO_3^-)_x(TBP)_2]}{[An^{x+}]} \quad \text{Eq. 2}$$

Another concern is which oxidation state is more extractable for a specific actinide. In Table 1-2, the distribution ratios of some actinides in the +4 and +6 oxidation state are compared. The actinides were dissolved in a 5 M  $HNO_3$  solution and extracted with 19 % v/v of TBP in kerosene.<sup>29, 30</sup> It was found that the tetravalent actinides were more extractable into the organic phase as the atomic number increased, and vice versa in the case of the hexavalent actinides.

Table 1-2 D values of actinides extracted with kerosene modified with 19% v/v TBP from 5 M  $HNO_3$ .<sup>29, 30</sup>

Actinide	Oxidation State	
	IV	VI
Th	2	
U		30
Np	4	10
Pu	18	3

Another important parameter to consider is the nitric acid (nitrate) concentration. According to Eq. 1, the formation of the neutral complex is necessary and therefore the



extractability of the metal ion depends on the concentration of nitrate ions (nitric acid) present. As shown in Figure 1-5, the distribution ratio increases with increasing nitric acid concentration.<sup>31</sup> For instance, the distribution ratio of U(VI) increases as a function of HNO<sub>3</sub> concentration, up to a maximum of 5-6 M HNO<sub>3</sub>, and then begins to decrease. The decrease in D is found to be due to the competition between HNO<sub>3</sub> and TBP.<sup>29-32</sup>

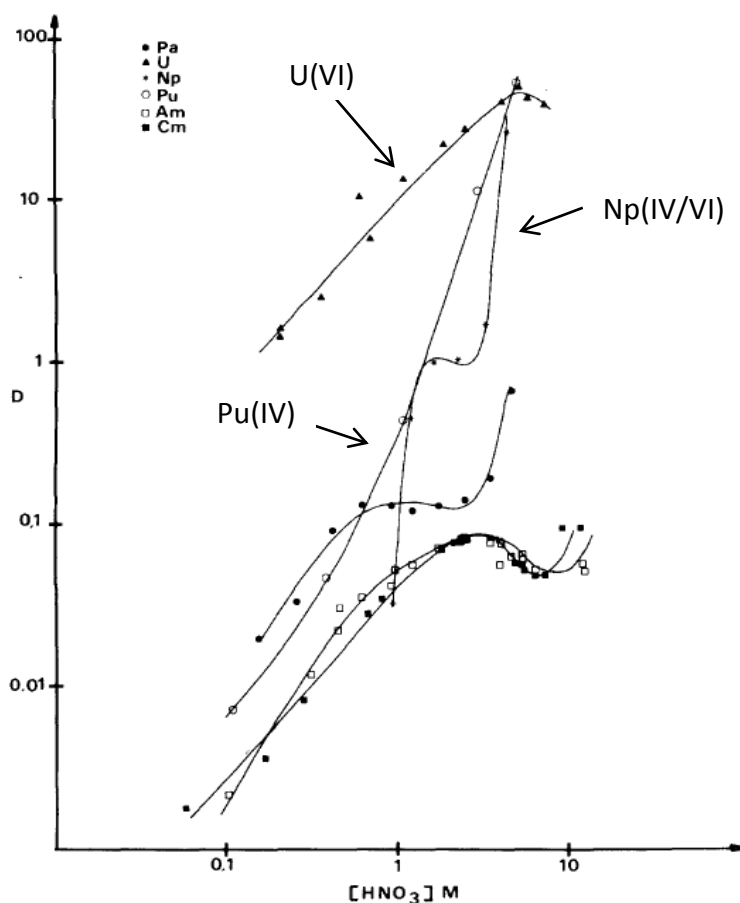


Figure 1-5 Distribution of actinides extracted from HLW by kerosene modified with 50% TBP (Reprinted with permission from ref 31. Copyright (1979), with permission from Elsevier . See Appendix A for documentation of permission to republish this material.

Based on Eq. 1, the addition of more TBP should increase actinide complex formation. This general trend is observed at 4.8 and 19% v/v TBP in kerosene as shown in Figure 1-6. Up to 1 g/L of uranium was dissolved in various HNO<sub>3</sub> solutions and partitioned

with 4.8 and 19% v/v TBP in kerosene.<sup>29</sup> It can be seen that the extraction of U(VI) was about an order of magnitude higher when 19% v/v of TBP in kerosene was used, compared to 4.8% v/v TBP in kerosene.

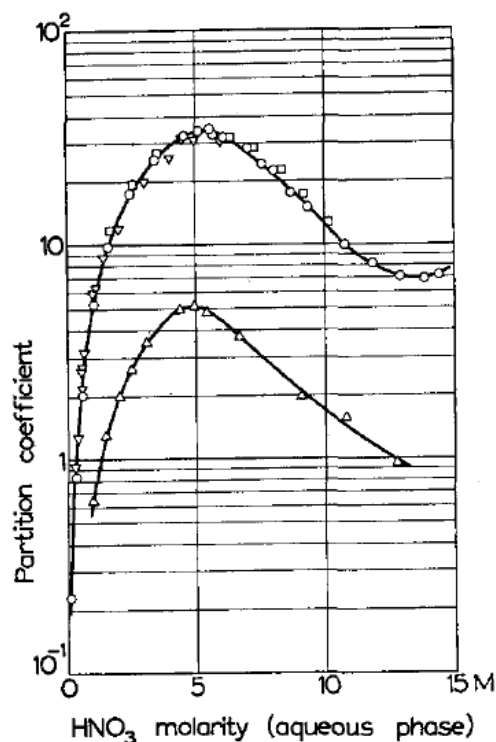


Figure 1-6 Distribution ratio of U(VI) extracted from HNO<sub>3</sub> solutions by, kerosene modified with 4.8% TBP (lower curve) and 19% TBP (upper curve) (Reprinted with permission from ref 29. Copyright (1958), with permission from Elsevier. See Appendix A for documentation of permission to republish this material.

The principle of chemical recycling of UNF relies essentially on liquid-liquid extraction. A flow chart of the PUREX process is reproduced in Figure 1-7. UNF is composed of 96% metals (95% uranium and 1% Pu) which can be recovered and 4% transuranic elements and fission products, rare earth elements (REE), and minor actinides (MA) which are disposed of.<sup>33</sup> Uranium is partitioned because it is the desired product, while removing the fission products substantially decreases the radiotoxicity and heat generated.

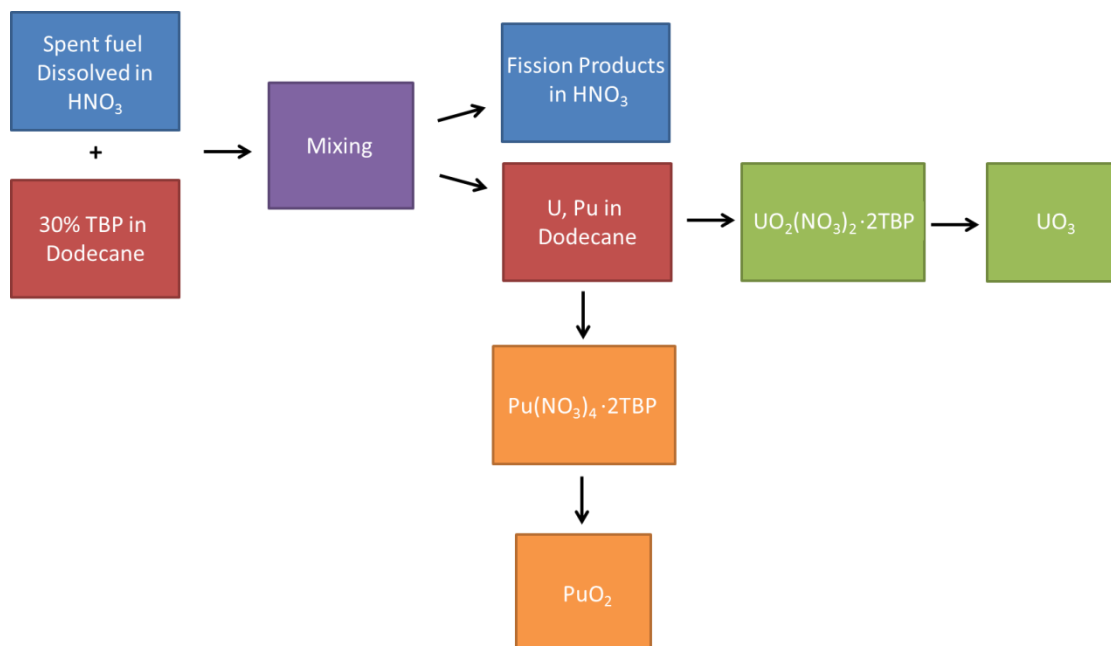
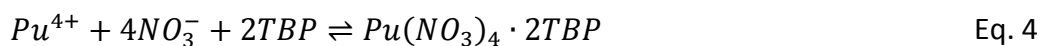
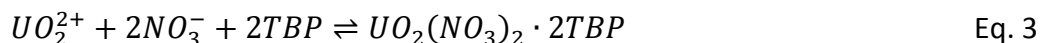
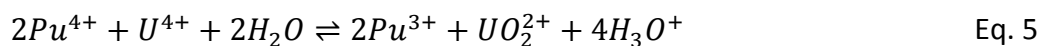


Figure 1-7 Flowsheet of the PUREX process.

The PUREX process begins with the fuel elements being disassembled to reveal the fuel rods, which are then chopped into pieces. These pieces are dissolved in  $\sim 6\text{-}8\text{ M HNO}_3$  in which  $\text{UO}_2$  undergoes dissolution to  $\text{U(VI)}$ . After dissolution of the fuel  $\text{U(VI)}$  is present in the form of  $\text{UO}_2(\text{NO}_3)_2$  and  $\text{Pu(IV)}$  is in the form  $\text{Pu}(\text{NO}_3)_4$ . Concurrently during the chopping and dissolution of the fuel, volatile gases are liberated and should be collected and treated. The non-dissolved pieces are removed by centrifugation and then the  $\text{HNO}_3$  concentration is adjusted to 3 M.  $\text{U(VI)}$  and  $\text{Pu(IV)}$  are co-extracted from the aqueous phase into the 30% v/v TBP/dodecane organic phase, which partitions them from fission products, trivalent actinides, and  $\text{Np(V)}$  in the aqueous phase. The separation of uranium and plutonium from the fission products is achieved by extraction of hexavalent and tetravalent metal nitrate complexes as shown in Eq. 3 and 4.



The separation of U(VI) from Pu(IV) is accomplished by reductive stripping of plutonium, where Pu(IV) is reduced to inextractable Pu(III) and then stripped into 1 M nitric acid, leaving U(VI) in the organic phase. The reductant chosen must be strong enough to reduce Pu(IV) to Pu(III); however, it must not change the oxidation state of U(VI). A typical reducing agent used is uranous nitrate, U(IV), as shown in Eq. 5.



Uranium is subsequently back-extracted with a very dilute nitric acid solution (0.01 M HNO<sub>3</sub>). At this point both U and Pu are isolated separately. Pu(III) is oxidized back to Pu(IV) by NO<sub>x</sub> gas, and then Pu(IV) reacts with oxalic acid to precipitate as a Pu(IV) oxalate. The Pu(IV) oxalate is dried and calcined to give PuO<sub>2</sub> powder. The uranium nitrate is converted to UO<sub>2</sub> powder by concentrating the nitric acid solution, followed by calcination, and then reduction of UO<sub>3</sub> by H<sub>2</sub> to produce UO<sub>2</sub>.<sup>8, 34</sup> Now U(IV) is ready to be re-used as recycled uranium in the form of a UO<sub>2</sub> fuel in a PWR and Pu(IV) to be mixed with UO<sub>2</sub> to form MOX fuel. Proliferation risk concerns and reduction of HLW volume, radiotoxicity, and heat generation encouraged the development of additional recycling methods such as UREX +, Trivalent Actinide - Lanthanide Separation by Phosphorus reagent Extraction from Aqueous Komplexes (TALSPEAK), and Trans-Uranium Extraction (TRUEX) in the US where minor actinides and lanthanides are selectively extracted.

## 1.4 Novel Non-Conventional Extraction Techniques

Despite the worldwide use of traditional solvent extraction for the recycling of used nuclear fuel, the generation of hazardous volatile organic solvent waste is an issue which cannot be ignored.<sup>13,25</sup> Extractions using sc-CO<sub>2</sub> and RTILs have been proposed as alternative non-conventional solvents for nuclear waste treatment, due to their potential to reduce the volume of organic solvent waste.<sup>20, 21</sup>

### 1.4.1 Supercritical Fluid

A fluid becomes supercritical when the temperature and pressure become elevated enough to exceed its critical point. Table 1-3 lists the critical constants of common molecules used as SCF solvents.<sup>35</sup>

Table 1-3 Critical constants of common molecules used as SCF solvents.<sup>36</sup>

Molecule	Critical Temperature, T <sub>c</sub> (°C)	Critical Pressure, P <sub>c</sub> (atm)
Ar	-122	49
CH <sub>4</sub>	-82	45
Xe	17	58
CF <sub>3</sub> H	26	47
CO <sub>2</sub>	31	73
C <sub>2</sub> H <sub>6</sub>	32	48
C <sub>3</sub> H <sub>8</sub>	97	42
NH <sub>3</sub>	133	111
H <sub>2</sub> O	374	218

A special characteristic of a SCF is that it possesses physical properties of both a liquid and a gas. Thus, by manipulating the pressure of the system, the SCF can mimic the physical properties of either a liquid or a gas. Characteristic values of gas, liquid, and supercritical states are listed in Table 1-4.<sup>36-39</sup> The density of SCF is similar to that of a liquid, which allows SCFs to dissolve and carry large amounts of solutes. The advantage of possessing gas-like properties is that higher extraction efficiencies can be achieved because the mass transfer rates between a solute and a SCF are related to the gas's high diffusivity and low viscosity properties.

Table 1-4 Physical properties of gases, supercritical fluids, and liquids.

State of the Fluid	Density (g/cm <sup>3</sup> )	Diffusivity (cm <sup>2</sup> /s)	Viscosity (g/(cm·s))	ref
Gas (ambient)	$1.0 \times 10^{-03}$	$1.0 \times 10^{-01}$	$1.0 \times 10^{-04}$	[36, 37]
	$(0.6 - 2.0) \times 10^{-03}$	$(1.0 - 4.0) \times 10^{-01}$	$(1.0 - 3.0) \times 10^{-04}$	[38, 39]
SCF ( $T_c, P_c$ )	$3.0 \times 10^{-01}$	$1.0 \times 10^{-03}$	$1.0 \times 10^{-04}$	[36, 37]
	$(2.0 - 5.0) \times 10^{-01}$	$7.0 \times 10^{-04}$	$(1.0 - 3.0) \times 10^{-04}$	[38, 39]
Liquid (ambient)	$1.0 \times 10^{+00}$	$5.0 \times 10^{-06}$	$1.0 \times 10^{-02}$	[36, 37]
	$(0.6 - 1.6) \times 10^{+00}$	$(0.2 - 2.0) \times 10^{-05}$	$(0.2 - 3.0) \times 10^{-02}$	[38, 39]

In particular, sc-CO<sub>2</sub> has several advantages over traditional organic solvents used in recycling UNF such as moderate critical points ( $P_c = 73.0$  atm,  $T_c = 31.1^\circ\text{C}$ ), low cost, and nonflammable nature. Also, the selectivity and dissolution of specific compounds may be easily achieved in sc-CO<sub>2</sub> by adjusting the pressure (density) of the fluid. Thus, sc-CO<sub>2</sub> possesses several features that would be advantageous to have in the recycling of UNF.

### 1.4.2 Room Temperature Ionic Liquids

VOCs (volatile organic compounds) are common solvents with high vapor pressures used in chemical processes such as nuclear waste processes. Using VOCs has a negative effect on the environment, including smog, ozone depletion and groundwater contamination, and this has raised alarm among environmentalists.<sup>40</sup> The commonly accepted definition of an RTIL is a compound composed of fully dissociated ions that melt at temperatures lower than 100°C. The most common RTILs are composed of the following organic cations: imidazolium, pyridinium, ammonium, and phosphonium and inorganic anions (Table 1-5).<sup>41</sup>

Table 1-5 Generic structures of common RTILs. See Appendix A for documentation that this material is in the public domain.<sup>41</sup>

Ionic liquid type	Structure	Ionic liquid type	Structure
Alkylammonium		Alkylpyridinium	
Alkylphosphonium		Alkylimidazolium	

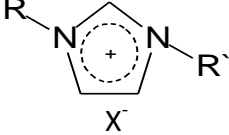
$X^-$ :  $BF_4^-$ ,  $PF_6^-$ ,  $AlCl_4^-$ ,  $SbF_6^-$ ,  $CF_3SO_3^-$ ,  $(CF_3SO_2)_2N^-$  etc.  $R_x$ : from  $-CH_3$  to  $-C_9H_{19}$

RTILs possess features that conventional molecular solvents do not. One of an RTILs most attractive characteristics is its potential of being “designed to order.” Thus, by choosing the appropriate cation and anion, the following physical properties may be varied:

density, moisture stability, viscosity or miscibility. Table 1-6 shows a comparison table of selected physical properties of two alkyimidazolium cations combined with different anions.<sup>41</sup> Two general parameters determine the properties of alkyimidazolium ionic liquids. The first is the anion, which affects the water miscibility and the second is the length of the alkyl chain on the cation, which affects the hydrophobicity, viscosity, and density of the IL. The lengthening of the alkyl chain increases the hydrophobicity and viscosity, while decreasing the density of the IL.<sup>42</sup> The widely tunable class of ILs has become important for synthetic,<sup>43, 44</sup> catalytic,<sup>43-45</sup> biochemical and electrochemical<sup>46</sup> applications and as liquid phases for separations processes.<sup>47-50</sup>



Table 1-6 Select physical properties of two alkyimidazolium cations with three anions. See Appendix A for documentation that this material is in the public domain.<sup>41</sup>

RTIL 	MP [°C]	Density [g mL <sup>-1</sup> ]	Viscosity [cP]	WaterSol ubility	References
[C <sub>4</sub> MIM][Cl]	41	1.08	716	S	[42]
[C <sub>4</sub> MIM][BF <sub>4</sub> ]	-81	1.12	219	S	[42, 51]
[C <sub>4</sub> MIM][PF <sub>6</sub> ]	10	1.37	371	NS	[42, 51, 52]
[C <sub>6</sub> MIM][Cl]	-70	1.03	-	S	[42, 53]
[C <sub>6</sub> MIM][BF <sub>4</sub> ]	-82	1.21	314	PS	[42]
[C <sub>6</sub> MIM][PF <sub>6</sub> ]	-61	1.30	582	NS	[42, 53, 54]
<p>R = Methyl; R' = Butyl or Hexyl; X<sup>-</sup> = Cl, BF<sub>4</sub>, PF<sub>6</sub>            S- Soluble, PS- Partially Soluble, NS- Not Soluble            [C<sub>4</sub>MIM][Cl] = 1-butyl-3-methylimidazolium chloride            [C<sub>4</sub>MIM][BF<sub>4</sub>] = 1-butyl-3-methylimidazolium tetrafluoroborate            [C<sub>4</sub>MIM][PF<sub>6</sub>] = 1-butyl-3-methylimidazolium hexafluorophosphate            [C<sub>6</sub>MIM][Cl] = 1-hexyl-3-methylimidazolium chloride            [C<sub>6</sub>MIM][BF<sub>4</sub>] = 1-hexyl-3-methylimidazolium tetrafluoroborate            [C<sub>6</sub>MIM][PF<sub>6</sub>] = 1-hexyl-3-methylimidazolium hexafluorophosphate</p>					

## 1.5 Overview of Dissertation

The goal of this research project is to develop a sustainable separation technique for the separation of uranium from other actinides and lanthanides. RTILs and sc-CO<sub>2</sub> will be used as solvents and are known to be superior in regards to minimizing the volume of waste produced as compared to the amount produced when using traditional solvents. A

review of literature on our current understanding of actinide and lanthanide separations in RTILs and sc-CO<sub>2</sub> will be summarized in Chapter 2.

The core of my dissertation is split into three sections, where each utilizes non-traditional solvents to contribute to the development of a sustainable technique for recycling UNF. The first uses a RTIL as the solvent (Chapter 3), the second includes the use of tristructural isotopic (TRISO) fuel particles and sc-CO<sub>2</sub> as the solvent (Chapter 4), and the third demonstrates the separation of uranium from other actinides and lanthanides by using sc-CO<sub>2</sub> (Chapter 5). A conclusion chapter will summarize the contents discussed in this dissertation (Chapter 6).

In Chapter 3, the coordination environment of uranyl ion in solutions of the RTIL, 1-butyl-3-methylimidazolium bis(trifluoromethylsulfonyl)imide ([C<sub>4</sub>MIM][Tf<sub>2</sub>N]) containing either tetrabutylammonium nitrate (TBAN), nitric acid, or TBAN and TBP characterized by using attenuated total reflection-Fourier transform infrared (ATR-FTIR) and ultraviolet-visible (UV-Vis) spectroscopy is presented. Both UO<sub>2</sub>(NO<sub>3</sub>)<sub>2</sub> and UO<sub>2</sub>(NO<sub>3</sub>)<sub>3</sub><sup>-</sup> species were detected in solutions containing TBAN and in solutions containing nitric acid only UO<sub>2</sub>(NO<sub>3</sub>)<sub>2</sub> was detected by ATR-FTIR. Furthermore, the complex UO<sub>2</sub>(NO<sub>3</sub>)<sub>2</sub>(TBP)<sub>2</sub> was identified in [C<sub>4</sub>MIM][Tf<sub>2</sub>N] by ATR-FTIR and UV-Vis spectroscopy.

In Chapter 4, whole TRISO fuel particles were  $\gamma$ -irradiated at 691 and 1047 kGy and then mechanically crushed with a mortar and pestle to a range of particle sizes. These were then subjected to sc-CO<sub>2</sub> extraction with the complex ligand TBP(HNO<sub>3</sub>)<sub>1.8</sub>(H<sub>2</sub>O)<sub>0.6</sub>. The extraction efficiency of U(VI) increased from 67  $\pm$  2% to 98  $\pm$  1% and 99  $\pm$  1% for the particle size of < 60 mesh when the TRISO fuel was irradiated to 691 and 1047 kGy, respectively.

The increase is believed to be caused by the carbon vacancy- interstitial pair formed when the TRISO fuel particles are irradiated. This phenomenon increases the diffusion of the extractant used which allows for higher dissolution of uranium for extraction. Furthermore, the feasibility of crushing TRISO fuels in liquid CO<sub>2</sub> is presented. The attempt to use an ultrasound pressure vessel to crushed TRISO fuels was unsuccessful.

In Chapter 5, several actinides (U(VI), Np(VI), Pu(IV), and Am(III)) were extracted in sc-CO<sub>2</sub> modified with TBP over a range of nitric acid concentrations and then the actinides were exposed to reducing and complexing agents to suppress their extractability. According to this study, the separation of uranium from plutonium in sc-CO<sub>2</sub> modified with TBP was successful at nitric acid concentrations of less than 3 M in the presence of AHA or oxalic acid (OA), and the separation of uranium from neptunium was successful at nitric acid concentrations of less than 1 M in the presence of AHA, OA, or sodium nitrite.

In addition, the sc-CO<sub>2</sub> extraction and separation of U(VI) from Np(VI), Pu(IV), Am(III), and the lanthanide series by using 1% mole fraction TBP, sodium nitrite, and oxalic acid from 1 M HNO<sub>3</sub> solution is presented. This will demonstrate an alternative to the PUREX process for recycling UNF. A series of stripping columns is used to simulate counter current columns in an actual industrial process. All Np(VI) was reduced to Np(V) upfront to prevent extraction and the trivalent Am and Ln series were not extractable. A large portion of Pu(IV) was stripped by an OA-HNO<sub>3</sub> solution. With a series of water stripping columns, U(VI) can be isolated.

## 1.6 References

1. *Nuclear Energy: Assuring Future Energy Supplies*, in *Oak Ridge National Laboratory Reviews*. 2002, 2-3.
2. *Nuclear Energy and the Environment*, ed. C. M. Wai and B. J. Mincher, ACS Symposium Series 1046, Washington DC, USA, 2010.
3. *U.S. Energy Information Administration*, 2012, Available from: <http://www.eia.gov/totalenergy/data/monthly/#electricity>.
4. P. J. Meier, *Life-cycle Assessment of Electricity Generation Systems and Applications for Climate Change Policy Analysis*, in *Land Resources*. 2002, University of Wisconsin-Madison: Madison.
5. R. E. Kasperson, *Daedalus*, 2013, **142**, 90-96.
6. *An Energy Landmark: Idaho's Pioneering Experimental Breeder Reactor-1*. Available from: <http://www.inl.gov/ebr/>.
7. Power Reactor Information System, IAEA. *United States of America*. 2013; Available from: <http://www.iaea.org/PRIS/CountryStatistics/CountryDetails.aspx?current=US>.
8. K. H. Lieser, *Nuclear and Radiochemistry*; 2 ed.; WILEY-VCH: New York, 2001.
9. G. Friedlander and J. W. Kennedy, *Introduction to Radiochemistry*; Wiley: New York, 1949.
10. *Radioactive Waste, United States Nuclear Regulatory Commission*; Available from: <http://www.nrc.gov/waste.html>.
11. C. Madic, *Radiat. Prot. Dosimetry*, 1989, **26**, 15-22.
12. D. O. Campbell and W. D. Burch, *J. Radioanal. Nucl. Chem.*, 1990, **142**, 303-320.
13. G. R. Choppin, *Solvent Extr. Res. Dev., Jpn.*, 2005, **12**, 1-10.
14. K. L. Nash, C. Madic, J. N. Mathur, and J. Lacquemont, *Actinide Separation Science and Technology in Chemistry of the Actinide and Transactinide Elements*, ed. L. R. Morss, N. M. Edelstein, and J. Fuger. 2006, Springer: The Netherlands. p. 2644-2666.
15. H. Lee, J. Hur, J. Kim, D. Ahn, Y. Cho, and S. Paek, *Energy Procedia*, 2011, **7**, 391-395.

16. G. Jarvenin, *Precipitation and Crystallization Processes*. 2008, Los Alamos National Laboratory.
17. R. O. A. Rahman, H. A. Ibrahim, and Y. Hung, *Water*, 2011, **3**, 551-565.
18. J. N. Mathur, M. S. Murali, and K. L. Nash, *Solvent Extr. Ion Exch.*, 2001. **19**, 357-390.
19. M. L. Dietz, *Sep. Sci. Technol.*, 2006, **41**, 2047-2063.
20. J. S. Wang, C. N. Sheaff, B. Yoon, R. S. Addleman, and C. M. Wai, *Chem. – Eur. J.*, 2009, **15**, 4458-4463.
21. C. M. Wai, Y. Liao, W. Liao, G. Tian, R. S. Addleman, D. Quach, and S. P. Pasilis, *Dalton Trans.*, 2011, **40**, 5039-5045.
22. C. Wai and B. Waller, *Ind. Eng. Chem. Res.*, 2000, **39**, 4837-4841.
23. F. G. Gosling, *The Manhattan Project: Making the Atomic Bomb*, 2010, **1**.
24. J. E. Birkett, M. J. Carrott, D. O. Fox, C. J. Jones, C. J. Maher, C. V. Roubé, R. J. Taylor, and D. A. Woodhead, *Chimia*, 2005, **59**, 898-904.
25. J. M. McKibben, *Radiochim. Acta*, 1984, **36**, 3-15.
26. W. B. Lanham and T. C. Runion, *PUREX Process for Plutonium and Uranium Recovery*. 1949, Oak Ridge National Laboratory.
27. R. Bari, L. Cheng, J. Phillips, J. Pilat, G. Rochau, I. Therios, R. Wigeland, E. Wonder, and M. Zentner, *Proliferation Risk Reduction Study of Alternative Spent Fuel Processing*. 2009, Brookhaven National Laboratory: Upton.
28. W. W. Schulz, L. L. Burger and J. D. Navratil, *Science and technology of tributyl phosphate Volume III: Applications of tributyl phosphate in nuclear fuel reprocessing*, CRC Press, Boca Raton, FL, USA, 1990.
29. K. Alcock, G. F. Best, E. Hesford, and A. C. McKay, *J. Inorg. Nucl. Chem.*, 1958, **6**, 328-333.
30. G. F. Best, A. C. McKay, and P. R. Woodgate, *J. Inorg. Nucl. Chem.*, 1957, **4**, 315-320.
31. I. Svantesson, I. Hagstrom, G. Persson, and J. Liljenzin, *J. Inorg. Nucl. Chem.*, 1979, **41**, 383-389.
32. K. Naito and T. Suzuki, *J. Phys. Chem.*, 1962, **66**, 989-995.

33. K. L. Nash, C. Madic, J. N. Mathur, and J. Lacquemont, *Actinide Separation Science and Technology in Chemistry of the Actinide and Transactinide Elements*, ed. L.R. Morss, N. M. Edelstein, and J. Fuger. 2006, Springer: The Netherlands. p. 2644-2666.
34. *The Nuclear Fuel Cycle From Ore to Waste*, ed. P.D. Wilson. 1996, New York: Oxford University Press.
35. Y. Arai, T. Sako, Y. Takebatashi, *Supercritical Fluids: Molecular Interactions, Physical Properties, and New Applications*. Materials Processing, ed. H. Warlimont, E. Weber, W. Michaeli, Vol. 2. 2002, New York: Springer.
36. U. Wasen, I. Swaid, G. M. Schneider, *Angew. Chem.*, 1980, **19**, 575-658.
37. T. H. Gouw and R. E. Jentoft, *J. Chromatogr.* 1972, **68**, 303-323.
38. E. Stahl, K. W. Quirin, and D. Gerard, *Dense Gases for Extraction and Refining*. 1988, New York: Springer-Verlag.
39. G. Brunner, *Chem. Ing. Tech*, 1987, **59**, 12-22.
40. M. C. Cann and M. W. Connelly, *Real-world cases in green chemistry*. 2000, Washington American Chemical Society.
41. P. Stepnowski, *Int. J. Mol. Sci.*, 2006, **7**, 497-509.
42. J. G. Huddleston, A. G. Visser, W. M. Reichert, H. D. Willauer, G. A. Broker, and R. D. Rogers, *Green Chem.*, 2001, **3**, 156-164.
43. T. Welton, *Chem. Rev.*, 1999, **99**, 2071-2083.
44. J. P. Hallett and T. Welton, *Chem. Rev.*, 2011, **111**, 3508-3576.
45. P. Wasserscheid and W. Keim, *Angew. Chem. Int. Ed.*, 2000, **39**, 3772-3789.
46. M. C. Buzzeo, R. G. Evans, and R. G. Compton, *Chem. Phys. Chem.*, 2004, **5**, 1106-1120.
47. J. G. Huddleston, H. D. Willauer, R. P. Swatloski, A. E. Visser, and R. D. Rogers, *Chem. Commun.*, 1998. **16**, 1765-1766.
48. N. V. Plechkova and K. R. Seddon, *Chem. Soc. Rev.*, 2008, **37**, 123-150.
49. R. D. Rogers and K. R. Seddon, *Science*, 2003, **302**, 792-793.
50. I. Billard and C. Gaillard, *Radiochim. Acta*, 2009, **97**, 355-359.

51. P. A. Z. Suarez, S. Einloft, J. E. L. Dullius, R. F. de Souza, J. Dupont, *J. Chim. Phys. Phys. Chim. Biol.*, 1998, **95**, 1626-1639.
52. K. R. Seddon, A. Stark, and M. J. Torres, *Pure Appl. Chem.*, 2000, **72**, 2275-2287.
53. M. A. Abraham and L. Moens, *Clean Solvents. Alternative media for chemical reactions and processing*, in ACS. 2002: Washington DC.
54. A. E. Visser, J. R. Holbrey, and R. D. Rogers, *Chem. Commun.*, 2001, 2484 – 2485.

## Chapter 2

### Literature Review

#### 2.1 Introduction

The extraction and separation of actinides and lanthanides from UNF is traditionally accomplished by solvent extraction processes. The inherent drawback of conventional solvent extraction is the use of VOCs and production of radioactive aqueous and organic wastes. A more environmentally-friendly technique is desired for treating used nuclear fuel, which would minimize waste generation, lower health risks, lower costs, and meet environmental regulations. SCF and RTILs are two non-conventional solvents with potential for treating used nuclear fuel. These novel solvents have received a lot of attention recently due to their tunable physical properties.<sup>1</sup> For the reasons just mentioned above, new techniques to partition uranium from transuranic and fission products based on the PUREX process are being developed. For instance, research on recycling methods using non-conventional solvents such as SCFs and RTILs are currently in progress and will be discussed further. This chapter provides a brief review of literature in the extraction and separation of actinides and lanthanides using various solvents.

##### 2.1.1 Supercritical Carbon Dioxide

Using sc-CO<sub>2</sub> as a solvent for the dissolution of used nuclear fuel offers a number of advantages compared with conventional nitric acid-organic solvent extraction processes.



As can be seen in Figure 2-1, by decreasing the pressure the sc-CO<sub>2</sub> becomes a gas. This allows for the minimization of secondary liquid waste generation and rapid separation of solute from solvent. Also, an advantage of using sc-CO<sub>2</sub> is being able to work in a closed system, thus providing containment of volatile fission products. Thus, sc-CO<sub>2</sub> has more advantages over using traditional solvents in the recycling of UNF.<sup>2,3</sup>

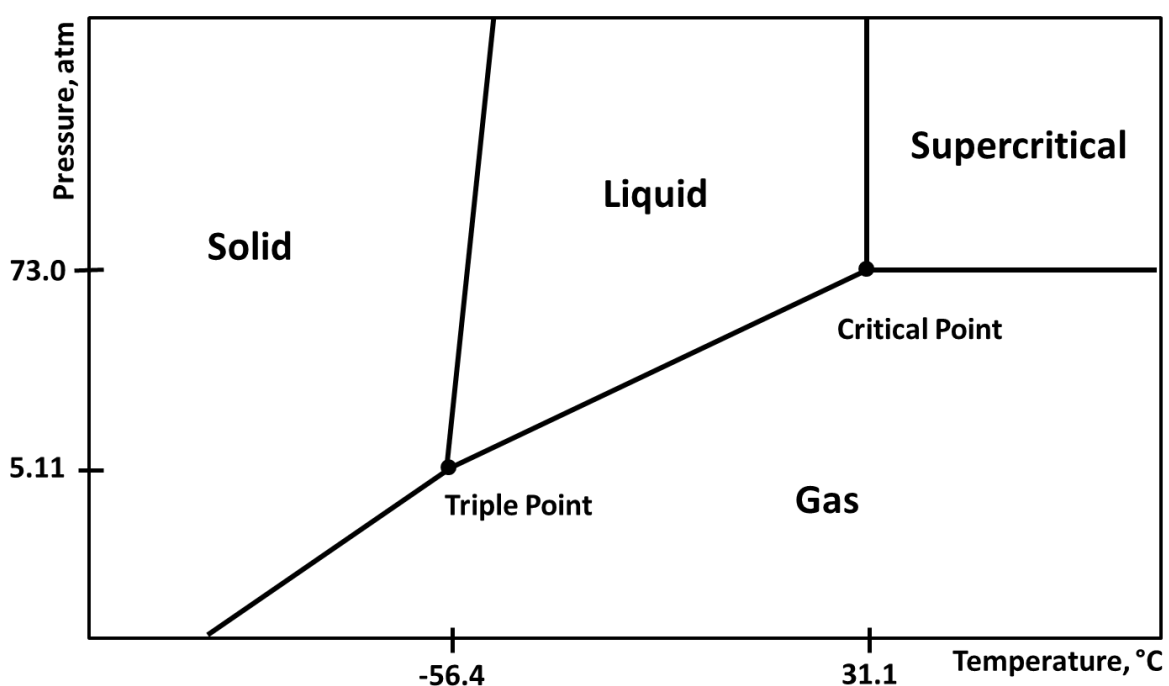


Figure 2-1 Phase diagram for carbon dioxide

However, since CO<sub>2</sub> is a linear molecule, it does not have any dipole moment, and therefore, sc-CO<sub>2</sub> is capable of effectively dissolving non-polar species, but not polar or ionic metal species. Therefore, a chelation technique has been developed for dissolving metal ions into the sc-CO<sub>2</sub> phase.<sup>4</sup> In 1992, Laintz et al.<sup>5</sup> was first to demonstrate the extraction of the metal ion Cu<sup>2+</sup> from aqueous and solid matrices by using the CO<sub>2</sub> soluble

ligand lithium bis(trifluoroethyl) dithiocarbamate (LiFDDC). It was found, when the temperature was constant at 35°C and the density of CO<sub>2</sub> varied, that the solubility of the Cu-FDDC complex varied when extractions were performed from both aqueous and solid matrices. The general trend was that, as the density increased, so did the extraction efficiency of Cu<sup>2+</sup>. When the density of CO<sub>2</sub> was at 0.37 g/mL, the extraction efficiency reached nearly 100% in 30 minutes when Cu<sup>2+</sup> was dissolved in an aqueous solution and about 42% in 30 mins when extraction was performed from a solid matrix. This proved that metal ions can be extracted by sc-CO<sub>2</sub> in the presence of a CO<sub>2</sub>-soluble chelate. However, LiFDDC is not available commercially and is not an effective ligand for complexation with the f-block elements. For a SCF extraction to be successful, the ligand used must be effective and readily available; therefore different CO<sub>2</sub> soluble ligands<sup>6-8</sup> have been explored to improve nuclear waste management.

### 2.1.2 sc-CO<sub>2</sub> as a Solvent for Actinide and Lanthanide Extraction

There has been an extensive amount of research done in the field of sc-CO<sub>2</sub> extraction of metal ions, including actinides and lanthanides. Not all the work done is mentioned in this literature review, but an overview of the progress made in the last two decades has been compiled, specifically focusing on the sc-CO<sub>2</sub> extraction of actinides and lanthanides.

Lin et al.<sup>9</sup> demonstrated the sc-CO<sub>2</sub> extraction of lanthanides and actinides from solid matrices by using the fluorinated β-diketone, 2,2-dimethyl-6,6,7,7,8,8,8-heptafluoro-

3,5 octanedione (FOD). In this paper, 10  $\mu\text{g}$  of the actinide  $\text{UO}_2^{2+}$  and lanthanides  $\text{La}^{3+}$ ,  $\text{Eu}^{3+}$ , and  $\text{Lu}^{3+}$  were each spiked on and extracted from filter paper at  $60^\circ\text{C}$  and 150 atm. When the sc- $\text{CO}_2$  phase was modified with FOD, the extraction efficiency of U(VI) was 12% from dry filter paper. With the addition of 10  $\mu\text{L}$  of water on to the dry filter paper, the extraction efficiency of U(VI) increased to 40%. The extraction efficiency of  $\text{La}^{3+}$ ,  $\text{Eu}^{3+}$ , and  $\text{Lu}^{3+}$  were 5, 10, and 12%, respectively, in the presence of FOD when the filter paper was dry. The extraction efficiency was slightly enhanced to 11, 14, and 18% for  $\text{La}^{3+}$ ,  $\text{Eu}^{3+}$ , and  $\text{Lu}^{3+}$  respectively when the filter paper was wet with water prior to extraction. Methanol is a polar molecule which can modify the polarity of the  $\text{CO}_2$  fluid phase; therefore, it was used to enhance the extraction efficiency of actinides and lanthanides in sc- $\text{CO}_2$ . Using 5 % methanol modified  $\text{CO}_2$ , 95% of the  $\text{UO}_2^{2+}$  and 69, 76, 79% of  $\text{La}^{3+}$ ,  $\text{Eu}^{3+}$ , and  $\text{Lu}^{3+}$ , respectively can be extracted from the dry filter paper.

To further actinide SCF extraction research Lin et al.<sup>10</sup> proceeded to combine organophosphorus reagents and the different fluorinated  $\beta$ -diketones hexafluoroacetylacetone (HFA), thienoyltrifluoroacetylacetone (TTA), and FOD to give a synergistic extraction effect on the complexation and extraction of  $\text{Th}^{4+}$  and  $\text{UO}_2^{2+}$  from aqueous and solid samples. It was reported that by combining the organophosphorus and fluorinated  $\beta$ -diketones, the extraction efficiency of  $\text{Th}^{4+}$  and  $\text{UO}_2^{2+}$  was significantly enhanced compared to when using either ligand alone.

Lin et al.<sup>11</sup> also reported SFE of uranium and thorium from nitric acid solutions using sc- $\text{CO}_2$  modified with different organophosphorus reagents. Solubility and extraction efficiency for TBP, tri-n-butyl phosphine oxide (TBPO), tri-n-octyl phosphine oxide (TOPO)

and triphenylphosphine oxide (TPPO) were obtained. High extraction efficiencies were observed for all of the organophosphorus reagents studied. The strong dependence of uranyl extraction efficiency on nitric acid concentration was noted. The beneficial effects of salting agents ( $\text{LiNO}_3$ ) were also found to be similar to results found in conventional solvent extraction systems. In addition, the uranyl species extracted by  $\text{sc-CO}_2$  is a neutral uranyl-nitrate-TBP complex,  $\text{UO}_2(\text{NO}_3)_2 \cdot 2\text{TBP}$ , which is identical to the species extracted in the PUREX process using TBP diluted in kerosene. Later in 1998, Carrot et al.<sup>12</sup> determined the complex  $\text{UO}_2(\text{NO}_3)_2 \cdot 2\text{TBP}$  was most soluble at the temperature and pressure of about 40°C and 200 atm by UV-Vis spectrophotometry. Addleman et al.<sup>13</sup> further investigated the solubility of  $\text{UO}_2(\text{NO}_3)_2 \cdot 2\text{TBP}$  in  $\text{sc-CO}_2$  and found that, when the  $\ln(\text{solubility})$  was plotted versus the  $\ln(\text{density})$  for various temperatures, the density of  $\text{sc-CO}_2$  played a larger role in the solubility of  $\text{UO}_2(\text{NO}_3)_2 \cdot 2\text{TBP}$  than temperature. Meguro et al.<sup>7</sup> studied the  $\text{sc-CO}_2$  extraction equilibrium for the uranyl nitrate-TBP system from nitric acid solutions. A linear relationship between the distribution ratio of the metal and the density of  $\text{sc-CO}_2$  was found to exist for liquid and  $\text{sc-CO}_2$  processes.

Meanwhile, at Nagoya University in Japan, Tomioka et al.<sup>14</sup> studied the  $\text{sc-CO}_2$  extraction of lanthanide oxides with a TBP- $\text{HNO}_3$  complex. The TBP- $\text{HNO}_3$  complex was dissolved in the  $\text{sc-CO}_2$  then carried to the extraction cell where the lanthanide oxides were placed. Extraction efficiencies of  $\text{Nd}^{3+}$  and  $\text{Gd}^{3+}$  were both about 50% at a temperature and pressure of 40 °C and 120 atm. In 2001, Tomioka et al.<sup>15</sup> expanded their work to  $\text{sc-CO}_2$  extraction of  $\text{U}_3\text{O}_8$  and  $\text{UO}_2$  with a TBP- $\text{HNO}_3$  complex. Furthermore, Samsonov et al.<sup>16</sup> demonstrated the capability of dissolving  $\text{UO}_3$  and  $\text{UO}_2$  in  $\text{sc-CO}_2$  with a TBP- $\text{HNO}_3$  complex

without any additional solvents. Concurrently, Trofimov et al.<sup>17</sup> used ultrasound to enhance the dissolution rate of metal oxides ( $\text{UO}_3$ ,  $\text{UO}_2$ ,  $\text{U}_3\text{O}_8$ ,  $\text{CeO}_2$ ,  $\text{La}_2\text{O}_3$  and  $\text{ThO}_2$ ) in  $\text{sc-CO}_2$  with TBP- $\text{HNO}_3$  complex and TTA. This study found  $\text{UO}_2$  was more extractable by TBP- $\text{HNO}_3$  than  $\text{ThO}_2$  which indicated possible separation between the two actinides. In 2002 Enokida<sup>18</sup> used ultrasound to enhance the  $\text{sc-CO}_2$  extraction of  $\text{UO}_2$  from glass beads with different TBP- $\text{HNO}_3$  complexes. These complexes have the chemical formula of  $\text{TBP}(\text{HNO}_3)_x(\text{H}_2\text{O})_y$ , where  $x$  and  $y$  depend on the ratio of TBP and  $\text{HNO}_3$  used in their preparation. The complex was characterized by Karl Fisher titration and  $^1\text{H}$  NMR (Nuclear Magnetic Resonance). It was found that  $x$  can be up to 2.5 and  $y$  varies from 0.4 to 0.8.<sup>19</sup>

Characterization of the  $\text{TBP}(\text{HNO}_3)_x(\text{H}_2\text{O})_y$  complex made a significant impact in the field of recycling used nuclear fuel because of its solubility in  $\text{sc-CO}_2$  and dissolution power. Russian<sup>20, 21</sup> and Japanese<sup>14, 15, 22, 23</sup> research groups took advantage of this complexing ability and took a step further towards  $\text{sc-CO}_2$  extraction and separation of actinide and lanthanide oxides and actinides in nitric acid solution. For example, Samsonov et al.<sup>20</sup> demonstrated the dissolution of uranium oxides ( $\text{UO}_2$ ,  $\text{U}_3\text{O}_8$ , and  $\text{UO}_3$ ) and separation from  $\text{ThO}_2$ ,  $\text{PuO}_2$ , and  $\text{NpO}_2$  with  $\text{TBP}(\text{HNO}_3)_{1.8}(\text{H}_2\text{O})_{0.6}$ . However, separation was possible due to the fact that thorium, plutonium, and neptunium did not undergo dissolution. In addition, Indian<sup>24-27</sup> research groups have shown interest in the recycling of used nuclear fuel because of their country's plan to build more nuclear power reactors in the near future. Also, the Chinese<sup>28, 29</sup> have similar plans to expand their fleet of nuclear power reactors, and so have been active in researching the treatment of TRISO fuels which are used in next generation reactors called very high temperature reactors (VHTR).

### 2.1.3 Room Temperature Ionic Liquids

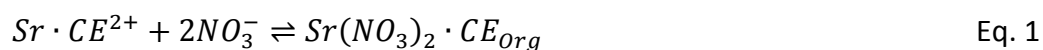
A new non-conventional class of solvents with negligible vapor pressure, called ionic liquids (ILs), has emerged with great promise for replacing VOCs. However, ILs are not newly discovered compounds, they have been known for over a century. In 1914, the first IL, ethylammonium nitrate, was reported by Paul Walden.<sup>30</sup> Some distinctive properties of RTILs are negligible vapor pressure, low viscosity, high conductivity, and good thermal stability, thus making RTIL an attractive replacement for volatile organic solvents.<sup>31, 32</sup> In addition, as mentioned in section 1.4.2, due to the fact that RTILs are composed of a cation and an anion, their properties can be varied based on the combination of cation and/or anion. The uniqueness of RTILs makes them a promising candidate for replacing VOCs for the treatment of used nuclear fuel. Use of RTILs as a solvent in actinide and lanthanide separation processes will be discussed further.

### 2.1.4 Room Temperature Ionic Liquids as a Solvent for Actinide and Lanthanide Extraction

Although Paul Walden's discovery of ILs occurred in 1914, air and water stable 1-ethyl-3-methylimidazolium based RTILs were not synthesized until the early 1990s.<sup>33</sup> The discovery opened up a whole new field of research in various areas of science especially as a potential replacement for VOCs in separation processes. The first demonstration of a liquid-liquid extraction of a metal ion from an aqueous solution into a RTIL was by Dai et al.<sup>34</sup> in 1999. Strontium nitrate was dissolved in an aqueous medium which was then contacted with a crown ether extractant dissolved in various imidazolium based RTILs as

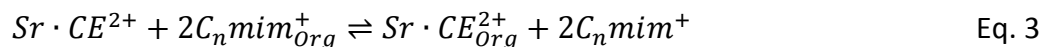
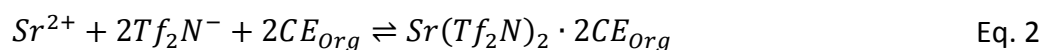
well as conventional organic solvents for comparison purposes. Dai et al.<sup>34</sup> observed higher extractability of  $Sr^{2+}$  from RTILs over the conventional solvents used. The crown ether extractant has a significant role in the partitioning of  $Sr^{2+}$ , since without the crown ether, essentially no  $Sr^{2+}$  was partitioned into the organic phase. Another feature in this study worth noting is that the distribution ratio of  $Sr^{2+}$  was 2-3 orders of magnitude higher when the bistrifluoromethylsulfonamide anion ( $Tf_2N^-$ ) was used over the hexafluorophosphate anion ( $PF_6^-$ ). Dai et al.<sup>34</sup> explained this difference by comparing the size of the anions. Since the crown ether and  $Sr^{2+}$  form a large cationic complex, it is stabilized by forming a neutral complex with a big anionic species. Thus, when the cationic complex is solvated by  $Tf_2N^-$  or  $PF_6^-$ , the extraction efficiency of  $Sr^{2+}$  in the  $Tf_2N^-$  system is higher than when compared to the  $PF_6^-$  system.

To further understand the role of RTILs as a diluent in a solvent extraction process, Dietz<sup>35, 36</sup> proposed possible mechanisms  $Sr^{2+}$  can be involved in when being transferred from acid solution into 1-alkyl-3-methylimidazolium based RTILs. For comparison purposes conventional solvents such as alkan-1-ols were also used. In a conventional molecular solution it is known that electro-neutrality is required for a metal ion to be transferred from an aqueous to an organic solution. Crown ether (CE) is not a charged extractant, thus the cationic complex is thought to be solvated by nitrate ions to obtain electro-neutrality as shown in Eq. 1.



To determine whether this mechanism occurred, Dietz et al.<sup>35</sup> used acid solutions not containing nitrate ( $H_2SO_4$  and  $HCl$ ) as the aqueous solution and varied the nitrate

concentration to examine how these factors would affect the distribution of  $Sr^{2+}$  between the aqueous and organic phase. It was observed that the distribution ratio of  $Sr^{2+}$  decreased as the nitric acid concentration increased when RTIL was the organic diluent, while the opposite is observed when octanol was used. This observation suggested the mechanism was most likely different when RTILs are used as the diluent. RTILs are only able to dissolve <2% w/w of water, which suggested that the  $Sr^{2+}$  partitioned into the  $C_nMIM^+$  system does not involve nitrate ion co-extraction. The following two possible mechanisms were considered.

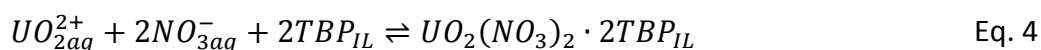


Dietz<sup>35</sup> concluded Eq. 3 was the most probable mechanism by which  $Sr^{2+}$  was being partitioned into the RTIL. When nitrate concentration increased this caused the decrease in extraction of  $Sr^{2+}$  and without the crown ether extractant no transfer was occurring. Thus, anions in the solution do not play a role in the partitioning of  $Sr^{2+}$ , so the only explanation would be a cation exchange.

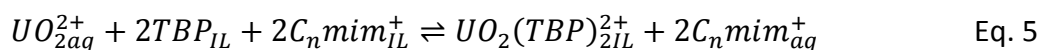
A series of papers related to the extraction of uranium from nitric acid solution by dissolving 1.1 M TBP into 1-alkyl-3-methylimidazolium hexafluorophosphate were reported by Giridhar et al.<sup>37,38</sup>. At < 4 M nitric acid, the distribution ratios of U(VI) into 1.1 M TBP/[ $C_4MIM$ ][ $Tf_2N$ ] or [ $C_4MIM$ ][ $PF_6$ ] are comparable to those obtained into 1.1 M TBP/dodecane was used. At > 4 M nitric acid, the distribution ratio of U(VI) continues to increase in the RTIL diluent; whereas, it decreased in dodecane.



The mechanism of U(VI) extraction by TBP dissolved in RTIL was investigated in detail by Dietz et al.<sup>39</sup> The effect of alkyl chain length on the distribution ratio of U(VI) in TBP/n-alkanes and TBP/[C<sub>n</sub>MIM][Tf<sub>2</sub>N] was compared. The variation in chain length for n-alkanes did not affect the distribution ratio of U(VI); however, a significant effect was observed in the RTIL system. When the alkyl chain length was n= 10, the extraction trend resembled what is seen with n-alkane. This suggested anion pair extraction mechanism as shown in Eq. 4.



When the alkyl chain was n= 5 or 8, the distribution ratio decreased when the nitric acid concentration ranged from 0.01 to 0.2 M then increased when the nitric acid concentration ranged from 0.2 to 1 M. When the nitric acid concentration was > 0.2 M the acid dependency curve started to resemble [C<sub>10</sub>MIM][Tf<sub>2</sub>N], which means the mechanism is the same as shown in Eq. 4. However at lower acid concentrations it is postulated that a cation exchange occurs as shown in Eq. 5. This extraction mechanism was observed in the case of the extraction of Sr<sup>2+</sup> as well<sup>35, 36</sup>.



Trivalent lanthanides and actinides are minimally extracted by TBP/dodecane in the PUREX process; however, they are extractable by CMPO (octyl(phenyl)-N,N-diisobutylcarbonoylmethyl-phosphine oxide ) and DGAs (diglycolamides). Diglycolamides are becoming more favorable as ligands, for separating trivalent actinides from UNF.<sup>40-44</sup> Diglycolamides are promising extractants because of their ability to form a tridentate

complex with trivalent species. The general chemical structure of a DGA is shown in Figure 2-2.

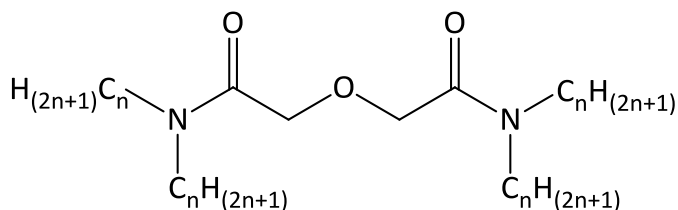
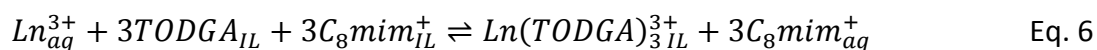
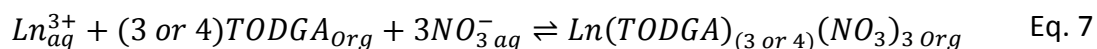


Figure 2-2 Schematic of the general chemical structure of diglycolamide (DGA).

Shimojo et al.<sup>43</sup> studied the solvent extraction of lanthanides ( $\text{Ln}^{3+}$ ) from aqueous solution by using a solution of N,N,N',N'-tetra(n-octyl)diglycolamide (TODGA) diluted in  $[\text{C}_n\text{MIM}][\text{Tf}_2\text{N}]$  ( $n=2,4,6$ ) and compared it to the isooctane system. When TODGA was used in conjunction with the RTIL, the extraction of  $\text{Ln}^{3+}$  was enhanced greatly in comparison to the isooctane system. As has been found in the previously discussed RTIL system, the transfer of  $\text{Ln}^{3+}$  into the organic phase occurred by a cation-exchange mechanism Eq. 6, which is different from the ion pair extraction mechanism as shown in Eq. 7. Also, it was found that TODGA provided selectivity for the intermediate lanthanide group in the RTIL systems, but heavier lanthanides were extracted better in the isooctane system.<sup>43</sup> When a cation-exchange mechanism occurs, the cation of the RTIL is released into the aqueous phase diluting the nitric acid solution, which largely hinders the back extraction of metal ions. This is a major drawback to their use in solvent extraction. A synergistic extraction technique has been used to overcome this disadvantage and will be discussed in the next section (2.1.5).





### 2.1.5 Supercritical Fluid-Ionic Liquid Coupled Extraction

As previously discussed sc-CO<sub>2</sub> and RTILs individually have several advantages as solvents for use in extracting actinides and lanthanides; thus, a possible synergistic effect may occur when the two solvents are coupled. In 1999, Blanchard et al.<sup>45</sup> reported that RTILs do not dissolve into the sc-CO<sub>2</sub> phase, but sc-CO<sub>2</sub> can be dissolved in RTILs effectively. By combining these two novel solvents, an effective extraction technique for recycling used nuclear fuel can be developed. The coupling of RTILs and sc-CO<sub>2</sub> for metal ion, actinide, and lanthanide extraction has been studied by the Wai group.<sup>46-49</sup> Mekki et al.<sup>46</sup> coupled sc-CO<sub>2</sub> and RTIL by using [C<sub>4</sub>MIM][Tf<sub>2</sub>N] as the RTIL and Cu<sup>2+</sup> as the metal ion to be extracted into sc-CO<sub>2</sub>. Fluorinated β-diketone and TBP were used as extractants. This was the first quantitative extraction of a metal ion from an RTIL into sc-CO<sub>2</sub>. It was found the extraction efficiency with fluorinated β-diketone and TBP were > 95%. The following year Mekki et al.<sup>47</sup> studied the extraction of lanthanides from aqueous solution by using an RTIL and sc-CO<sub>2</sub> in conjunction. This technique was successful in extracting > 87% of La<sup>3+</sup> and Eu<sup>3+</sup> with fluorinated β-diketone and TBP. Based on the reports by Mekki et al.<sup>46, 47</sup>, sc-CO<sub>2</sub> is an effective organic solvent for extracting metal species from an RTIL phase. In addition, sc-CO<sub>2</sub> may be used to effectively remove metal species to recycle the RTIL for reuse. Therefore, an innovative recycling technique including water, RTIL, and sc-CO<sub>2</sub>, may be incorporated to form a two-step extraction process. This theory was studied by Wang et al.<sup>48</sup> by extracting U(VI) from nitric acid by using RTIL and sc-CO<sub>2</sub> in conjunction. Although

this two-step extraction method is more environmentally friendly than the traditional PUREX process, aqueous waste is still being produced. A technique bypassing the dissolution of metal species, actinides, and lanthanides in acid solution would be a better method to reduce the amount of hazardous aqueous waste produced. Just recently Wai et al.<sup>49</sup> reported the dissolution of  $\text{UO}_2$  into  $[\text{C}_4\text{MIM}][\text{Tf}_2\text{N}]$  directly by using  $\text{TBP}(\text{HNO}_3)_{1.8}(\text{H}_2\text{O})_{0.6}$  and then extraction of U(VI) by  $\text{sc-CO}_2$ . The extracted species  $\text{UO}_2(\text{NO}_3)_2(\text{TBP})_2$  was identified by the two spectroscopic methods Raman and UV-Vis.

## 2.2 Conclusions

From what has been discussed previously, it is clear  $\text{sc-CO}_2$  and RTILs are excellent alternative solvents as compared to VOCs. Not only are these solvents safer for the environment, the use of these solvents in the extraction of metal ions, actinides, and lanthanides show higher efficiencies than in conventional solvent systems. Also an advantage to using  $\text{sc-CO}_2$  is that conventional stripping of RTILs is very difficult and this is a major drawback to their use in solvent extraction. This is because ionic complexes can't be back extracted simply by lowering the acidity of the aqueous phase.

Studies showed extractions using RTILs as the organic phase illustrated a cation exchange mechanism which is different from the ion-pair mechanism seen in conventional solvents. The  $\text{sc-CO}_2$  extraction of actinides and lanthanides from aqueous solutions is possible with the chelation of fluorinated  $\beta$ -diketones and phosphine oxides. This method was later extended to RTILs. The development of the direct dissolution of  $\text{UO}_2$  solid into an

RTIL and then extraction into sc-CO<sub>2</sub> shows great promise for the future of recycling used nuclear fuel. In general, there has been great progress in researching sc-CO<sub>2</sub> and RTILs with the promise of still more discoveries to be made.

## 2.3 References

1. K. R. Seddon, *Nature*, 2003, **2**, 363-365.
2. J. S. Wang, C. N. Sheaff, B. Yoon, R. S. Addleman, and C. M. Wai, *Chem. – Eur. J.*, 2009, **15**, 4458-4463.
3. C. M. Wai, Y. Liao, W. Liao, G. Tian, R. S. Addleman, D. Quach, and S. P. Pasilis, *Dalton Trans.*, 2011, **40**, 5039-5045.
4. K. E. Laintz, J. J. Yu, and C. M. Wai, *Anal. Chem.*, 1992, **64**, 311-315.
5. K. E. Laintz, C. M. Wai, C. R. Yonker, and R. D. Smith, *Anal. Chem.*, 1992, **22**, 2875-2878.
6. N. G. Smart, T. Carleson, T. Kast, A. A. Clifford, M. D. Burford, and C. M. Wai, *Talanta*, 1997, **44**, 137-150.
7. Y. Meguro, S. Iso, T. Sasaki, and Z. Yoshida, *Anal. Chem.*, 1998, **70**, 774-779.
8. N. G. Smart, T. E. Carleson, S. Elshani, S. Wang, and C. M. Wai, *Ind. Eng. Chem. Res.*, 1997, **36**, 1819-1826.
9. Y. Lin, R. D. Brauer, K. E. Laintz, and C. M. Wai, *Anal. Chem.*, 1993, **65**, 2549-2551.
10. Y. Lin, C. M. Wai, F. M. Jean, and R. D. Brauer, *Environ. Sci. Technol.*, 1994, **28**, 1190-1193.
11. Y. Lin, N. G. Smart, and C. M. Wai, *Environ. Sci. Technol.*, 1995, **29**, 2706-2711.
12. M. J. Carrott, B. E. Waller, N. G. Smart, and C. M. Wai, *Chem. Commun.*, 1998, 373-374.
13. R. S. Addleman, M. J. Carrott, and C. M. Wai, *Anal. Chem.*, 2000, **72**, 4015-4021.
14. O. Tomioka, Y. Enokida, and I. Yamaoto, *J. Nucl. Sci. Technol.*, 1998, **35**, 515-516.

15. O. Tomioka, Y. Meguro, Y. Enokida, I. Yamamoto, and Z. Yoshida, *J. Nucl. Sci. Technol.*, 2001, **38**, 1097-1102.
16. M. D. Samsonov, C. M. Wai, S. Lee, Y. Kulyako, and N. G. Smart, *Chem. Commun.*, 2001, 1868-1869.
17. T. I. Trofimov, M. D. Samsonov, S. Lee, B. F. Myasoedova, and C. M. Wai, *Mendeleev Commun.*, 2001, **11**, 129-130.
18. Y. Enokida, S. A. El-Fatah, and C. M. Wai, *Ind. Eng. Chem. Res.*, 2002, **41**, 2282-2286.
19. Y. Enokida, O. Tomioka, S. Lee, A. Rustenholtz, and C. M. Wai, *Ind. Eng. Chem. Res.*, 2003, **42**, 5037-5041.
20. M. D. Samsonov, T. I. Trofimov, S. E. Vinokurov, S. C. Lee, B. F. Myasoedov, and C. M. Wai, *J. Nucl. Sci. Technol.*, 2002, **3**, 263-266.
21. T. I. Trofimov, M. D. Samsonov, Y. M. Kulyako, and B. F. Myasoedov, *C. R. Chimie*, 2004, **7**, 1209-1213.
22. S. Iso, S. Uno, Y. Meguro, T. Sasaki, and Z. Yoshida, *Prog. Nucl. Energy*, 2000, **37**, 423-428.
23. O. Tomioka, Y. Enokida, and I. Yamamoto, *Prog. Nucl. Energy*, 2000, **37**, 417-422.
24. B. Kumar, S. M. Kumar, S. D. Sivakumar, U. K. Mudali, and R. Natarajan, *J. Radioanal. Nucl. Chem.*, 2011, **288**, 443-445.
25. K. Sujatha, K. C. Pitchaiah, N. Sivaraman, T. G. Srinivasan, P. R. Rao, and V. Rao, *Am. J. Anal. Chem.*, 2012, **3**, 916-922.
26. P. Kumar, A. Pal, M. K. Saxena, and K. L. Ramakumar, *Desalination*, 2008, **232**, 71-79.
27. A. Rao, N. V. Rathod, D. D. Malkhede, V. V. Rau, and K. L. Ramakumar, *Sep. Sci. Technol.*, 2013, **48**, 644-651.
28. L. Zhu, W. Duan, J. Xu, and Y. Zhu, *J. Hazard. Mater.*, 2012, **241-242**, 456-462.
29. W. Duan, L. Zhu, and Y. Zhu, *Prog. Nucl. Energy*, 2011, **53**, 664-667.
30. P. Walden, *Bull. Imper. Acad. Sci. (St Petersburg)*, 1914, **8**, 405-422.
31. K. Binnemans, *Chem. Rev.*, 2007, **107**, 2592-2614.
32. P. Stepnowski, *Int. J. Mol. Sci.*, 2006, **7**, 497-509.
33. J. S. Wilkes and M. J. Zaworotko, *Chem. Commun.*, 1992, **13**, 965-967.

34. S. Dai, Y. H. Ju, and C. E. Barnes, *Dalton Trans. Commun.*, 1999, **8**, 1201-1202.
35. M. L. Dietz and J. A. Dzielawa, *Chem. Commun.*, 2001, **20**, 2124-2125.
36. M. L. Dietz, J. A. Dzielawa, I. Laszak, B. A. Young, and M. P. Jensen, *Green Chem.*, 2003, **5**, 682-685.
37. P. Giridhar, K. A. Venkatesan, T. G. Srinivasan, and P. R. V. Rao, *J. Nucl. Radiochem. Sci.*, 2004, **5**, 21-26.
38. P. Giridhar, K. A. Venkatesan, T. G. Srinivasan, and P. R. V. Rao, *J. Radioanal. Nucl. Chem.*, 2005, **265**, 31-38.
39. M. L. Dietz and D. C. Stepinski, *Talanta*, 2008, **75**, 598-603.
40. Y. Sasaki, and G. R. Choppin, *Anal. Sci.*, 1996, **12**, 225-230.
41. S. A. Ansari, P. N. Pathak, V. K. Manchanda, M. Husain, A. K. Prasad, and V. S. Parmar, *Solvent Extr. Ion Exch.*, 2005, **23**, 463-479.
42. G. Modolo, H. Asp, H. Vijgen, R. Malmbeck, D. Magnusson, and C. Sorel, *Solvent Extr. Ion Exch.*, 2008, **26**, 62-76.
43. K. Shimojo, K. Kurahashi, and H. Naganawa, *Dalton Trans.*, 2008, **37**, 5083-5088.
44. M. E. Mincher, D. L. Quach, Y. J. Liao, B. J. Mincher, and C. M. Wai, *Solvent Extr. Ion Exch.*, 2012, **30**, 735-747.
45. L. A. Blanchard, D. Hancu, E. J. Beckman, and J. F. Brennecke, *Nature*, 1999, **399**, 28-29.
46. S. Mekki, C. M. Wai, I. Billard, G. Moutiers, C. H. Yen, J. S. Wang, A. Ouadi, C. Gaillard, and P. Hesemann, *Green Chem.*, 2005, **7**, 421-423.
47. S. Mekki, C. M. Wai, I. Billard, G. Moutiers, J. Burt, B. Yoon, J. S. Wang, C. Gaillard, A. Ouadi, and P. Hesemann, *Chem. Eur. J.*, 2006, **12**, 1760-1766.
48. J. S. Wang, C. N. Sheaff, B. Yoon, R. S. Addleman, and C. M. Wai, *Chem. Eur. J.*, 2009, **15**, 4458-4463.
49. C. M. Wai, Y. Liao, W. Liao, G. Tian, R. S. Addleman, D. Quach, and S. P. Pasilis, *Dalton Trans.*, 2011, **40**, 5039-5045.

## Chapter 3

# Attenuated Total Reflection-Fourier Transform Infrared and Ultraviolet-Visible Spectrometry Studies of Uranyl Coordination with Nitrate and Tri-n-butyl Phosphate in a Room Temperature Ionic Liquid\*

### 3.1 Introduction

Used nuclear fuel (UNF) should be recycled to recover unused uranium and fission and transuranic products, which would help extend the supply of uranium and to alleviate the shortage of space to store the highly radioactive waste. Although the US does not currently recycle UNF, in the past UNF was reprocessed by the PUREX method to partition uranium and plutonium, which are then reused as mixed oxide nuclear fuel, (as described in Chapter 1).<sup>1</sup> This process uses volatile organic compounds and produces radioactive aqueous and organic waste; thus a more environmentally friendly technique is desired. Currently researchers use the basic principles of the PUREX method to develop new recycling methods with the goal of minimizing the volume of toxic waste produced.<sup>2-6</sup> One innovative development in UNF recycling technology is the introduction of non-traditional

(\*Modified version of the following manuscript: *Inorg. Chem.* 2010, **49**, 8568–8572, Copyright 2010 American Chemical Society) See Appendix A for documentation of permission to republish this material.



solvents, such as RTILs and sc-CO<sub>2</sub>. These solvents are thought to be superior to conventional molecular organic solvents, due to their low volatility and capability to minimize organic waste produced, (as described in Chapter 1). In fact, a recycling method has been reported by Wai et al.<sup>5</sup> which includes the use of both RTIL and sc-CO<sub>2</sub> as solvents. In this method, uranium dioxide was dissolved directly into the RTIL 1-butyl-3-methylimidazolium bis(trifluoromethylsulfonyl)imide [C<sub>4</sub>MIM][Tf<sub>2</sub>N] using the Lewis acid-base complex TBP(HNO<sub>3</sub>)<sub>1.8</sub>(H<sub>2</sub>O)<sub>0.6</sub>. Furthermore, the extractable uranyl complex UO<sub>2</sub>(NO<sub>3</sub>)<sub>2</sub>(TBP)<sub>2</sub> is extracted into the sc-CO<sub>2</sub> phase from the RTIL solution and then recovered by depressurization into a dodecane trap solution. This RTIL-sc-CO<sub>2</sub> coupled dissolution and extraction technique demonstrates its potential use in recycling UNF.

To further develop more sustainable recycling techniques, the basic solution chemistry of actinides and lanthanides in RTILs needs to be investigated thoroughly. One of the most important and extensively studied radionuclides in nuclear fuel research is uranium. Uranium may exist in several oxidation states (Figure 1-4), but +6 is the most stable oxidation state for uranium. The hexavalent species is called uranyl (UO<sub>2</sub><sup>2+</sup>). The complex formation, coordination chemistry, electrochemistry, and extraction behavior of uranyl and its complexes in several RTILs have been studied and reported in several review papers.<sup>6-12</sup> Nitrate anions are commonly studied in relation to uranyl because nitric acid is used as the solvent in the dissolution of uranyl in the PUREX process.

The majority of researchers use extended X-ray absorption fine structure (EXAFS) and UV-Vis to identify and characterize UO<sub>2</sub><sup>2+</sup> species in RTILs. Observation of uranyl nitrate coordination in traditional organic diluents by UV-Vis spectroscopy dates back to 1956.<sup>13</sup>

The spectra observed when 0.02 M  $\text{UO}_2(\text{NO}_3)_2 \cdot 6\text{H}_2\text{O}$  was dissolved in acetone, methyl isobutyl ketone, or cyclohexanone are shown in Figure 3-1. These spectra arise from the dinitrato complex. Kaplan et al.<sup>13</sup> observed sharp and intense peaks at 426, 440, 455, and 470 nm in the spectrum when uranyl nitrate hexahydrate (0.02 M) was dissolved in acetone and then 0.02 M tetrabutylammonium nitrate (TBAN) was added (Figure 3-1). These peaks are characteristic of the trinitrato complex.

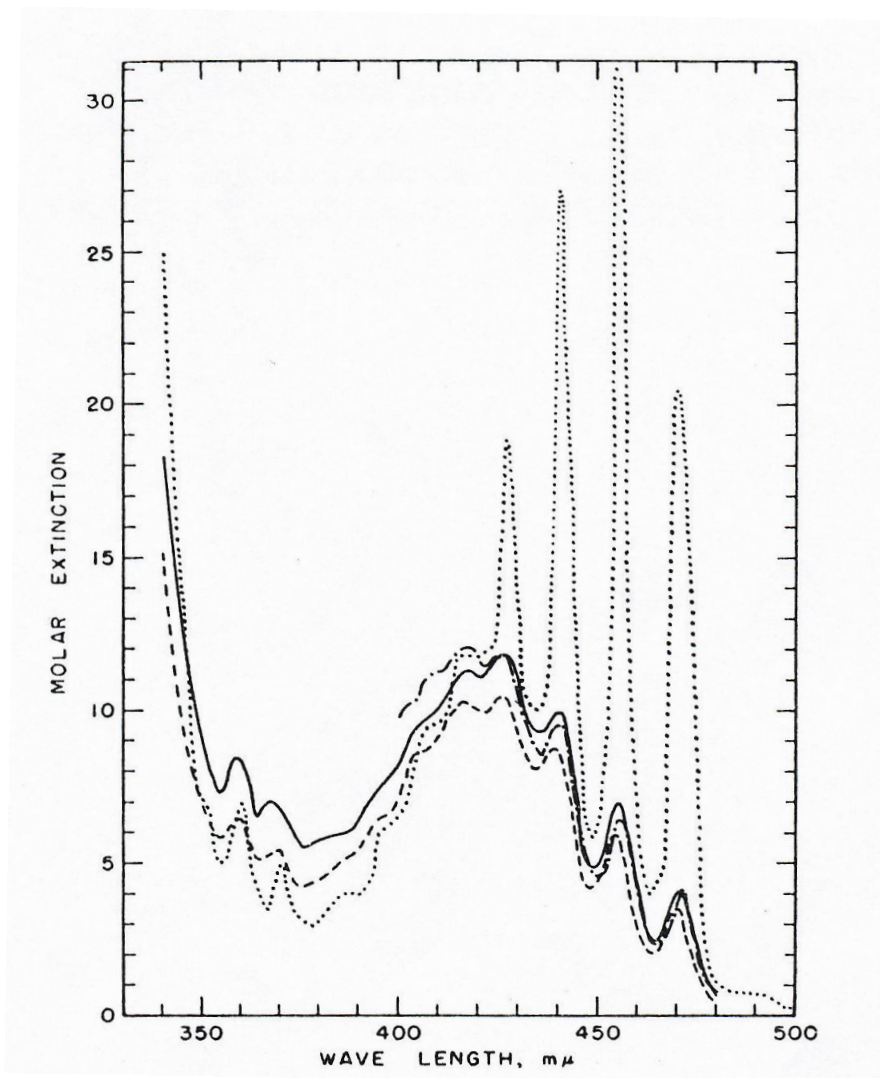


Figure 3-1 UV-Vis spectra of 0.02 M  $\text{UO}_2(\text{NO}_3)_2 \cdot 6\text{H}_2\text{O}$  dissolved in ketonic solvents. The less intense spectra acquired contain 0.02 M  $\text{UO}_2(\text{NO}_3)_2 \cdot 6\text{H}_2\text{O}$  dissolved in acetone (solid line), methyl isobutyl ketone (dashed line), and cyclohexanone (dashed-dotted line). The spectrum having the most intense peaks was acquired from a solution containing 0.02 M  $\text{UO}_2(\text{NO}_3)_2 \cdot 6\text{H}_2\text{O}$  and 0.02 M TBAN in acetone (dotted line). (Reprinted with permission from ref 13. Copyright (1956), with permission from Elsevier) See Appendix A for documentation of permission to republish this material.

Servaes and co-workers<sup>14, 15</sup> have extensively studied uranyl nitrate speciation in RTILs. The presence of the characteristic absorption bands in their spectra indicated that the trinitrato complex,  $[\text{UO}_2(\text{NO}_3)_3]^-$ , were observed in RTIL as well. To determine how the nitrate ion is coordinated to uranyl in the RTIL, X-ray absorption fine structure (EXAFS) spectroscopy was

used and provided the bond length of U=O, U-O, and U-N.<sup>14</sup> The measurement indicated that the nitrate ligand was bound to uranyl in a bidentate manner in both [C<sub>4</sub>MIM][Tf<sub>2</sub>N] and acetonitrile. In addition, different uranyl nitrate complexes form in RTIL when uranyl and nitrate are dissolved in a RTIL. The possible species, as determined using UV-vis and EXAFS are UO<sub>2</sub>(NO<sub>3</sub>)<sup>+</sup>, UO<sub>2</sub>(NO<sub>3</sub>)<sub>2</sub>, UO<sub>2</sub>(NO<sub>3</sub>)<sub>3</sub><sup>-</sup>, and UO<sub>2</sub>(NO<sub>3</sub>)<sub>4</sub><sup>2-</sup>.<sup>14-18</sup> Gaillard et al.<sup>16</sup> have suggested that UO<sub>2</sub>(NO<sub>3</sub>)<sub>2</sub> can disproportionate into UO<sub>2</sub>(NO<sub>3</sub>)<sup>+</sup> and UO<sub>2</sub>(NO<sub>3</sub>)<sub>3</sub><sup>-</sup>. However, when excess nitrate was present, the trinitrato complex formed and was confirmed with the presence of the characteristic bands in the UV-Vis absorption spectrum. Furthermore, Gaillard et al.<sup>16</sup> investigated the complexation of NO<sub>3</sub><sup>-</sup> with uranyl in the form of UO<sub>2</sub>(Tf<sub>2</sub>N)<sub>2</sub> in [C<sub>4</sub>MIM][Tf<sub>2</sub>N]. When uranyl was dissolved in [C<sub>4</sub>MIM][Tf<sub>2</sub>N], addition of nitrate easily displaced the Tf<sub>2</sub>N<sup>-</sup> anion. Thus, nitrate is a stronger complexing ligand than the Tf<sub>2</sub>N<sup>-</sup> anion.

Also, it is of interest to study TBP in the uranyl-nitrate-TBP system because it is an important extractant in the recycling of uranyl. For example, in the PUREX process, UO<sub>2</sub>(NO<sub>3</sub>)<sub>2</sub> is extracted by the ligand TBP. Healy and McKay<sup>19</sup> studied the complexation of TBP by several actinyl nitrates, including uranyl nitrate. Uranyl nitrate was dissolved in a saturated solution of TBP and formed the neutral complex UO<sub>2</sub>(NO<sub>3</sub>)<sub>2</sub> · 2TBP. Giridhar et al.<sup>20</sup> extracted uranyl nitrate using TBP diluted in dodecane and [C<sub>4</sub>MIM][PF<sub>6</sub>] and found a linear relationship between the logD and log[NO<sub>3</sub><sup>-</sup>]. Based on the slope of 1.7 and 2.1 when dodecane and [C<sub>4</sub>MIM][PF<sub>6</sub>] were used, respectively, they were able to conclude that two molecules of TBP are involved in the extraction of uranyl nitrate. In contrast to Giridhar et al.<sup>20</sup>, Murali et al.<sup>21</sup> did not observe the neutral complex in [C<sub>4</sub>MIM][PF<sub>6</sub>], but a charged species [UO<sub>2</sub>(NO<sub>3</sub>)<sub>2</sub> · 2TBP]<sup>+</sup>. The same charged species was also observed in [C<sub>4</sub>MIM][Tf<sub>2</sub>N].

In addition, Billard et al.<sup>22</sup>, did not observe the neutral complex  $\text{UO}_2(\text{NO}_3)_2 \cdot 2\text{TBP}$ , but charged complexes in  $[\text{C}_4\text{MIM}][\text{Tf}_2\text{N}]$ .

Vibrational spectroscopic and NMR techniques<sup>5, 23</sup> offer valuable information in addition to the important information absorption spectroscopy can give, such as the bond length in a complex. For example, in infrared spectroscopy, changes in the  $\text{UO}_2^{2+}$  chemical environment are easily detected by the shift in wavenumber. The anti-symmetric stretching mode of  $\text{UO}_2$  ( $\nu_{\text{as}}(\text{UO}_2)$ ) is infrared active and the symmetric stretching mode of  $\text{UO}_2$  ( $\nu_{\text{s}}(\text{UO}_2)$ ) is Raman active. Both modes are sensitive to changes in the uranyl coordination environment. It is known that complexation of uranyl by a ligand causes the O=U=O bond to weaken, thus shifting the  $\nu_{\text{as}}(\text{UO}_2^{2+})$  band to a lower wavenumber.<sup>24</sup> The magnitude of the shift depends on the strength of the complex formed. This shift can be tracked to systematically study the complexes formed between uranyl and nitrate species in solution. Wai et al.<sup>5</sup> used Raman spectroscopy to study the  $[\text{UO}_2(\text{NO}_3)_x(\text{TBP})_2]^{2-x}$  ( $x= 1-3$ ) complex in  $[\text{C}_4\text{MIM}][\text{Tf}_2\text{N}]$  and  $\text{sc-CO}_2$ . The addition of extractants affected the coordination chemistry of the uranyl nitrate system in RTILs. For example, when 0.34 M TBP was added to 0.17 M  $\text{UO}_2(\text{NO}_3)_2 \cdot 6\text{H}_2\text{O}$  in  $[\text{C}_4\text{MIM}][\text{Tf}_2\text{N}]$ , the coordination environment was disturbed, thus the  $\nu_{\text{s}}(\text{UO}_2^{2+})$  shifted from 868 to 860  $\text{cm}^{-1}$ . Furthermore, when 0.2 M TBP was added to 0.1 M  $\text{UO}_2^{2+}$ , the complex formed in  $[\text{C}_4\text{MIM}][\text{Tf}_2\text{N}]$  was confirmed by the position of the  $\nu_{\text{s}}(\text{UO}_2^{2+})$  mode. When the molar ratio of  $\text{UO}_2^{2+}:\text{TBP}$  was greater than 2 the  $\nu_{\text{s}}(\text{UO}_2^{2+})$  mode appeared at 860  $\text{cm}^{-1}$ . The position of the mode was the same as discussed above, when the molar ratio of uranyl nitrate:TBP was 1:2. Thus, it was postulated the  $\text{UO}_2(\text{NO}_3)_2 \cdot 2\text{TBP}$  complex was likely formed in  $[\text{C}_4\text{MIM}][\text{Tf}_2\text{N}]$ , due to the fact that neutral complexes are

extracted into the sc-CO<sub>2</sub> phase. Pasilis and Blumenfeld<sup>23</sup> investigated the speciation of uranyl with three different ligands: nitrate, water, and perchlorate in the RTIL 1-ethyl-3-methylimidazolium bis(trifluoromethylsulfonyl)imide ([C<sub>2</sub>MIM][Tf<sub>2</sub>N]) using Raman, FTIR, and <sup>2</sup>H and <sup>17</sup>O NMR spectroscopies. It was found that water and perchlorate in the first coordination sphere were easily displaced by nitrate; however, the ligands water and perchlorate are present in the outer coordination sphere in [C<sub>2</sub>MIM][Tf<sub>2</sub>N]. In this current work, we use UV-Vis and ATR-FTIR to investigate the effect of nitrate and TBP on uranyl speciation in the RTIL ([C<sub>4</sub>MIM][Tf<sub>2</sub>N]).

## 3.2 Experimental

### 3.2.1 Chemicals and reagents

Uranium trioxide, UO<sub>3</sub>, and uranyl nitrate hexahydrate, UO<sub>2</sub>(NO<sub>3</sub>)<sub>2</sub> · 6H<sub>2</sub>O, were purchased from Internal Bio-Analytical Industries, Inc. (Boca Raton, FL). Concentrated nitric acid (70% w/w), tri-n-butylphosphate (TBP), 1-butyl-3-methylimidazolium chloride, [C<sub>4</sub>MIM]Cl, tetrabutylammonium nitrate (TBAN), and bis(trifluoromethane) sulfonimide lithium salt, [LiN(CF<sub>3</sub>SO<sub>2</sub>)<sub>2</sub>], were purchased from Sigma-Aldrich (Milwaukee, WI). Acetonitrile and methylene chloride were purchased from Fisher Scientific (Pittsburg, PA). Toluene was purchased from EMD Chemicals Inc (Gibbstown, NJ). Deuterated chloroform was purchased from Cambridge Isotope Laboratory, Inc (Andover, MA).

### 3.2.2 Instruments

A Bruker 300 MHz NMR spectrometer was used to check the purity of [C<sub>4</sub>MIM][Tf<sub>2</sub>N] after synthesis. Other NMR spectra were acquired using a Bruker 500 MHz NMR spectrometer. ATR-FTIR spectra were acquired using a Nicolet Magna 760 FTIR spectrometer equipped with a DTGS detector. ATR-FTIR measurements were made with a Diamond Splitpea™ attenuated total reflection accessory (Harrick Scientific Corporation). A silicon ATR crystal element was used as a reflectance medium. Absorption spectra were acquired using a Model 440 UV/vis spectrophotometer with a CCD (charge coupled device) array detector (Spectral Instruments Inc., Tucson AZ).

### 3.2.3 Synthesis of 1-butyl-3-methylimidazolium bis(trifluoromethylsulfonyl)imide [C<sub>4</sub>MIM][Tf<sub>2</sub>N]

[C<sub>4</sub>MIM][Tf<sub>2</sub>N] was synthesized from the metathesis of [C<sub>4</sub>MIM]Cl and [LiN(CF<sub>3</sub>SO<sub>2</sub>)<sub>2</sub>] following an established literature procedure.<sup>25</sup> The resulting ionic liquid was washed and extracted with dichloromethane and deionized water. The excess dichloromethane was removed by evaporation under reduced pressure using a rotary evaporator. The sample was left under high vacuum overnight at 68°C to remove excess water. The purity of the ionic liquid was evaluated using <sup>1</sup>H NMR. The concentration of water in the final product was 10 mM.

### 3.2.4 Synthesis of uranyl bis(trifluoromethylsulfonyl)imide [UO<sub>2</sub>(Tf<sub>2</sub>N)<sub>2</sub>]

Uranyl bis(trifluoromethylsulfonyl)imide (UO<sub>2</sub>(Tf<sub>2</sub>N)<sub>2</sub> · xH<sub>2</sub>O) was synthesized according to the method of Nockeman et al.<sup>15</sup> The synthesis of uranyl

bis(trifluoromethylsulfonyl)imide began with the conversion of 2 M lithium bis(trifluoromethylsulfonyl)imide into the corresponding acid,  $\text{H}(\text{Tf}_2\text{N})$  with the addition of excess 20%  $\text{H}_2\text{SO}_4$ . In the process of converting the salt into an acid, lithium sulfate was produced. The desired acid was extracted with diethyl ether and washed with water to remove trace amounts of lithium sulfate. Evaporation of diethyl ether under reduced pressure gave  $\text{H}(\text{Tf}_2\text{N})$ . In the next step, uranium (VI) oxide (0.023 mol) was suspended in water, and a small excess of  $\text{H}(\text{Tf}_2\text{N})$  (0.033 mol) was added to a round bottom flask. This mixture was allowed to react for 3 days at  $50^\circ\text{C}$  with stirring, and then the temperature was increased to  $75^\circ\text{C}$  to react for an additional 24 hours. Water was removed under reduced pressure to give a viscous yellow substance. This product was then washed with dichloromethane to remove non-reacted  $\text{H}(\text{Tf}_2\text{N})$ . The desired product was then dissolved in methanol and stirred for 1 hour. Non-reacted  $\text{UO}_3$  was filtered off to give a clear yellow solution, which upon evaporation under reduced pressure of methanol resulted in a viscous dark yellow substance. The product was left under reduced pressure to further remove excess solvent. The final product was stored in a desiccator. The water content was analyzed by Karl Fischer titration. The synthesized  $\text{UO}_2(\text{Tf}_2\text{N})_2 \cdot x\text{H}_2\text{O}$  was estimated to have three  $\text{H}_2\text{O}$  molecules coordinated to uranyl according to Liao.<sup>26</sup>

### 3.2.5 Sample preparation

For ATR-FTIR measurements, samples were prepared by dissolving uranyl nitrate hexahydrate and uranyl bis(trifluoromethylsulfonyl)imide in  $[\text{C}_4\text{MIM}][\text{Tf}_2\text{N}]$  to a final concentration of 0.1 M. Nitrate was added in the form of TBAN or concentrated  $\text{HNO}_3$ , which ranged from 0.05-0.5 M in  $[\text{C}_4\text{MIM}][\text{Tf}_2\text{N}]$ . The samples were sonicated to completely



homogenize all solutes in the ionic liquid. A small drop of sample was placed directly on the Si ATR crystal element prior to analysis by ATR-FTIR.

### **3.3 Results and Discussion**

#### **3.3.1 Coordination study of uranyl nitrate complexes formed in [C<sub>4</sub>MIM][Tf<sub>2</sub>N]**

In this study, ATR-FTIR is used to attempt to identify the different uranyl nitrate species present in [C<sub>4</sub>MIM][Tf<sub>2</sub>N]. In the recycling of UNF, nitric acid is used in the dissolution of the UNF. Thus, it is of interest to study the coordination of uranyl with nitric acid as the nitrate source. The spectra acquired from solutions containing UO<sub>2</sub>(Tf<sub>2</sub>N)<sub>2</sub> and varying amounts of HNO<sub>3</sub> in [C<sub>4</sub>MIM][Tf<sub>2</sub>N] are shown in Figure 3-2 a-d.

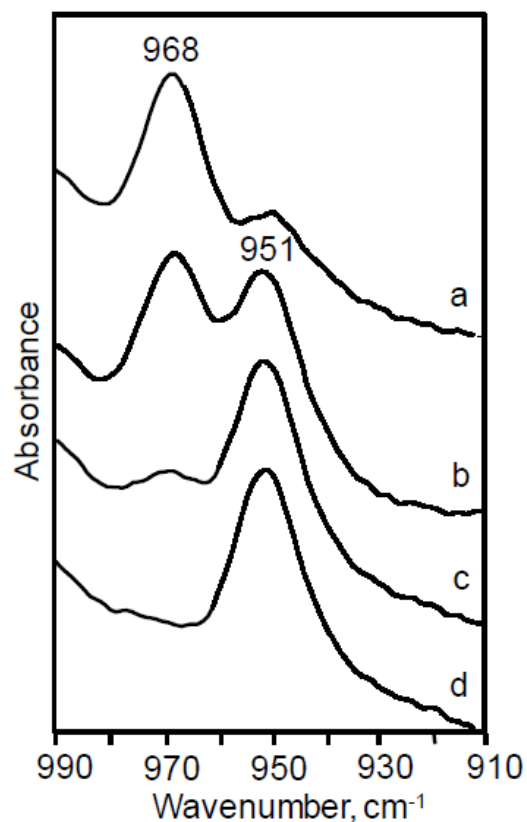


Figure 3-2 ATR-FTIR spectra showing the  $\nu_{as}(\text{UO}_2^{2+})$  region for solutions of 0.1 M  $\text{UO}_2(\text{Tf}_2\text{N})_2$  in  $[\text{C}_4\text{MIM}][\text{Tf}_2\text{N}]$  containing a) no  $\text{HNO}_3$ , b) 0.1 M  $\text{HNO}_3$ , c) 0.2 M  $\text{HNO}_3$ , and d) 0.3 M  $\text{HNO}_3$ . (\*Reprinted with permission).

When 0.1 M  $\text{UO}_2(\text{Tf}_2\text{N})_2$  was dissolved in  $[\text{C}_4\text{MIM}][\text{Tf}_2\text{N}]$  without the addition of  $\text{HNO}_3$ , the  $\nu_{as}(\text{UO}_2^{2+})$  band appeared at  $968 \text{ cm}^{-1}$  (Figure 3-2 a). This band can be assigned to  $\text{UO}_2(\text{Tf}_2\text{N})_2$ , since there is no other competing anion present to complex with uranyl. A small band at a lower wavenumber is a vibrational mode arising from the  $[\text{C}_4\text{MIM}][\text{Tf}_2\text{N}]$ . When the uranyl to nitrate molar ratio is 1:1, the  $\nu_{as}(\text{UO}_2^{2+})$  band at  $968 \text{ cm}^{-1}$  decreases in intensity and a new band at  $951 \text{ cm}^{-1}$  starts to grow in (Figure 3-2 b). Since nitrate has been introduced into the  $\text{UO}_2(\text{Tf}_2\text{N})_2$  and  $[\text{C}_4\text{MIM}][\text{Tf}_2\text{N}]$  system, the anion  $\text{Tf}_2\text{N}^-$  complexed to uranyl is now displaced by the stronger complexing ligand nitrate. The  $\text{UO}_2(\text{NO}_3)^+$  band at

956  $\text{cm}^{-1}$  was reported by Liao<sup>26</sup> when the uranyl to nitrate molar ratio was 1:1 in the RTIL, 1-octyl-3-methylimidazolium bis(trifluoromethylsulfonyl)imide ( $[\text{C}_8\text{MIM}][\text{Tf}_2\text{N}]$ ). Also the  $\text{UO}_2(\text{NO}_3)^+$  species was reported as the major species when the molar ratio of uranyl to nitrate is 1:1 in the  $\text{UO}_2(\text{Tf}_2\text{N})_2$  and  $[\text{C}_4\text{MIM}][\text{NO}_3]$  system.<sup>17</sup> However, in the  $\text{UO}_2(\text{Tf}_2\text{N})_2$  and  $[\text{C}_4\text{MIM}][\text{Tf}_2\text{N}]$  system the  $\text{UO}_2(\text{NO}_3)^+$  species is not observed. This may be due to the overlapping of the  $\text{UO}_2^{2+}$  mode of the  $\text{UO}_2(\text{NO}_3)^+$  species and a vibrational mode arising from  $[\text{C}_4\text{MIM}][\text{Tf}_2\text{N}]$  because the observation of the  $\text{UO}_2(\text{NO}_3)^+$  species was detected when dissolved in  $[\text{OMIM}][\text{Tf}_2\text{N}]$  and  $[\text{C}_4\text{MIM}][\text{NO}_3]$ . As the nitric acid concentration is increased so that the molar ratio of uranyl to nitrate is 1:2, the band at 968  $\text{cm}^{-1}$  disappears and the band at 951  $\text{cm}^{-1}$  becomes more intense (Figure 3-2 c). This  $\nu_{\text{as}}(\text{UO}_2^{2+})$  band can be assigned to the neutral  $\text{UO}_2(\text{NO}_3)_2$  species. Increasing the concentration of nitric acid did not cause the  $\nu_{\text{as}}(\text{UO}_2^{2+})$  band to shift beyond 951  $\text{cm}^{-1}$  (Figure 3-2d). Examining the  $\nu(\text{NO})$  mode at 1537  $\text{cm}^{-1}$  (Figure 3-3) indicates the band appears to grow in intensity as the nitrate concentration increases. This growth in intensity represents uranyl and nitrate complexation.

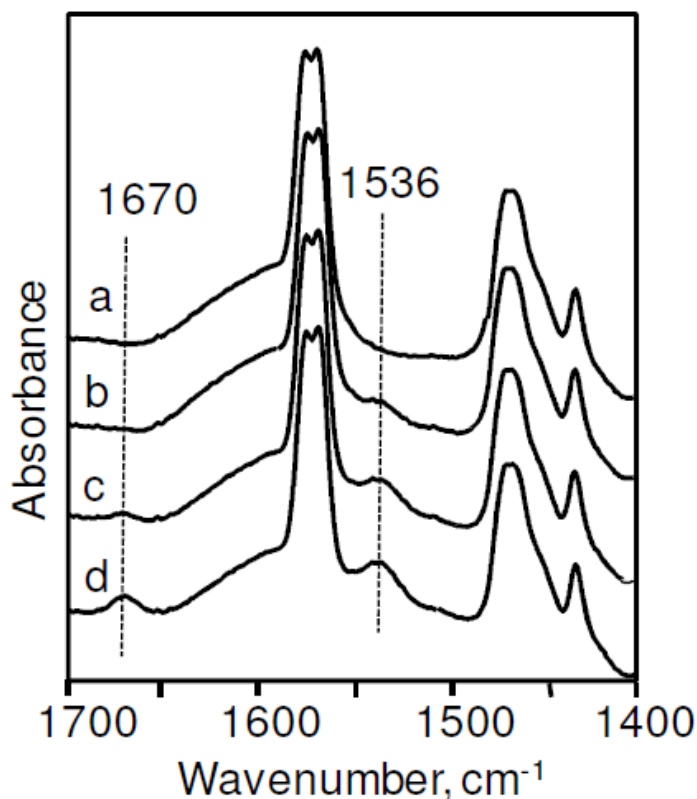


Figure 3-3 ATR-FTIR spectra showing the  $\nu(\text{NO})$  region for solutions of 0.1 M  $\text{UO}_2(\text{Tf}_2\text{N})_2$  in  $[\text{C}_4\text{MIM}][\text{Tf}_2\text{N}]$  containing a) no  $\text{HNO}_3$ , b) 0.1 M  $\text{HNO}_3$ , c) 0.2 M  $\text{HNO}_3$ , and d) 0.3 M  $\text{HNO}_3$ . (\*Reprinted with permission).

Previous work by Servaes et al.<sup>14</sup> and Georg et al.<sup>17</sup> found that when excess amounts of nitrate are present in RTIL solutions,  $\text{UO}_2(\text{NO}_3)_3^-$  can be detected using UV-Vis absorption spectroscopy and bond lengths can be determined using EXAFS. In our study, absorption spectroscopy was used to aid in identifying uranyl nitrate species, because absorption spectroscopy is more sensitive than FTIR. When the absorption spectra are examined (Figure 3-4), the characteristic peaks appear at 423, 437, 451, and 467 nm when excess amounts of nitrate (as nitric acid) are present, indicating that  $\text{UO}_2(\text{NO}_3)_3^-$  is present. However, the peaks are not as intense as they would be if a significant amount of

$\text{UO}_2(\text{NO}_3)_3^-$  was present in solution. Thus, we can say  $\text{UO}_2(\text{NO}_3)_3^-$  is present in only very low concentrations, which means the presence of a competing ligand does not allow the third nitrate to coordinate in a bidentate form around the uranyl ion.

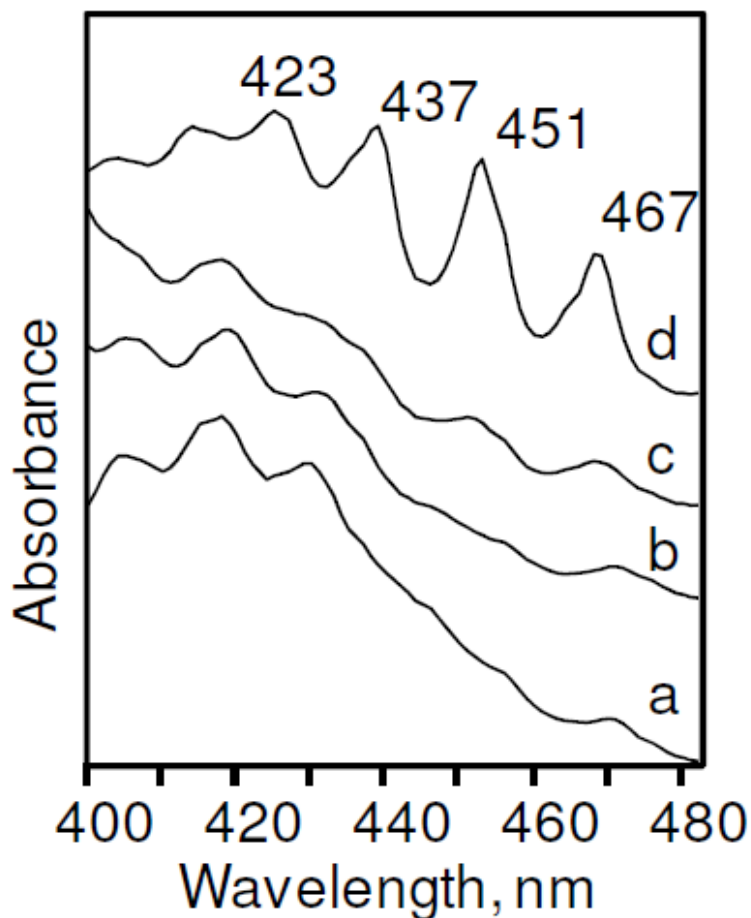


Figure 3-4 UV/visible absorption spectra of solutions of 0.1 M  $\text{UO}_2(\text{Tf}_2\text{N})_2$  in  $[\text{C}_4\text{MIM}][\text{Tf}_2\text{N}]$  containing a) no  $\text{HNO}_3$ , b) 0.2 M  $\text{HNO}_3$ , c) 0.3 M  $\text{HNO}_3$ , and d) 0.4 M  $\text{HNO}_3$ . (\*Reprinted with permission).

In this study, water is introduced into the  $\text{UO}_2(\text{Tf}_2\text{N})_2$  and  $[\text{C}_4\text{MIM}][\text{Tf}_2\text{N}]$  system, because 70% w/w nitric acid is used as the nitrate source. As each aliquot of 0.1 M  $\text{HNO}_3$  is added, the water content in  $[\text{C}_4\text{MIM}][\text{Tf}_2\text{N}]$  solution increases. The water saturation point in  $[\text{C}_4\text{MIM}][\text{Tf}_2\text{N}]$  is  $\sim 0.9$  M.<sup>22</sup> When 0.3 M  $\text{HNO}_3$  and 0.1 M  $\text{UO}_2(\text{Tf}_2\text{N})_2 \cdot 3\text{H}_2\text{O}$  are added to the

[C<sub>4</sub>MIM][Tf<sub>2</sub>N] solution the [H<sub>2</sub>O] is ~0.8 M, which is near the saturation point. Kaplan<sup>13</sup> and Billard et al.<sup>27</sup> showed that the trinitrato complex is affected by the presence of water in acetone and [C<sub>4</sub>MIM][Tf<sub>2</sub>N], respectively. Kaplan et al.<sup>13</sup> added 10% and 20% H<sub>2</sub>O to anhydrous acetone solution containing 0.02 M UO<sub>2</sub>(NO<sub>3</sub>)<sub>2</sub> · 6H<sub>2</sub>O and 0.02 M TBAN and then collected the UV-Vis spectra of these solutions. The change in intensity of the 470 nm peak was monitored. The 470 nm peak decreased in intensity with the addition of 10 % and 20 % H<sub>2</sub>O. Billard et al.<sup>27</sup> collected the UV-Vis spectra of UO<sub>2</sub><sup>2+</sup> dissolved in [C<sub>4</sub>MIM][Tf<sub>2</sub>N], which contained about 0.237, 0.6 and > 0.95 M H<sub>2</sub>O. In these experiments, the 423, 436, 451, and 466 nm absorption bands decreased in intensity with each addition of H<sub>2</sub>O. Both Kaplan<sup>13</sup> and Billard et al.<sup>27</sup> suggested that nitrate ions and water molecules compete for a coordination position around the uranyl ion. However, Pasilis and Blumenfeld<sup>23</sup> investigated uranyl speciation with several ligands including nitrate and water using FTIR and <sup>2</sup>H NMR. The uranyl perchlorate hexahydrate contributed 0.6 M H<sub>2</sub>O to the RTIL solutions. The growth of new ν<sub>as</sub>HOH and ν<sub>s</sub>HOH bands and chemical shifts in <sup>2</sup>H NMR indicated that water could be displaced by nitrate. The key difference between the coordination study by Billard et al.<sup>27</sup> and Pasilis and Blumenfeld<sup>23</sup> is that nitrate was in large excess (U:NO<sub>3</sub><sup>-</sup> was 1:12) in the study by Billard et al.<sup>27</sup>; whereas, nitrate was not in large excess in the study by Pasilis and Blumenfeld<sup>23</sup> (U:NO<sub>3</sub><sup>-</sup> was 1:4). The spatial arrangement of nitrate and water molecules is not clear. In this HNO<sub>3</sub>/[C<sub>4</sub>MIM][Tf<sub>2</sub>N] study, the trinitrato species does not form in a great abundance, because of the high water content. Although we have assigned uranyl nitrate complexes to a particular ν<sub>as</sub>(UO<sub>2</sub><sup>2+</sup>) vibrational band, it

should be mentioned that other uranyl nitrate species may be present. The band assigned to a certain uranyl nitrate complex is the most dominant species detected.

In the interest of detecting the  $\text{UO}_2(\text{NO}_3)_3^-$  species in  $[\text{C}_4\text{MIM}][\text{Tf}_2\text{N}]$  using FTIR, TBAN was utilized as the nitrate source. The introduction of excess water to the system can be minimized since TBAN is a salt. The speciation of uranyl nitrate can be tracked by systematically varying the uranyl to nitrate molar ratio and then acquiring the FTIR spectrum of each solution, as was done for the uranyl/ $\text{HNO}_3$  system. The spectra are shown in Figure 3-5 a-d.

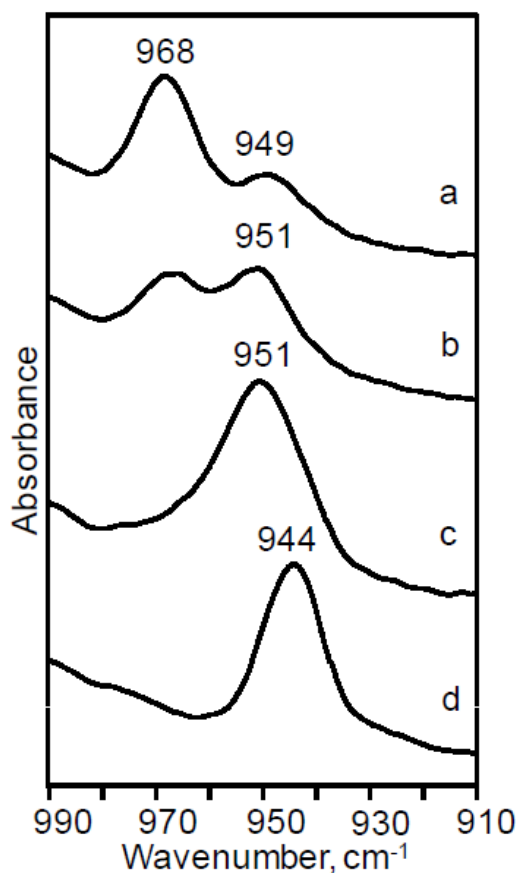


Figure 3-5 ATR-FTIR spectra showing the  $\nu_{\text{as}}(\text{UO}_2^{2+})$  region for solutions of 0.1 M  $\text{UO}_2(\text{Tf}_2\text{N})_2$  in  $[\text{C}_4\text{MIM}][\text{Tf}_2\text{N}]$  containing a) no TBAN, b) 0.1 M TBAN, c) 0.2 M TBAN, and d) 0.3 M TBAN. (\*Reprinted with permission).

When  $\text{UO}_2(\text{Tf}_2\text{N})_2$  is dissolved in  $[\text{C}_4\text{MIM}][\text{Tf}_2\text{N}]$ , the  $\nu_{\text{as}}(\text{UO}_2^{2+})$  band appears at  $968\text{ cm}^{-1}$  and is assigned to the  $\text{UO}_2^{2+}$  ion that is coordinated to the  $\text{Tf}_2\text{N}$  anion as previously discussed (Figure 3-5 a). Also, a small band appears at  $949\text{ cm}^{-1}$  and is attributed to  $[\text{C}_4\text{MIM}][\text{Tf}_2\text{N}]$ . With the addition of 0.1 M TBAN, the  $\nu_{\text{as}}(\text{UO}_2^{2+})$  mode at  $968\text{ cm}^{-1}$  decreases in intensity and a new  $\nu_{\text{as}}(\text{UO}_2^{2+})$  band at  $951\text{ cm}^{-1}$  grows in (Figure 3-5 b). Based on the position of the mode, the  $\text{UO}_2(\text{NO}_3)_2$  species is present. Once again no band appears at  $956\text{ cm}^{-1}$ , thus the  $\text{UO}_2(\text{NO}_3)^+$  species is not detected. When the total nitrate concentration is increased to 0.2 M the mode at  $968\text{ cm}^{-1}$  disappears and the  $\nu_{\text{as}}(\text{UO}_2^{2+})$



mode at  $951\text{ cm}^{-1}$  becomes more intense (Figure 3-5 c). The band can be assigned to the dinitrato complex  $\text{UO}_2(\text{NO}_3)_2$ . With the continual addition of TBAN to a total concentration of  $0.3\text{ M}$ , the  $\nu_{\text{as}}(\text{UO}_2^{2+})$  shifts to  $944\text{ cm}^{-1}$  (Figure 3-5 d). As previously discussed, this band may be assigned to the  $\text{UO}_2(\text{NO}_3)_3^-$  complex. The growth in the  $\nu(\text{NO})$  mode at  $1536\text{ cm}^{-1}$  (Figure 3-6) as nitrate concentration increases again indicates nitrate is coordinated to uranyl.

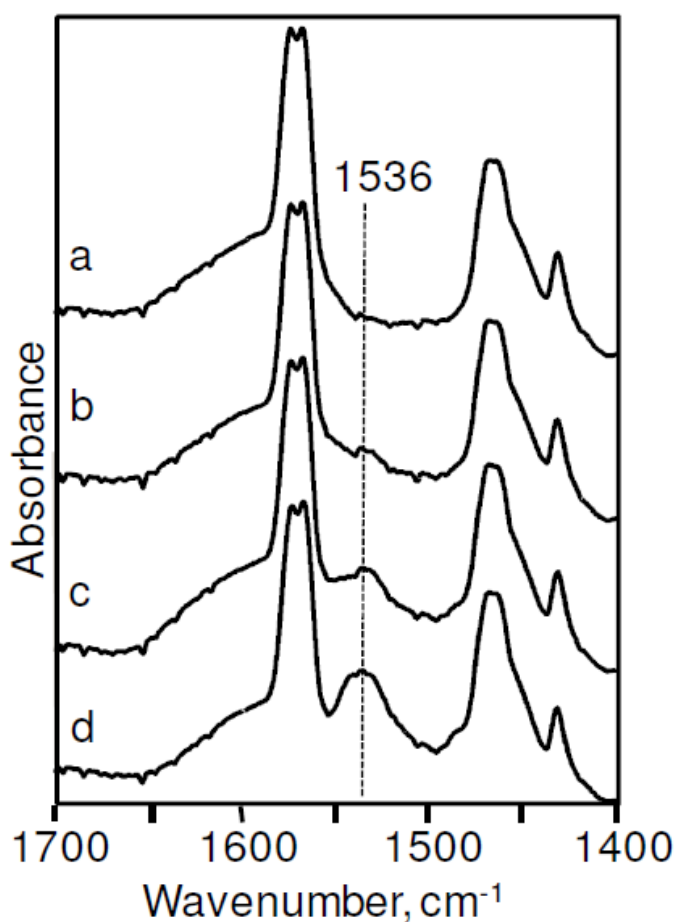


Figure 3-6 ATR-FTIR spectra showing the  $\nu(\text{NO})$  region for solutions of  $0.1\text{ M UO}_2(\text{Tf}_2\text{N})_2$  in  $[\text{C}_4\text{MIM}][\text{Tf}_2\text{N}]$  containing a) no TBAN, b)  $0.1\text{ M TBAN}$ , c)  $0.2\text{ M TBAN}$ , and d)  $0.3\text{ M TBAN}$ . (\*Reprinted with permission).

The same solutions used to acquire the ATR-FTIR spectra were analyzed using UV-Vis absorption spectroscopy. The spectra are shown in Figure 3-7. Characteristic bands at 424, 438, 450, 466 nm were seen when a molar excess nitrate was present.

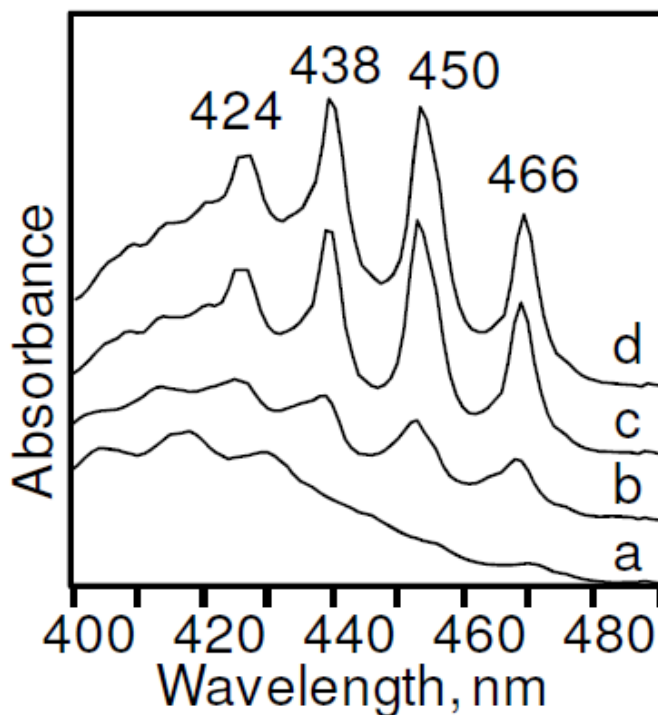


Figure 3-7 UV/visible absorption spectra of solutions of 0.1 M  $[\text{UO}_2(\text{Tf}_2\text{N})_2]$  in  $[\text{C}_4\text{MIM}][\text{Tf}_2\text{N}]$  containing a) no TBAN, b) 0.2 M TBAN, c) 0.3 M TBAN, and d) 0.4 M TBAN. (\*Reprinted with permission).

Even at lower nitrate concentrations the characteristic bands are present, although they are less intense. In comparison to Figure 3-4, the characteristic bands are more prominent in Figure 3-7, meaning the concentration of the trinitrato complex is greater in the TBAN system than in the  $\text{HNO}_3$  system. Also, the  $\nu_{\text{as}}(\text{UO}_2)$  bands are relatively broad, leading to the possibility that a mixture of uranyl nitrate species co-exist in the  $[\text{C}_4\text{MIM}][\text{Tf}_2\text{N}]$  solution.

Using TBAN as the nitrate source, both the  $\text{UO}_2(\text{NO}_3)_2$  and  $\text{UO}_2(\text{NO}_3)_3^-$  species were detected by FTIR.

### 3.3.2 Coordination study of uranyl-nitrate TBP complexes formed in $[\text{C}_4\text{MIM}][\text{Tf}_2\text{N}]$

It is of interest to characterize the uranyl-nitrate TBP complex formed in  $[\text{C}_4\text{MIM}][\text{Tf}_2\text{N}]$  because the  $\text{UO}_2(\text{NO}_3)_2$  and  $\text{UO}_2(\text{NO}_3)_3^-$  complexes are not extractable into  $\text{sc-CO}_2$ . Therefore, a complexing agent with high solubility in  $\text{sc-CO}_2$  is required to recover uranium. Alkyl phosphates and phosphine oxides form complexes with uranyl and nitrate and are soluble in  $\text{sc-CO}_2$ .<sup>28, 29</sup> TBP is a highly  $\text{sc-CO}_2$  soluble ligand and as discussed in Chapter 1, it is a well-known complexing agent used in the PUREX process. Thus in this section, the complex formed when TBP is introduced into solutions containing the di- and trinitrato complexes is studied by FTIR and UV-Vis. Figure 3-8 shows a graph showing the shift of  $\nu_{\text{as}}(\text{UO}_2^{2+})$  as the TBP concentration increases. Two trends are seen as the TBP concentration increases.

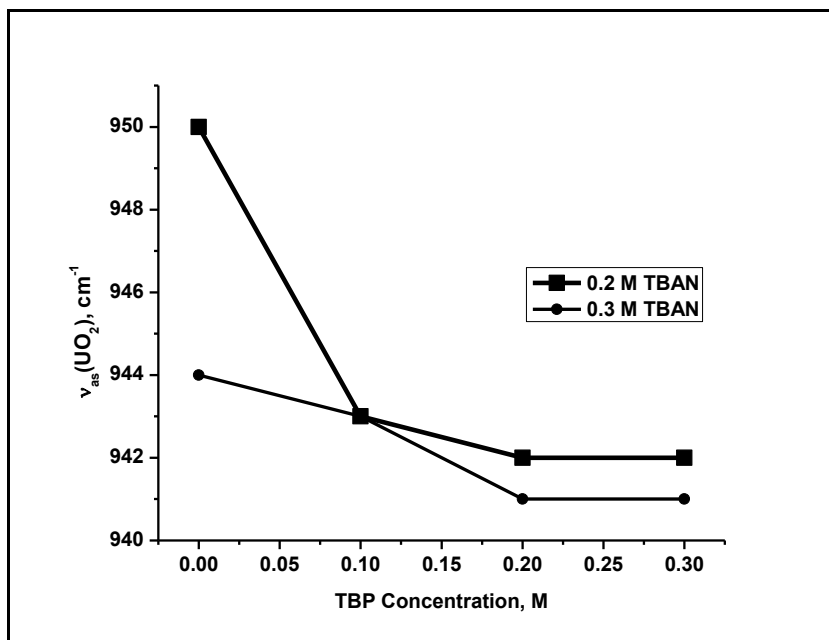


Figure 3-8 Graph showing the shift in  $v_{as}(\text{UO}_2^{2+})$  mode for solutions of 0.1 M  $\text{UO}_2(\text{Tf}_2\text{N})_2$  in  $[\text{C}_4\text{MIM}][\text{Tf}_2\text{N}]$  containing 0.2 M TBAN or 0.3 M TBAN upon the addition of 0.1 M TBP, 0.2 M TBP, and 0.3 M TBP.

When no TBP is present in solution, the  $v_{as}(\text{UO}_2^{2+})$  band lies at  $950 \text{ cm}^{-1}$  where the  $\text{UO}_2(\text{NO}_3)_2$  species is the most dominant species present in the  $[\text{C}_4\text{MIM}][\text{Tf}_2\text{N}]$  solution and at  $944 \text{ cm}^{-1}$  where the  $\text{UO}_2(\text{NO}_3)_3^-$  species is the predominant species present. Addition of 0.1 M TBP to a solution containing  $\text{UO}_2(\text{NO}_3)_2$  causes the  $v_{as}(\text{UO}_2^{2+})$  band to shift to  $943 \text{ cm}^{-1}$ , indicating weakening of the  $\text{O}=\text{U}=\text{O}$  bonds. Another 0.1 M aliquot of TBP was added to the  $[\text{C}_4\text{MIM}][\text{Tf}_2\text{N}]$  solution causing the  $v_{as}(\text{UO}_2^{2+})$  band shift to  $942 \text{ cm}^{-1}$ . Additional TBP did not cause the  $v_{as}(\text{UO}_2^{2+})$  band to shift any further. When 0.1 M TBP was added to the  $[\text{C}_4\text{MIM}][\text{Tf}_2\text{N}]$  solution containing the  $\text{UO}_2(\text{NO}_3)_3^-$  species, the  $v_{as}(\text{UO}_2^{2+})$  band shifts slightly from  $944 \text{ cm}^{-1}$  to  $943 \text{ cm}^{-1}$ . When the TBP concentration was increased to a total concentration of 0.2 M, the  $v_{as}(\text{UO}_2^{2+})$  band shifted to  $941 \text{ cm}^{-1}$ . Addition of an excess amount of TBP did not cause the  $v_{as}(\text{UO}_2^{2+})$  band to shift any further. This FTIR data

suggests that TBP is coordinated to uranyl ion in  $[\text{C}_4\text{MIM}][\text{Tf}_2\text{N}]$ ; however, the number of TBP molecules coordinated to uranyl in  $[\text{C}_4\text{MIM}][\text{Tf}_2\text{N}]$  solution is not clear. Also, the number of nitrate ions coordinated to uranyl in  $[\text{C}_4\text{MIM}][\text{Tf}_2\text{N}]$  solution is not known. Even though the starting uranyl nitrate complexes were different, there was no further shift in either case after the TBP concentration reached 0.2 M. A Raman study by Wai et al.<sup>5</sup> showed that the  $\nu_s(\text{UO}_2^{2+})$  mode shifted from 870 to 860  $\text{cm}^{-1}$ , when the molar ratios of  $\text{UO}_2^{2+}:\text{TBP}$  increased from 1:0.25 to 1:2 in  $[\text{C}_4\text{MIM}][\text{Tf}_2\text{N}]$ . The  $\nu_s(\text{UO}_2^{2+})$  mode did not shift further when an additional 0.1 M TBP was added to the  $[\text{C}_4\text{MIM}][\text{Tf}_2\text{N}]$  solution. It was concluded that two molecules of TBP was coordinated to  $\text{UO}_2^{2+}$  in  $[\text{C}_4\text{MIM}][\text{Tf}_2\text{N}]$ .<sup>5</sup> The  $\nu(\text{NO})$  band at 1536  $\text{cm}^{-1}$  decreases in intensity as shown in Figure 3-9, which is indicative of  $\text{NO}_3^-$  being displaced, due to the addition of TBP.

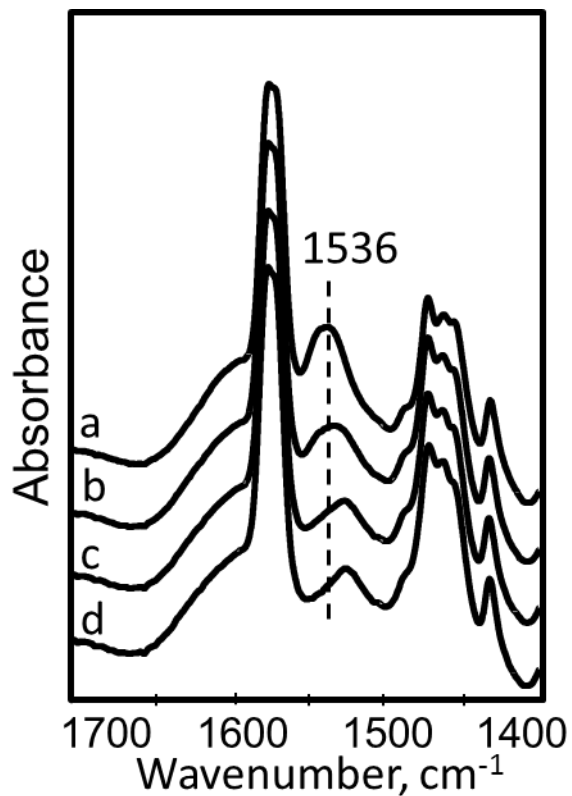


Figure 3-9 ATR-FTIR spectra showing the  $\nu(\text{NO})$  region for solutions of 0.1 M  $\text{UO}_2(\text{Tf}_2\text{N})_2$  and 0.3 M TBAN in  $[\text{C}_4\text{MIM}][\text{Tf}_2\text{N}]$  containing a) no TBP, b) 0.1 M TBP, c) 0.2 M TBP, and d) 0.3 M TBP.

Absorption spectroscopy was used for further clarification. Figure 3-10 a shows the spectrum of  $\text{UO}_2(\text{Tf}_2\text{N})_2$  dissolved in  $[\text{C}_4\text{MIM}][\text{Tf}_2\text{N}]$ . Figure 3-10 b shows the spectrum of  $\text{UO}_2(\text{Tf}_2\text{N})_2$  dissolved in a solution of  $[\text{C}_4\text{MIM}][\text{Tf}_2\text{N}]$  containing only 0.1 M TBP. Figure 3-10 c-f shows the UV-vis spectra of the  $[\text{C}_4\text{MIM}][\text{Tf}_2\text{N}]$  solution when 0.1 M TBP aliquots were added to a solution containing the  $\text{UO}_2(\text{NO}_3)_3^-$  species.

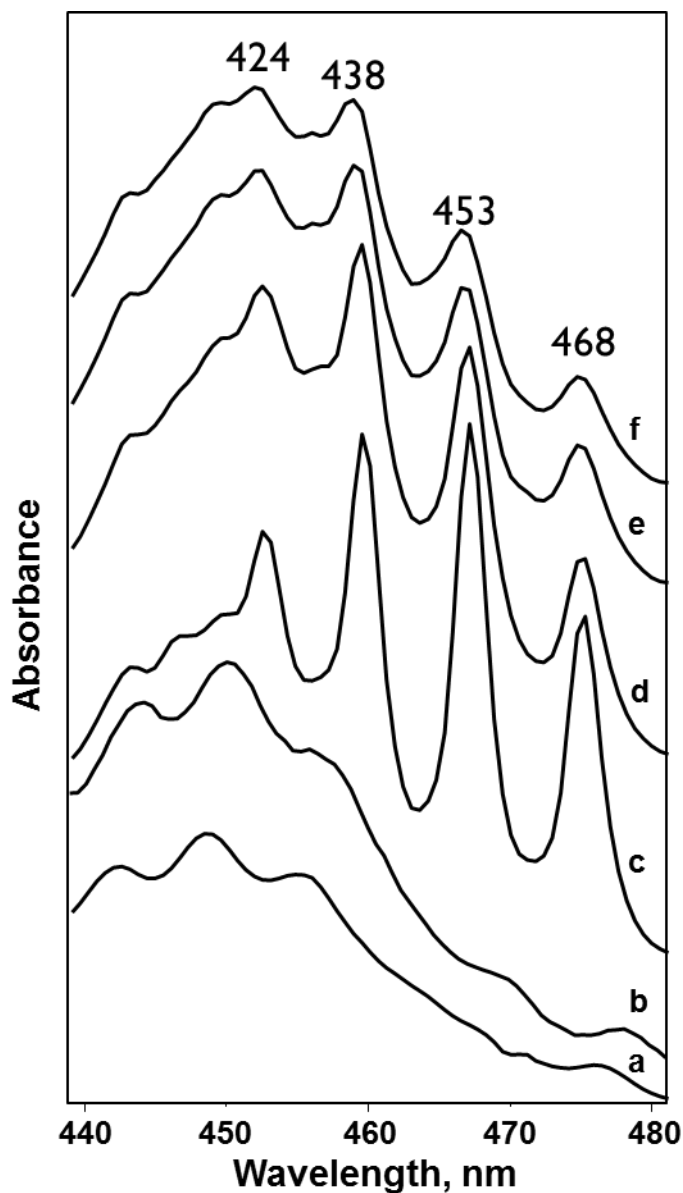


Figure 3-10 UV/visible absorption spectra of solutions of 0.1 M  $\text{UO}_2(\text{Tf}_2\text{N})_2$  in  $[\text{C}_4\text{MIM}][\text{Tf}_2\text{N}]$  containing a) no TBAN or TBP, b) no TBAN and 0.1 M TBP, c) 0.3 M TBAN and no TBP, d) 0.3 M TBAN and 0.1 M TBP, e) 0.3 M TBAN and 0.2 M TBP, and f) 0.3 M TBAN and 0.3 M TBP.

As shown in Figure 3-10 c, the characteristic peaks of the  $\text{UO}_2(\text{NO}_3)_3^-$  species in  $[\text{C}_4\text{MIM}][\text{Tf}_2\text{N}]$  solution are present. Once 0.1 M TBP aliquots were added, the intensity of the peaks characteristic to the  $\text{UO}_2(\text{NO}_3)_3^-$  species started to decrease, indicating the loss of

a nitrate ion (Figure 3-10 d-f). Based on these absorption spectra and  $\nu(\text{NO})$  mode, it can be concluded that the TBP ligand causes the displacement of the nitrate ion from the  $\text{UO}_2(\text{NO}_3)_3^-$  species to form a uranyl-nitrate-TBP complex which likely includes two molecules of nitrate and TBP. As discussed above, Wai et al.<sup>5</sup> found that the uranyl-nitrate-TBP complex contains two molecules of TBP. The results of a Raman spectroscopic study suggested that the neutral complex  $\text{UO}_2(\text{NO}_3) \cdot 2\text{TBP}$  and a  $\text{HNO}_3$  adduct complex form when the  $\text{TBP}(\text{HNO}_3)_{1.8}(\text{H}_2\text{O})_{0.6}$  complex dissolves  $\text{UO}_2$  in  $[\text{C}_4\text{MIM}][\text{Tf}_2\text{N}]$ ; as well as, when 0.34 M TBP is added to 0.17 M of uranyl nitrate hexahydrate in  $[\text{C}_4\text{MIM}][\text{Tf}_2\text{N}]$ . These results are contradictory to what was observed by Billard et al.<sup>22</sup> When they performed liquid-liquid extractions of uranyl from nitric acid solution into the  $[\text{C}_4\text{MIM}][\text{Tf}_2\text{N}]$  solution, they concluded charged complexes were being partitioned. It is postulated, at low  $\text{HNO}_3$  concentrations,  $[\text{UO}_2(\text{TBP})_x]^{2+}$  was extracted and at high  $\text{HNO}_3$  concentration,  $[\text{UO}_2(\text{NO}_3)_3(\text{TBP})_y]^-$  was extracted.<sup>22</sup> RTILs are unique solvents because of their ability to solvate both ionic species and neutral species, making identifying the uranyl-nitrate-TBP species in RTIL difficult.

### 3.4 Conclusion

The coordination environment of uranyl nitrate and uranyl-nitrate TBP complexes were examined by varying the nitrate and TBP concentration in  $[\text{C}_4\text{MIM}][\text{Tf}_2\text{N}]$  and then analyzing the resulting solutions using ATR-FTIR spectroscopy. Nitrate was added in the form of  $\text{HNO}_3$  or TBAN. When the source of nitrate was TBAN, ATR-FTIR spectra indicated the presence of both the  $\text{UO}_2(\text{NO}_3)_2$  and  $\text{UO}_2(\text{NO}_3)_3^-$  complexes, but the  $\text{UO}_2(\text{NO}_3)^+$  species



was not detected. The  $\nu_{\text{as}}(\text{UO}_2^{2+})$  mode arising from uranyl complexed to the anion  $\text{Tf}_2\text{N}^-$  appeared at  $968\text{ cm}^{-1}$ , while the  $\nu_{\text{as}}(\text{UO}_2^{2+})$  mode for the  $\text{UO}_2(\text{NO}_3)_2$  species was found to appear at  $950\text{ cm}^{-1}$  and the  $\nu_{\text{as}}(\text{UO}_2^{2+})$  mode for the  $\text{UO}_2(\text{NO}_3)_3^-$  species appeared at  $945\text{ cm}^{-1}$ . Formation of the uranyl nitrate complexes may be monitored by the growth of the  $\nu(\text{NO})$  mode at  $1537\text{ cm}^{-1}$ , as well. The  $\text{UO}_2(\text{NO}_3)_3^-$  species was not detected in  $[\text{C}_4\text{MIM}][\text{Tf}_2\text{N}]$  solutions using ATR-FTIR, when the source of nitrate was  $\text{HNO}_3$  and this is believed to be due to the role water plays in this system. In addition, a uranyl-nitrate-TBP complex was formed when TBP was added to  $[\text{C}_4\text{MIM}][\text{Tf}_2\text{N}]$  solutions containing uranyl and nitrate. It is likely two molecules of TBP are coordinated to uranyl nitrate.  $\nu_{\text{as}}(\text{UO}_2^{2+})$  for the complex  $\text{UO}_2(\text{NO}_3)_2(\text{TBP})_2$  appears at  $942\text{ cm}^{-1}$ . Overall our results show ATR-FTIR is a valuable spectroscopic tool and may be added to the suite of analytical tools to detect changes in uranyl nitrate and uranyl-nitrate-TBP complex chemical environments.

### 3.5 Acknowledgement

The authors would like to acknowledge the DOE Nuclear Energy University Program (NE-UP #TO 00058) for financial support.

### 3.6 References

1. W. B. Lanham and T. C. Runion, *PUREX Process for Plutonium and Uranium Recovery*. 1949, Oak Ridge National Laboratory
2. *Nuclear Energy and the Environment*, ed. C. M. Wai and B. J. Mincher, ACS Symposium Series 1046, Washington DC, USA, 2010.

3. J. S. Wang, C. N. Sheaff, B. Yoon, R. S. Addleman, and C. M. Wai, *Chem. Eur. J.*, 2009, **15**, 4458-4463.
4. J. N. Mathur, M. S. Murali, and K. L. Nash, *Solvent Extr. Ion Exch.*, 2001, **19**, 357-390.
5. C. M. Wai, Y. Liao, W. Liao, G. Tian, R. S. Addleman, D. Quach, and S. P. Pasilis, *Dalton Trans.*, 2011, **40**, 5039.
6. X. Sun, H. Luo, and S. Dai, *Chem. Rev.*, 2012, **112**, 2100.
7. V. A. Cocalia, K. E. Gutowski, and R. D. Rogers, *Coord. Chem. Rev.* 2006, **250**, 755.
8. K. Binnemans, *Chem. Rev.*, 2007, **107**, 2592.
9. I. Billard and C. Gaillard, *Radiochim. Acta*, 2009, **97**, 355.
10. A. Mudring and S. Tang, *Eur. J. Inorg. Chem.*, 2010, **2010**, 2569.
11. S. H. Ha, R. N. Menchavez, and Y.-M. Koo, *Korean J. Chem. Eng.*, 2010, **27**, 1360.
12. K. Takao, T. J. Bell, and Y. Ikeda, *Inorg. Chem.*, 2013, **52**, 3459
13. L. Kaplan, R. A. Hildebrandt, and M. J. Ader, *Inorg. Nucl. Chem.*, 1956, **2**, 153.
14. K. Servaes, C. Hennig, I. Billard, C. Gaillard, K. Binnemans, C. Gorller-Walrand, and R. Van Deun, *Eur. J. Inorg. Chem.*, 2007, 5120.
15. P. Nockemann, K. Servaes, R. Van Deun, K. Van Hecke, L. Van Meervelt, K. Binnemans, and C. Goerller-Walrand, *Inorg. Chem.*, 2007, **46**, 11335. 17
16. C. Gaillard, A. Chaumont, I. Billard, C. Hennig, A. Ouadi, and G. Wipff, *Inorg. Chem.*, 2007, **46**, 4815.
17. S. Georg, I. Billard, A. Ouadi, C. Gaillard, L. Petitjean, M. Picquet, and V. Solov'ev, *J. Phys. Chem. B*, 2010, **114**, 4276.
18. C. Gaillard, O. Klimchuk, A. Ouadi, I. Billard, and C. Hennig, *Dalton Trans.*, 2012, 41, 5476-5479.
19. T. V. Healy and H. A. C. McKay, *Trans. Faraday Soc.*, 1956, 633-642.
20. P. Giridhar, K. A. Venkatesan, T. G. Srinivasan, and P. R. V. Rao, *J. Radioanal. Nucl. Chem.*, 2005, **265**, 31-38.
21. M. S. Murali, N. Bonville, G. R. Choppin, *Solvent Extr. Ion Exch*, 2010, **28**, 495-509.
22. I. Billard, A. Ouadi, E. Jobin, J. Champion, C. Gaillard, and S. Georg, *Solvent Extr. Ion Exch.*, 2011, **29**, 577-601.

23. S. P. Pasilis and A. Blumenfeld, *Inorg. Chem.*, 2012, **50**, 8302-8307.
24. S. P. McGlynn, J. K. Smith, and W. C. Neely, *J. Chem. Phys.*, 1961, **35**, 105-116.
25. S. Mekki, C. M. Wai, I. Billard, G. Moutiers, J. Burt, B. Yoon, J. S. Wang, C. Gaillard, A. Ouadi, and P. Hesemann, *Chem. Eur. J.*, 2006, **12**, 1760.
26. Y. Liao, *Actinide and Lanthanide Species in Ionic Liquid and in Supercritical CO<sub>2</sub>: Dissolution, Coordination, and Separation*, Doctoral Dissertation, University of Idaho, 2012.
27. I. Billard, C. Gaillard, and C. Hennig, *Dalton Trans.*, 2007, 4214.
28. Y. Lin, N. G. Smart, and C. M. Wai, *Environ. Sci. Technol.*, 1995, **29**, 2706-2711.
29. M. J. Carrott, B. E. Waller, N. G. Smart, and C. M. Wai, *Chem. Commun.*, 1998, 373-374.

## Chapter 4

# Recycling Uranyl from TRISO Fuel Particles using Supercritical CO<sub>2</sub>

### 4.1 Introduction

TRISO fuels have been used in the reactors called very high temperature reactors (VHTR) in which inert gases are used as the cooling fluid. One advantage of using VHTR for power production is that the conversion efficiency of heat to work increases with temperature. These reactors are being proposed for wider deployment in the future, and the TRISO fuels will likely see increased production and use.

The TRISO fuel consists of several layers to contain any fission products present from escaping during irradiation. Figure 4-1 shows the structure of a typical TRISO fuel particle.

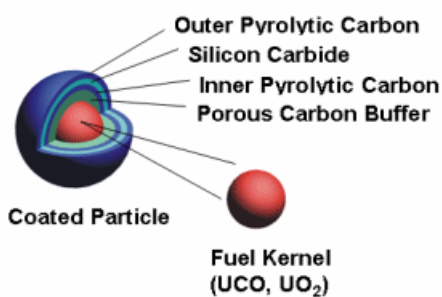


Figure 4-1 Schematic diagram showing the five different layers of a TRISO particle. (Slightly modified version from: [http://aris.iaea.org/ARIS/reactors.cgi?requested\\_doc=report&doc\\_id=70&type\\_of\\_output=html](http://aris.iaea.org/ARIS/reactors.cgi?requested_doc=report&doc_id=70&type_of_output=html)).

The fuel kernel consisting of uranium in the form of uranium oxycarbide or uranium dioxide (UCO or  $\text{UO}_2$ ) can be found at the center of the TRISO fuel particle. In addition, plutonium, thorium, or transuranic elements (TRU) can be used as the fuel kernel. The fuel kernel is surrounded by a porous carbon buffer, where volatile fission products accumulate. Three additional outer layers surround the fuel and buffer carbon layer. The three layers are the inner pyrolytic carbon (IPyC) layer, silicon carbide layer, and outer pyrolytic (OPyC) layer. The IPyC layer provides support to the buffer carbon layer by acting as another diffusion barrier to prevent fission products from escaping. The SiC layer keeps the fuel intact by withstanding any compression and expansion caused by volatile fission products. Lastly, the OPyC layer acts as a shield and protects the SiC layer from chemical attack and retains any fission gas product from escaping.<sup>1</sup> About a billion of these one mm in diameter coated fuel particles are incorporated into the final fuel element placed in the VHTR as shown in Figure 4-2. This design makes proliferation for weapons production difficult because a small amount of U(IV) is in the fuel kernel. The fuel element is placed in a VHTR core and  $^{235}\text{U}$  is exposed to thermal neutrons to undergo nuclear fission to produce electricity.

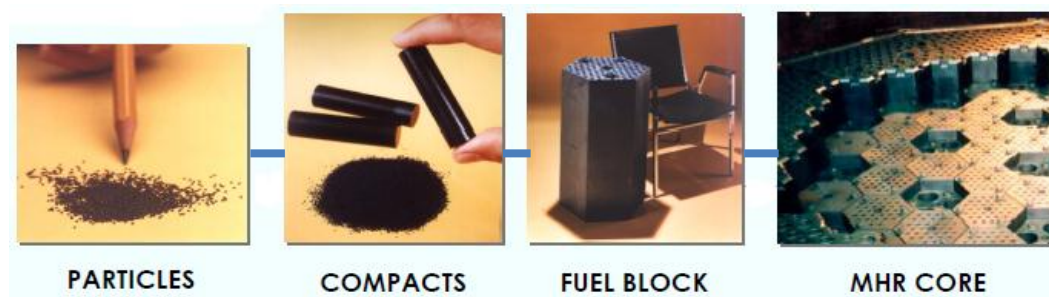


Figure 4-2 Illustration of TRISO fuel particles being processed into a fuel element for a nuclear reactor. See Appendix A for documentation that this material is in the public domain.<sup>2</sup>

Uranium carbide (UC) is more attractive as a fuel for the VHTR than  $\text{UO}_2$  because of its ability to withstand high temperatures, conduct heat, and more fissile atoms can be compacted into the TRISO fuel core. Also, since the fusion temperature of UC is high, metallic elements, plutonium, and minor actinides can be combined with UC to give higher burn-up values.<sup>3</sup> A burn-up value of 10% is achieved when metallic elements are combined with UC; however, if plutonium and minor actinides are incorporated in UC, a burn-up value of 20% is possible.<sup>4</sup> Generally, there is useful uranium left over in the fuel element from spent fuel; this is recovered using the PUREX process. However, recycling methods for extracting uranium and other fission products from these TRISO fuels have not been developed.

The use of  $\text{sc-CO}_2$  for uranium recovery from used TRISO fuel would be ideal because it possesses both gas-like and liquid-like properties; therefore, it is capable of penetrating into porous materials and dissolving constituents in a solid matrix. In addition,  $\text{sc-CO}_2$  is an attractive solvent because it is non-toxic, recyclable, cheap, relatively inert, and non-flammable. Unfortunately,  $\text{sc-CO}_2$  is unable to penetrate the silicon carbide layer. Currently there is no method of cracking the TRISO other than mechanically crushing the TRISO fuel itself. By doing this, there is the risk of spreading gaseous fission products and radioactive contamination.

A technique to access the UC in a TRISO fuel particle, while containing the volatile fission products is an ultrasound pressure vessel. Irradiation from ultrasound causes acoustic cavitation and forms hot spots while bubbles collapse. Hot spots with temperatures up to  $5000^\circ\text{C}$  and pressures of 500 atm occur on the order of microseconds.

This phenomenon is capable of exposing new surfaces when cavitation occurs near a liquid-solid interface.<sup>5</sup> There has been no report of such an instrument being used for crushing any solid material. However, several reports have shown an enhancement in extraction yield when ultrasound was used before or during a sc-CO<sub>2</sub> extraction. For example, the rate of extraction of uranyl by sc-CO<sub>2</sub> with a CO<sub>2</sub>-soluble extractant of the formula TBP(HNO<sub>3</sub>)<sub>1.8</sub>(H<sub>2</sub>O)<sub>0.6</sub> at 50 °C and 150 atm can be enhanced by an order of magnitude with the assistance of ultrasound.<sup>6</sup>

Another concern in developing a recycling process, for TRISO fuel particles is that gamma irradiation resulting from radioactive decay affects the fuel during nuclear fission of the <sup>235</sup>U. Gamma irradiation can cause point defects in metal, alloy, and ionic crystals such as UC. Uranium carbide crystallizes in a NaCl structure. Crystal structures do not form perfectly even when there has been no exposure to radiation. Various types of point defects can occur within a crystal structure. These include vacancies, self-interstitials, substitutional defects, or interstitial impurity atoms.<sup>7</sup> Figure 4-3 illustrates the different types of point defects present in a 2D crystal lattice.<sup>4, 8, 9</sup> It is unknown how these point defects will affect the extraction efficiency of U(VI).

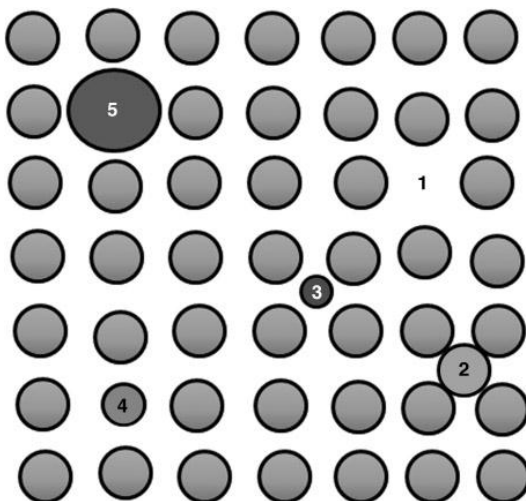


Figure 4-3 Several point defects are shown on a 2D crystal lattice. 1. monovacancy, 2. self-interstitial, 3. interstitial impurity atom, 4. undersize substitutional atom, and 5. oversize substitutional atom. (Reprinted with permission from ref 7. Copyright Wiley-VCH Verlag GmbH & Co. KGaA.). See Appendix A for documentation of permission to republish this material.

In this chapter, the extraction efficiency of U(VI) from non-irradiated and gamma irradiated TRISO fuel particles—by using the complex  $\text{TBP}(\text{HNO}_3)_{1.8}(\text{H}_2\text{O})_{0.6}$  and  $\text{sc-CO}_2$  for the dissolution and extraction—are compared. Also, by developing an ultrasound pressure vessel, the recycling of TRISO fuel particles will be safer due to the containment of volatile fission products during the crushing step. This chapter describes an attempt to crack TRISO fuel particles with an ultrasound pressure vessel in liquid  $\text{CO}_2$  and/or  $\text{sc-CO}_2$ .

## 4.2 Experimental

### 4.2.1 Chemicals and Reagents

TRISO fuel particles with a uranium oxycarbide core (39.87% U) were purchased from Babcock & Wilcox Company (Charlotte, NC). The oxycarbide is a solid solution of  $\text{UO}_2$  and UC. This solid solution is generated during a high temperature sintering process (1800-



1900°C) in a mixture of H<sub>2</sub> and CO gas. Concentrated nitric acid (70%w/w), tri-n-butylphosphate (TBP), and dodecane (ReagentPlus) were purchased from Sigma-Aldrich (Milwaukee, WI). Hydrofluoric acid (HF) was purchased from Fischer Chemicals (Santa Clara, CA). A tank of liquid carbon dioxide, Supercritical Fluid Chromatography grade (SFC), equipped with a full length eductor tube for liquid withdrawal was obtained from Norco (Boise, ID).

#### 4.2.2 Experimental Setup and Instruments

The supercritical fluid apparatus used is comprised of an ISCO syringe pump (Model 206D, Lincoln, NB) with a series D pump controller connected to the CO<sub>2</sub> tank. The pump supplies CO<sub>2</sub> via lines and valves (Autoclave Engineering, Erie, PA) linking it to the sample cell pressure vessels (home-made) containing the sample and extractant. The pressure and temperature are monitored by a pressure gauge (High Pressure Equipment Co., Erie, PA) and thermocouple (Omega Engineering, Stamford, CT), respectively. The CO<sub>2</sub> exit line and valve are wrapped with heating tape (Brisk Heat, Columbus, OH) and contain thermocouples controlled by a temperature controller (Omega Engineering, Stamford, CT). The CO<sub>2</sub> exit line is dipped in a trap vial containing dodecane.

Radiation effects on the TRISO fuel particles were tested by  $\gamma$ -irradiating two sets of TRISO fuel particles with a <sup>60</sup>Co irradiator (Nordion Gamma Cell 220E), one to an absorbed dose of 1047 kGy and the other to 691 kGy. Dose rate was determined using Fricke dosimetry at low absorbed doses. Initial experiments involved the crushing of irradiated and non-irradiated TRISO fuel particles using a mortar and pestle and then sieving the

particles to a range of particle sizes. A sample of crushed TRISO was placed in the sample pressure cell and the extractant,  $\text{TBP}(\text{HNO}_3)_{1.8}(\text{H}_2\text{O})_{0.6}$ , was added directly to the sample. The temperature and pressure were set at  $40^\circ\text{C}$  and 200 atm, respectively. During the entire extraction, mechanical stirring with a stir bar was applied. The static extraction was performed for 30 min. and a dynamic extraction was performed for 45 min., followed by complete depressurization at a flow rate of 0.345 mL/min. After depressurization was complete, the leftover TRISO particles were collected for neutron activation analysis (NAA) at Washington State University. The extraction efficiencies standard deviation error found was based on duplicate extractions. The extraction efficiencies of U(VI) were calculated based on Eq. 1, where D is the distribution ratio (amount of U(VI) extracted, divided by the amount of U(VI) not extracted).

$$\%E = 100 [D/(D+1)] \quad (\text{Eq. 1})$$

In the ultrasound experiments, the pressure vessel described above was replaced with an ultrasound pressure vessel (Manning Applied Technology, Troy, ID). The schematic of the ultrasound pressure vessel is shown in Figure 4-4. The ultrasonic system is composed of a power piezoelectric transducer (Langevin type), which delivers adjustable continuous output of a 500 W capacity and a fixed frequency of 20 kHz. This ultrasound cell is connected to a controller (Sonics, Newton, CT), allowing different amplified acoustic waves to be delivered. This ultrasound pressure vessel was designed and fabricated by Manning Applied Technologies, INC. (Troy, ID).

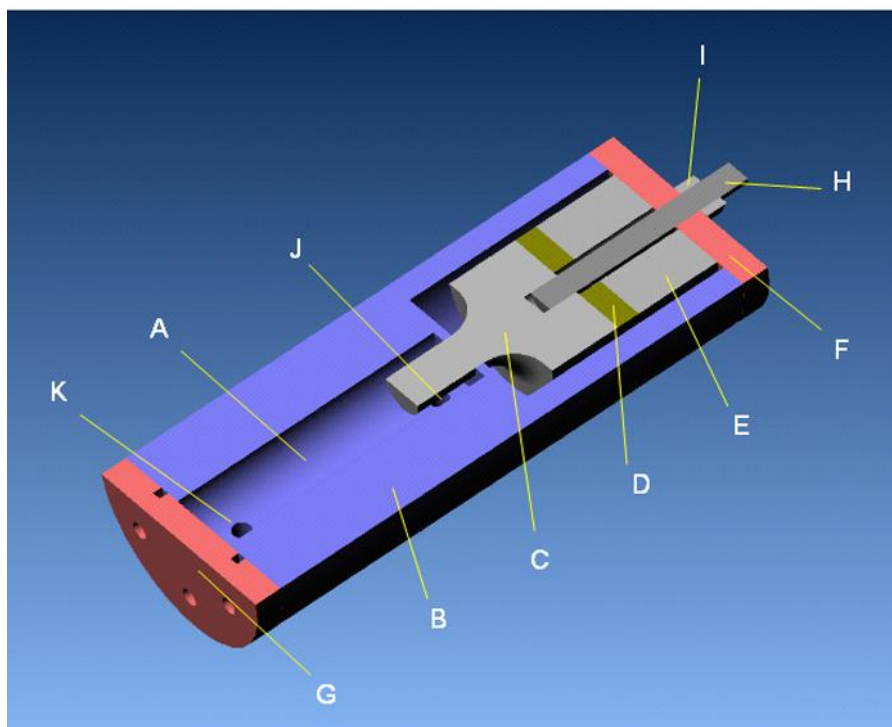


Figure 4-4 Schematic of the ultrasound pressure vessel. Details: A. SCF extraction chamber, B. Stainless steel cell body, C. Langevin horn, D. Piezoelectric transducer, E. Countermass, F. Endplate G. Endplate with o-ring seal H. Tensioning threaded rod, I. Tensioning nut, J. Fluid outlet port, and K. Fluid inlet port.

This study tested the feasibility of cracking TRISO fuel particles using ultrasound in liquid  $\text{CO}_2$ . A sample of 0.27 g of TRISO fuel particles was placed directly in the ultrasound pressure vessel and exposed to ultrasound. A total of 21,806 J of energy was applied. No container was used to hold the particles. A separate attempt to crack the TRISO fuel particle was made in which the TRISO fuel particle was pretreated with concentrated HF and then sonicated, in a sonication bath, for 1 hour. Afterwards, the HF was removed by evaporation and addition of concentrated  $\text{HNO}_3$ . The TRISO fuel particles were placed in the ultrasound pressure vessel and exposed to ultrasound resulting in a total of 44,494 J of energy. The temperature and pressure were at room temperature ( $20.1^\circ\text{C}$ ) and 80 atm. The

instrument was set to pulse ultrasound waves for 10 s and then pause for 15 s to prevent overheating of the machine. The amplitude was set to the manufacturer's suggested maximum of 30%. The length of time ultrasound was applied was varied. The system was depressurized after ultrasound application was complete and the TRISO was collected for scanning electron microscopy (SEM) analysis of any cracks. The SEM used was a Zeiss (Leo) 1455 VP. In addition, the ultrasound pressure vessel was also used to shatter glass.

### 4.3 Results and Discussion

#### 4.3.1 sc-CO<sub>2</sub> Extraction of U(VI) from Non-Irradiated and $\gamma$ -Irradiated TRISO Fuel Particles

The use of  $\gamma$ -irradiation can change the crystal structure of UC and enhance diffusion of the extractant in sc-CO<sub>2</sub>, which may increase the extraction yield of U(VI).<sup>8</sup> Shown in Table 4-1, TRISO fuel particles were irradiated at 691 and 1047 kGy and were found to have more than 30% higher extraction efficiencies than TRISO fuel particles that were not exposed to  $\gamma$ -irradiation.

Table 4-1 Comparison of the extraction yield of uranium from different particle sizes of TRISO fuel particles either not  $\gamma$  irradiated or  $\gamma$  irradiated at 691 or 1047 kGy.

Particle size, mesh	% U extracted		
	untreated	691 kGy	1047 kGy
x < 60	67 ± 2	98 ± 1	99 ± 1
60 < x < 500	53 ± 2	91 ± 3	95 ± 3

Carbon diffusion has been found to occur faster than uranium diffusion and carbon vacancies require the least amount of energy (0.65 eV/atom) to form.<sup>4,8</sup> The density of the

fuel decreases due to the movement of carbon and fission products produced. In theory, the vacancy- interstitial pairs would increase the volume of the fuel by 1.5 times; however, experimentally this has not been observed, except for the slight volume increase in the region where the fuel kernel is located due to the creation of void space.<sup>7</sup> The open space allows for the complexing ligand  $\text{TBP}(\text{HNO}_3)_{1.8}(\text{H}_2\text{O})_{0.6}$  dissolved in  $\text{sc-CO}_2$  to easily diffuse throughout the crystal structure to extract U(VI). Defects in the crystal structure, thus allowed the extraction yield to be significantly greater than when compared to non-irradiated TRISO fuel particles.

#### 4.3.2 The Effect of TRISO Exposed to Ultrasound in Liquid $\text{CO}_2$

The untreated TRISO fuel particle has a rough surface, as can be seen in Figure 4-5 A. The surface of the irradiated TRISO fuel particle changed from a rough hill-like surface to areas with pits and a smooth surface as shown in Figure 4-5 B. Also, carbon particles were found in the cell. It is apparent that exposure to ultrasound had an effect on the graphite surface. Though no cracks on the surface were seen, the experiment proves that TRISO fuels are extremely robust and failure safe. As can be seen in Figure 4-5 C, pre-treatment with concentrated HF had a greater effect on the removal of graphite than no pre-treatment. It appears craters have formed on the surface of the TRISO fuel particle.

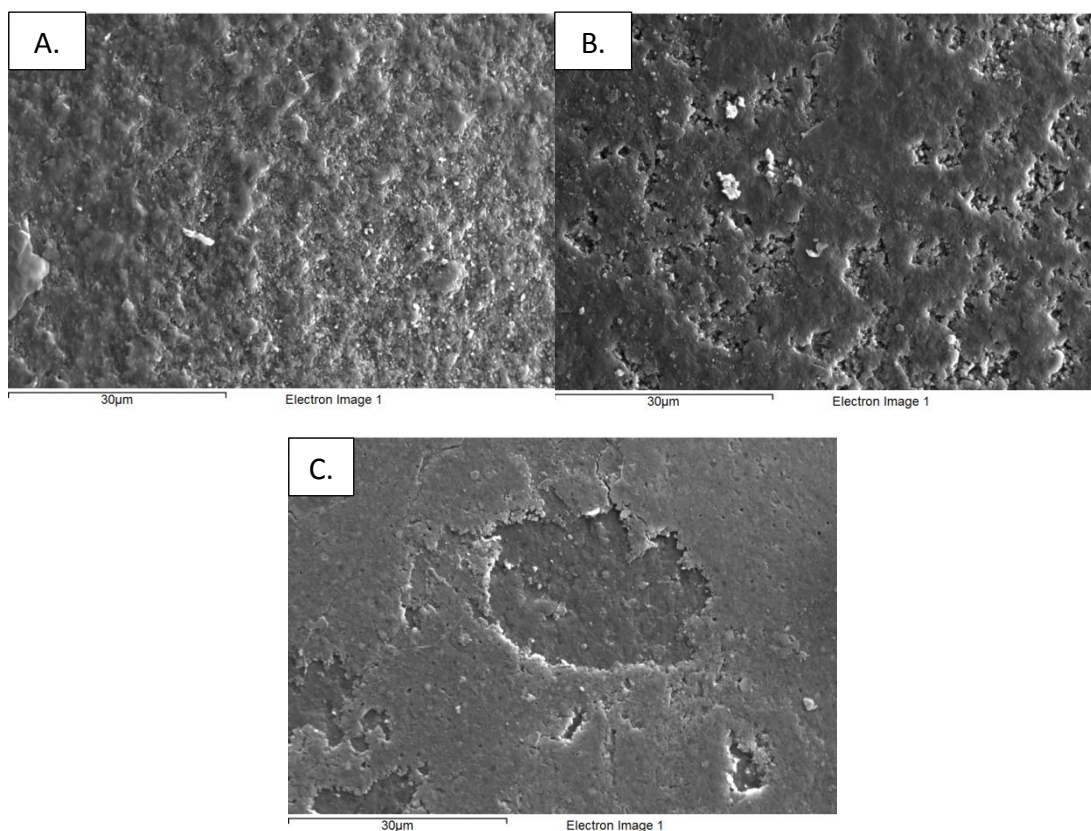


Figure 4-5 SEM images of the surface of TRISO fuel particles. A. Untreated TRISO fuel particle; B. Exposure to ultrasound; C. HF treatment and then exposure to ultrasound.

By exposing the TRISO fuel particle to HF and sonication, the HF was able to penetrate further into the graphite layer. Unfortunately, no crevices were observed on the surface of the TRISO fuel particle when examined by SEM.

#### 4.4 Conclusions

TRISO fuel particles were exposed to gamma irradiation to study the effect on the extraction of U(VI). The extraction yield of U(VI) was observed to have increased by more than 30 % when crushed TRISO fuel particles were gamma irradiated at 691 and 1041 kGy.

The reason for this increase is thought to be due to the creation of carbon vacancy sites to allow higher diffusion of the complex ligand dissolved in sc-CO<sub>2</sub>. Also, the feasibility of cracking TRISO fuel particles was tested by using an ultrasound pressure vessel in liquid CO<sub>2</sub>. It was observed that TRISO fuel cannot be fractured with the power of ultrasound alone. The addition of HF increased the penetration of the outer graphite layer, but was still unable to break through the tough silicon carbide shell. More research needs to be done to further develop this technology.

## 4.5 Acknowledgement

This work is supported by INL-LDRD Program under Idaho Operations Contract DE-AC07-05ID14517.

## 4.6 References

1. J. J. Power and B. Wirth, *J. Nucl. Mater.*, 2010, **405**, 74-82.
2. T. Allen, J. Busby, M. Meyer, and D. Petti, *Mater. Today*, 2010, **13**, 14-23.
3. M. Virost, S. Szenknect, T. Chave, N. Dacheux, P. Moisy, and S. I. Nikitenko, *J. Nucl. Mater.*, 2013, **441**, 421-430.
4. R. Ducher, R. Dubourg, M. Barrachin, and A. Pasturel, *Phys. Rev. B*, 2011, **83**, 104107-(1-12).
5. K. S. Suslick, *Science*, 1990, **247**, 1439-1445.
6. Y. Enokida, S. A. El-Fatah, and C. M. Wai, *Ind. Eng. Chem. Res.*, 2002, **41**, 2282-2286.
7. K. L. Murty and I. Charit, *An Introduction to Nuclear Materials : Fundamentals and Applications*. 2013, Hoboken: Wiley.
8. H. Matzke, *J. Less Common Met.*, 1986, **121**, 537-564.

9. M. Freyss, *Phys. Rev. B*, 2010, **81**, 014101-(1-16).



## Chapter 5

# Supercritical Fluid Extraction and Separation of Uranium from Other Actinides and Lanthanides\*

### 5.1 Introduction

An alternative to the traditional organic solvents used in liquid/liquid extraction is sc-CO<sub>2</sub>. Among its advantages are a significant reduction in the volume of secondary liquid waste generation, rapid separation of solutes from the solvent for stripping, and containment of the volatile fission products in an entirely closed system. However, little is known regarding actinide separations in sc-CO<sub>2</sub> and this knowledge is essential prior to real nuclear applications.

Strong inorganic acids such as the nitric acid used in fuel dissolution are typically not soluble in sc-CO<sub>2</sub> because carbon dioxide is a linear triatomic molecule with no dipole moment. However, phosphorus-containing organic compounds such as TBP are highly soluble in sc-CO<sub>2</sub>. These Lewis bases are used as carriers to bring inorganic acids into the supercritical fluid phase to provide the charge neutralization requirement needed to extract metal complexes from the aqueous phase into the non-polar fluid.<sup>1</sup> Using TBP as the carrier for nitric acid is of particular interest here not only because lanthanides and

\*(Modified version of the following manuscript: J. Hazard. Mater., 2014, **274**, 360-366., Copyright 2014 Elsevier B.V.) See Appendix A for documentation of permission to republish this material.

actinides form nitrate-TBP complexes which are soluble in CO<sub>2</sub>, but also because nitric acid is the aqueous phase used in current fuel reprocessing. The extraction of trivalent lanthanides and actinides requires higher TBP and nitrate concentrations than for the higher-valent actinides.

A number of reports have appeared using TBP as a ligand for the extraction of U(VI) into CO<sub>2</sub>, including the recovery of uranium from nitric acid solution.<sup>1-3</sup> Meguro et al.<sup>4</sup> proposed that the same neutral metal complex species was extracted into sc-CO<sub>2</sub> as was known from liquid/liquid extraction; namely UO<sub>2</sub>(TBP)<sub>2</sub>(NO<sub>3</sub>)<sub>2</sub>. The presence of this species in the sc-CO<sub>2</sub> phase was confirmed by UV/Vis absorbance spectroscopy by Wai et al.<sup>5</sup> It has been reported that metal extraction efficiency is a function of the solubility of the metal/ligand complex in the CO<sub>2</sub> phase,<sup>4,6</sup> which was in turn a function of the density of the sc-CO<sub>2</sub>. Thus, extraction efficiency could be altered by appropriate choices of temperature and pressure. Rao et al.<sup>7</sup> performed a comprehensive investigation of the factors affecting the efficiency of TBP-assisted U(VI) extraction into sc-CO<sub>2</sub>, confirming the importance of sc-CO<sub>2</sub> density during U(VI) extraction. Over the pressure range 15-30 MPa, U(VI) extraction from nitric acid decreased with increasing pressure, and was a function of the equilibrium distribution ratio of U(VI) at that density. Outside this range non-equilibrium conditions prevailed and extraction efficiency was not related only to density. These authors also reported that increased extraction efficiency was found for extractions from higher aqueous nitric acid concentrations, in analogy with the results from liquid/liquid extractions.

Extraction of metals including U has also been performed directly from solid metal oxides using TBP•HNO<sub>3</sub> complexes dissolved in sc-CO<sub>2</sub>. These solids include simulated ores<sup>8</sup> and metal oxides,<sup>9</sup> as well as incinerator ash,<sup>10</sup> and crushed UO<sub>2</sub> fuel pellets.<sup>11-13</sup> The separation of U(VI) from the other actinides has, until now, received much less attention. Actinide separations are important because used fuel contains not only unused enriched U(VI) but also transuranic products. Uranium can be recovered to extend the U(VI) supply and the other actinides to reduce the toxicity of the radioactive waste destined for the long-term repository. Among previous work, Lin et al.<sup>14</sup> used several different organophosphorus ligands, including TBP, at different nitric acid concentrations to extract U(VI) and Th(IV) from aqueous solutions into sc-CO<sub>2</sub>, with U moderately better extracted than Th(IV) from 1 M HNO<sub>3</sub>. They also reported that increasing nitrate concentration and more basic ligands increased the extraction efficiency of U(VI) and Th(IV), as is also found for conventional liquid/liquid extraction. In another case, Iso et al.<sup>15</sup> were able to manipulate the extraction efficiency of U(VI) and Pu(IV) from 3 M HNO<sub>3</sub> solution by adjusting the pressure and thus the density of sc-CO<sub>2</sub>, which suggested that it might be possible to design a separation scheme. This may prove effective when dealing with two species; however, it's unknown whether a more complex mixture of actinides could be so easily separated. Trofimov et al.<sup>16</sup> investigated the direct dissolution and extraction of actinides from solid oxide mixtures of U-Th, U-Np, and U-Pu, as well as calcined solid solutions of U-Pu, U-Np, U-Am, and U-Pu-Eu oxides using sc-CO<sub>2</sub> containing the TBP/HNO<sub>3</sub> complex. The two types of actinide containing solids exhibited differing extraction characteristics. It was concluded that U(VI) was well separated from Th(IV), Np(IV), and

Pu(IV) in the solid oxide mixture case with separation factors of greater than 1100; however, all species in the calcined solid solutions were extracted with efficiency of greater than 84%. Thus, the ability to dissolve and extract actinides directly from their oxides may depend on the solid state structure of the particular oxide mixture.

The purpose of this study was to investigate the separation of U from other actinides from nitric acid solution using TBP in sc-CO<sub>2</sub>. Although several reports have appeared in which ligands other than TBP have been used in sc-CO<sub>2</sub> extraction,<sup>14, 17-19</sup> TBP was used in this study because it is the conventional fuel reprocessing ligand. Selective stripping and/or hold back reagents (nitrite, AHA, or OA) were used to demonstrate the selective extraction of U in the presence of neptunium, plutonium, and americium. These data allow the proposal that a sc-CO<sub>2</sub> extraction system could be designed in which co-extracted U(VI), Np(VI), and Pu(IV) could be selectively stripped using these reagents.

## 5.2 Experimental

### 5.2.1 Chemicals and reagents

Concentrated nitric acid, TBP, AHA, and dodecane (ReagentPlus) were purchased from Sigma-Aldrich (Milwaukee, WI, USA). Sodium nitrite was obtained from Fisher Chemical (Santa Clara, CA, USA). Oxalic acid was purchased from EM Science (Cherry Hill, NJ, USA). A tank of liquid carbon dioxide equipped with a full length eductor tube for liquid withdrawal was obtained from Norco (Boise, ID, USA). Actinide stock solutions containing <sup>242</sup>Pu (7260 ppm in 1 M HNO<sub>3</sub>), <sup>237</sup>Np (6162 ppm in 2 M HNO<sub>3</sub>), and <sup>243</sup>Am (541 ppm in 0.5

M HNO<sub>3</sub>) were used at the Idaho National Laboratory (INL), and diluted to working concentrations of 28, 30, and 1 μM, respectively, in the appropriate nitric acid concentration (1, 3, 6, and 8 M) prior to use. Uranium solutions were prepared by dilution to 3 mM in the appropriate nitric acid concentration following dissolution of depleted UO<sub>2</sub> powder (Internal Bio-Analytical Industries, Inc., Boca Raton, FL, USA) in nitric acid.

### 5.2.2 Experimental setup and instruments

The supercritical fluid apparatus used is shown in Figure 5-1 and is comprised of an ISCO syringe pump (Model 206D, Lincoln, NB, USA) with a series D pump controller connected to the CO<sub>2</sub> tank. The pump supplies CO<sub>2</sub> via lines and valves (Autoclave Engineering, Erie, PA, USA) linking it to the extractant and two 15-mL pressure vessels (home-made) containing the TBP ligand and actinide samples, respectively. The extractant vessel contained 2 mL of neat TBP, and was placed upstream to the sample cell to allow the TBP to be dissolved in the sc-CO<sub>2</sub> and then delivered to the sample cell for metal ion complex formation. Carbon dioxide was delivered to the sample cell using a stainless steel tube dipping down into the sample solution to allow better contact between the ligand and dissolved metal species. A relief valve was placed in line to relieve pressures above 34 MPa and a pressure transducer (Omegadyne, Sunbury, OH, USA) was used to measure the pressure of the system. The lines and valves were wrapped with heating tape (Brisk Heat, Columbus, OH, USA) containing thermocouples controlled by a pressure and temperature monitor and controller (Omega Engineering, Stamford, CT, USA). A micrometering valve (Autoclave Engineering, Erie, PA, USA) assisted the control of the CO<sub>2</sub> flow exiting to the

collection vial containing a dodecane trap solution. Dodecane was chosen to solubilize the metal/TBP complex that precipitates from gaseous CO<sub>2</sub>.

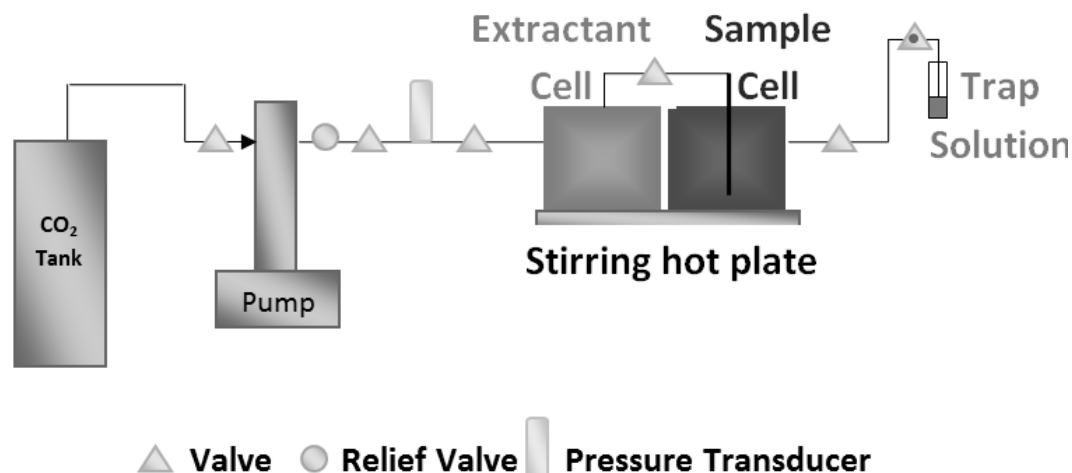


Figure 5-1 sc-CO<sub>2</sub> apparatus showing extractant and sample cells, and trap solution in the collection vial.

Neptunium, Pu and Am are  $\alpha$ -emitting radionuclides with the Am also having a significant  $\gamma$ -dose rate. To mitigate the radiological hazards the lowest specific activity isotopes available were chosen: <sup>237</sup>Np, <sup>242</sup>Pu, and <sup>243</sup>Am, respectively. The lowest possible chemical concentrations were also employed, consistent with adequate analytical detection limits. The extraction system was housed in a high efficiency particulate air (HEPA) filtered fume hood, and within a drip pan to contain any potential leakage from system fittings. Routine radiological surveys were performed to ensure adequate contamination control.

After the extraction, the aqueous residue (post-extraction raffinate) in the sample cell was analyzed for metal content. The <sup>237</sup>Np and <sup>243</sup>Am were determined by  $\gamma$ -counting using a GEM High-Purity Germanium (HPGE) Detector (Ortec, Oak Ridge, TN, USA) to

determine the  $^{237}\text{Np}$  (86.6 KeV) and  $^{243}\text{Am}$  (74.6 KeV) activities, the  $^{242}\text{Pu}$  was analyzed using a Tri-carb 3170TR/SL liquid scintillation analyzer (Perkin-Elmer, Waltham, MA, USA), and the  $^{238}\text{U}$  was analyzed using a Thermo X7 ICP-MS (Inductively Coupled Plasma Mass Spectrometry). All results are reported as % metal extracted. The standard deviations for these extraction efficiencies based on duplicate extractions were found to be  $\pm 7\%$  for Np,  $\pm 0.6\%$  for Pu and  $\pm 2\%$  for U.

### 5.2.3 sc-CO<sub>2</sub> extraction procedure

The extraction of metal ions from the acidic aqueous phase was conducted with sc-CO<sub>2</sub> modified with 1 mol % of TBP. The extraction temperature was 40°C at a pressure of 20 MPa. This pressure was chosen because the extracted neutral metal complex  $\text{UO}_2(\text{NO}_3)_2 \cdot 2\text{TBP}$  is known to have high solubility under these conditions.<sup>1</sup> The procedure consisted of a static contact between the TBP and the CO<sub>2</sub> for 20 min to dissolve the ligand, followed by a static extraction of the 1 mL sample in the 15-mL vessel for 30 min. The phase ratio is thus 15:1. This was followed by depressurization for 2 hours at a flow rate of approximately 0.375 mL min<sup>-1</sup>, during which the loaded CO<sub>2</sub> was bubbled through the dodecane trap solution vial, followed by a large volume of clean CO<sub>2</sub> which dissolved any remaining TBP in the extractant vessel and flushed the system, ensuring maximum recovery of the extracted metal. Acetohydroxamic acid, sodium nitrite and/or OA were used as reducing and/or complexing agents to enable selective extraction of the U. They were prepared at 0.5 M in 18 MΩ water and were directly added to the acidic metal ion sample solution to a final concentration of 0.1 M. For comparison, equal volume phase ratio liquid/liquid extractions

were done with 7% v/v (6 mol %) TBP in dodecane at room temperature ( $21 \pm 2^\circ\text{C}$ ) and ambient pressure. Typically, liquid/liquid extraction of U is performed using 30% v/v TBP (26 mol %), however, U is quantitatively extracted, especially from higher nitric acid concentrations, obscuring any trends that might otherwise be visible. A lower concentration was used here to purposefully decrease the extraction efficiency, and to bring the TBP concentration closer to that used in sc-CO<sub>2</sub> extractions. These liquid/liquid contacts were shaken by hand for 5 min and then separated by gravity. Based on previous experience, the kinetics of liquid/liquid TBP extraction are fast and the system was considered to be at equilibrium in less than this contact time. Phase disengagement was fast and considered complete within less than 5 min. Other than the lower TBP concentration, the techniques used here for the liquid/liquid extractions are standard for batch contact measurements. The post-contact aqueous solutions were analyzed as reported above. For liquid/liquid extractions, results are usually reported as distribution ratios ( $D$ ), where  $D$  is the ratio of the analytical concentration of the metal of interest in the organic phase divided by its concentration in the aqueous phase.<sup>20</sup> However, for comparison to sc-CO<sub>2</sub> extraction results, the distribution ratios have been converted to % extracted values, using the relationship:<sup>20</sup>

$$\%E = 100 [D/(D+1)] \quad (\text{Eq. 1})$$

where 1 is the phase ratio. It can be seen that high distribution ratios correspond to very high percent extraction.



### 5.3 Results and Discussion

It is well-known that the extraction efficiencies of metal ions depend on their valence states, with high charge density ions generally being better extracted. Hexavalent uranium, Pu(IV) and Am(III) are the natural oxidation states of the actinide metals in nitric acid, and these valence states are assumed here in the absence of attempts to purposefully alter them. The Np valence is more labile and the Np(VI) oxidation state was prepared by repetitive metathesis in nitric acid.

The extraction of metal ions into a non-polar solution, whether it be dodecane or CO<sub>2</sub> requires ligand solvation and charge neutralization. The phase transfer equilibrium for the extraction of neutral actinide ions with TBP is:<sup>21</sup>



The value of m is found to be 2 for divalent UO<sub>2</sub><sup>2+</sup> and 4 for tetravalent Pu<sup>4+</sup>. The formation of the neutral complex and therefore the extractability of the metal ion depends on the concentration of nitrate ions (nitric acid) present.

#### 5.3.1 Liquid liquid extraction of U(VI), Np(VI), and Pu(IV) from nitric acid solution

The liquid liquid extraction (Figure 5-2 a) of the hexavalent ions increased until reaching a maximum at about 6 M HNO<sub>3</sub>, but then decreased again at nitric acid concentrations above that. This phenomenon is common for the extraction of neutral complexes into organic solvents from nitric acid and has been attributed to competition for the ligand by nitric acid itself:<sup>22</sup>



In contrast to the hexavalent metals, Pu(IV) extraction efficiency continued to increase across the entire range of acid concentrations used here, eventually exceeding the efficiency of extraction for the hexavalent species, due to its higher ionic charge density which results in increased affinity for TBP complex formation. Although not measured here, the Pu extraction efficiency would also be expected to decrease at still higher nitric acid concentrations, also due to competition for the ligand as was shown in Eq. 3 above. As expected, the extraction of Am(III) was low. These results are consistent with previous literature reports.<sup>21</sup>

### 5.3.2 sc-CO<sub>2</sub> extraction of U(VI), Np(VI), and Pu(IV) from nitric acid solution

It can be seen in Figure 5-2 b that the sc-CO<sub>2</sub> extraction of U and Pu was more efficient than in liquid/liquid extraction, even though the mole ratio of TBP was lower for the sc-CO<sub>2</sub> solution. This may be attributed to the greater CO<sub>2</sub>:aqueous phase ratio for the sc-CO<sub>2</sub> extraction, although it should be noted that the higher mass transfer rate in sc-CO<sub>2</sub> allows for faster transfer of the complex into the sc-CO<sub>2</sub> phase. The extraction of Am(III) remained low in the sc-CO<sub>2</sub> system. This is not surprising since low charge density, trivalent metal ion species are well-known to be nearly inextractable by TBP in liquid/liquid systems, except at very high TBP concentrations. Kumar et al.<sup>23</sup> and Mincher et al.<sup>24</sup> used octylphenyldiisobutylcarbamoymethylphosphine oxide and thenoyltrifluoroacetone, respectively, as ligands when efficient extraction of Am into sc-CO<sub>2</sub> was required.

As can be seen in Figure 5-2 b, the sc-CO<sub>2</sub> extraction efficiency for U, Np, and Pu increased as the nitric acid concentration increased. This result also agrees with many previous reports.<sup>2, 7, 14</sup> However, the efficiency of nominally Np(VI) extraction appears to be less in the sc-CO<sub>2</sub> case. Neptunium valence control is difficult even in well-characterized PUREX liquid/liquid extraction, and these results suggest that some fraction of the Np may have been present as inextractable Np(V), having undergone reduction following preparation of the Np(VI) solution.

Uranium extraction using 1 mol% TBP in sc-CO<sub>2</sub> at 40°C and 20 MPa was efficient. It can be seen in Figure 5-2 b that U was quantitatively extracted from 3 M HNO<sub>3</sub>. Meguro et al.<sup>2</sup> reported ~70% U extraction from 3 M HNO<sub>3</sub>, at 60°C and 15 MPa, using 1.5 mol% TBP and a 30 min dynamic extraction. Rao et al.<sup>7</sup> reported U extraction of ~ 65% from 3 M HNO<sub>3</sub>, at 60 °C and 15 MPa, using 6 mol% TBP and a 30 min dynamic extraction. We attribute the higher efficiency found here to the combination of static and dynamic extractions performed.

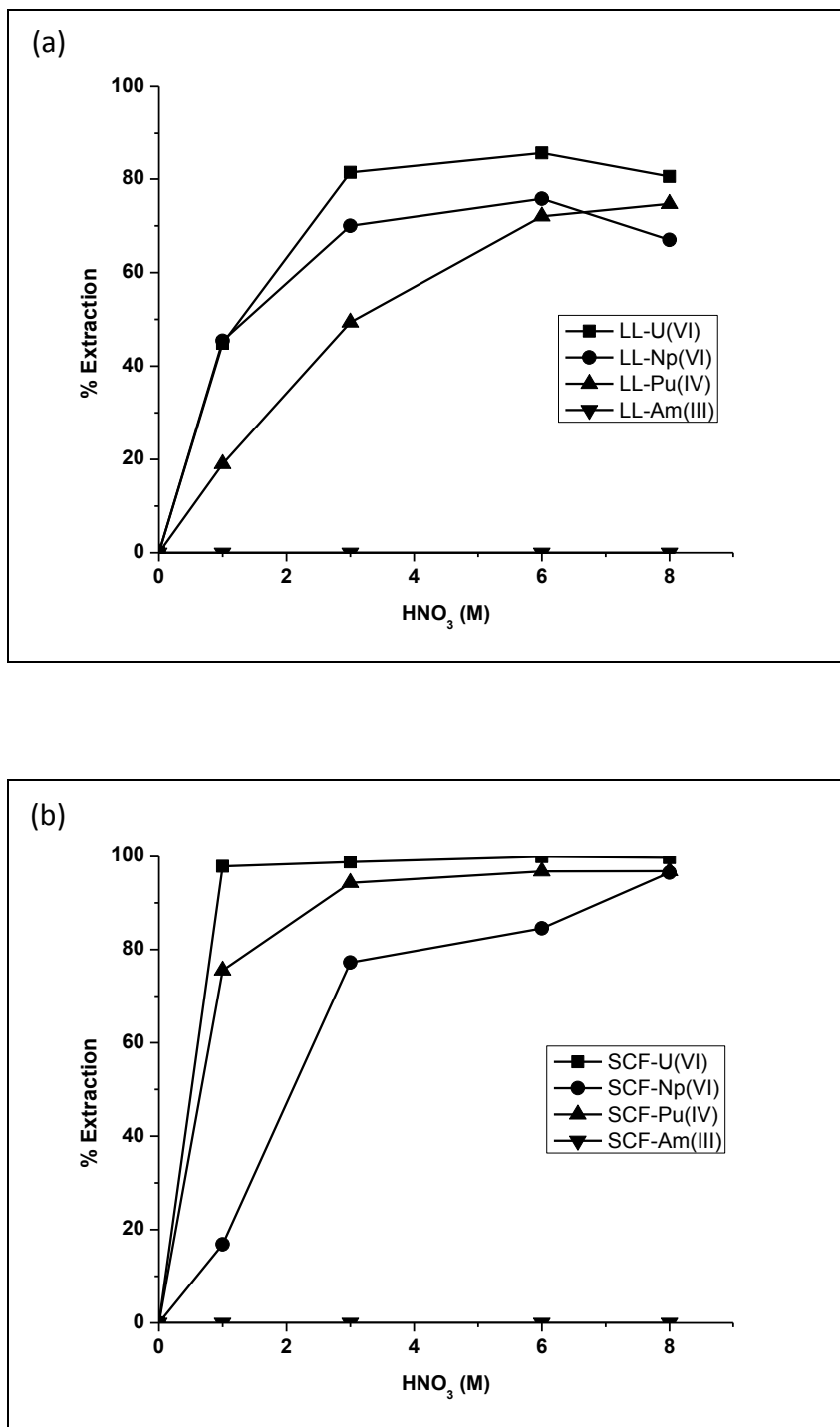


Figure 5-2 Extraction efficiency of U(VI), Np(VI), and Pu(IV) from nitric acid solution. (a) 6 mol % TBP liquid-liquid extraction (b) 1 mol % TBP SCF extraction at 40°C and 20 MPa. The lines connecting the data points are meant merely to guide the eye. (\*Reprinted with permission).

### 5.3.3 sc-CO<sub>2</sub> extraction of Pu and Np from nitric acid solution in the presence of reducing/complexing agents

There have been many studies related to the use of reducing and/or complexing agents to mitigate the extraction of Np and Pu for the selective extraction of U in liquid/liquid systems.<sup>25-32</sup> Among these, reducing/complexing agents such as AHA and OA are attractive because they are composed of only C, H, O, and N atoms and therefore can be decomposed to gases so that their incorporation into industrial processes does not lead to increased waste volumes. Hydroxamic acids such as AHA preferentially form complexes with tetravalent metals, especially Pu(IV), thus preventing it from co-extracting into the organic phase.<sup>33</sup> The stability constant trend for the actinide-hydroxamic acid complexes increases in the order:

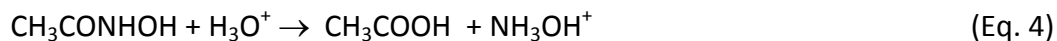
$\beta_{U(VI)} < \beta_{H^+} < \beta_{U(IV)} < \beta_{Np(IV)} < \beta_{Pu(IV)}$ .<sup>34-36</sup> Hydroxamic acids may also be capable of reducing Np(VI) to inextractable Np(V).

Oxalic acid is a complexing agent that also quickly reduces Np(VI) to Np(V).<sup>37</sup> The stability constants of this complex for Np(IV) and Pu(IV) in 1 M perchloric acid are high, at  $1.66 \times 10^9$  and  $5.42 \times 10^9$ , respectively.<sup>38</sup>

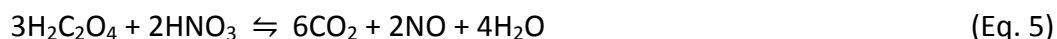
Finally, sodium nitrite is a conventional and convenient reagent for the reduction of extractable Np(VI) to the inextractable Np(V) oxidation state.<sup>39</sup> Based on these considerations, these reagents were investigated for their ability to allow for the selective sc-CO<sub>2</sub> extraction of U from a mixture of actinides.

The effect on the sc-CO<sub>2</sub> extraction of Pu(IV) from nitric acid solutions of 0.1 M AHA is shown in Figure 5-3. In 3 M HNO<sub>3</sub>, in the absence of AHA, over 95% of Pu(IV) was

extracted into the sc-CO<sub>2</sub> phase, similarly to the extraction of U(VI) under the same conditions as Pu(IV) (Figure 5-2). However, in the presence of the AHA, Pu(IV) was complexed sufficiently such that its extraction was only achieved at higher acid concentrations, where AHA probably hydrolyzed according to the following reaction:<sup>40</sup>



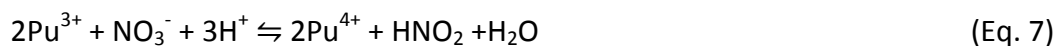
In 3 M HNO<sub>3</sub> only a small fraction of the Pu was extracted (Figure 5-3). Oxalic acid shows an even more pronounced effect on the extraction of Pu, also shown in Figure 5-3, although at higher nitric acid concentrations, OA was also less effective. Kubota<sup>41</sup> studied the decomposition of OA at various nitric acid concentrations and found about 50% of OA could be decomposed with 6 M HNO<sub>3</sub>:



In addition, it has been reported OA may be oxidized by Pu(IV) via the following reaction:<sup>42</sup>



However, in nitric acid solution the Pu(III) ions produced are easily oxidized back to Pu(IV):<sup>43, 44</sup>



Based on these reactions, the increase in extraction efficiency of Pu(IV) with increasing HNO<sub>3</sub> concentration can be attributed to the decrease in OA concentration by acid and metal ion catalyzed hydrolysis.

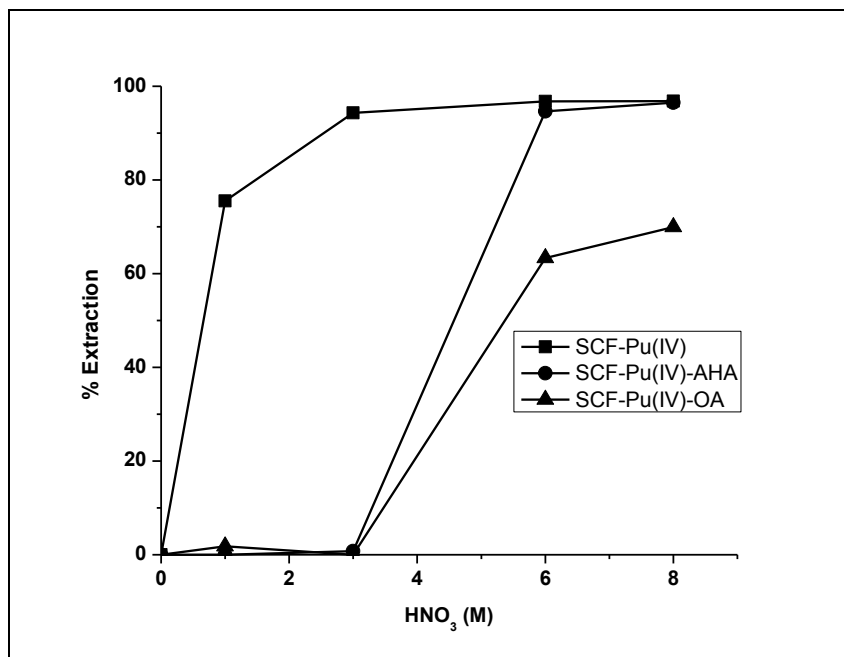


Figure 5-3 Extraction of Pu(IV) from nitric acid solutions into sc-CO<sub>2</sub> phase containing 1 mole % TBP in the presence and absence of reducing and/or complexing agents. AHA is acetohydroxamic acid, OA is oxalic acid. The lines connecting the data points are meant merely to guide the eye. (\*Reprinted with permission).

Table 5-2 shows the extraction results for a mixture of U and Pu from 3 M nitric acid using 1 mol% TBP modified sc-CO<sub>2</sub> in the presence of AHA or OA. The results indicate that it is possible to separate U from a mixture of U and Pu at this acidity by sc-CO<sub>2</sub> extraction. These results also suggest that U and Pu already dissolved in sc-CO<sub>2</sub> could be separated by selective stripping with 3 M nitric acid containing AHA or OA.

Table 5-1 Extraction efficiencies of U and Pu in the absence and presence of 0.1 M acetohydroxamic acid (AHA) or oxalic acid (OA) in 3 M nitric acid. NE = no extraction. (\*Reprinted with permission).

3M HNO <sub>3</sub>	% U(VI) extraction	% Pu(IV) extraction
U/Pu untreated	98.8 ± 1.0	94.3 ± 0.7
U/Pu + AHA	97.9 ± 1.0	7.5 ± 0.7
U/Pu + OA	96.8 ± 1.0	NE

Neptunium is especially problematic for actinide separations chemistry. The oxidation state of Np easily varies depending on its chemical environment, and extractable Np(IV) and Np(VI) may co-exist in nitric acid solution with inextractable Np(V). Pentavalent Np is oxidized to Np(VI) in the presence of HNO<sub>3</sub>, but is reduced by HNO<sub>2</sub>, according to the equilibrium first reported by Siddall and Dukes:<sup>39</sup>



Further, Np(V) slowly disproportionates, generating Np(VI) and Np(IV) in the presence of highly acidic solution.<sup>45</sup> Since both Np(IV) and Np(VI) are readily co-extractable in the PUREX process with U(VI) and Pu(IV), and Np(V) is not, the reliable extraction of Np is not easily controlled, resulting in Np-contaminated waste/product streams. Research into the factors controlling the Np valence in the fuel recycling process is currently being conducted in countries such as the USA, UK and Japan.<sup>46</sup>

Since Np(VI) is extracted into CO<sub>2</sub> as shown in Figure 5-2 b, its reduction to Np(V) is one way to provide separation from U(VI). The valence state of Np may be observed by UV/Vis absorption spectroscopy as shown in Figure 5-4. The appearance of a tail in the



range of 350–450 nm is associated with Np(VI). When an appropriate amount of  $\text{NaNO}_2$  is added to the acid solution, the growth of the absorbance band at 980 nm and disappearance of the tailing indicates Np(VI) was reduced to inextractable Np(V). The major absorbance below 400 nm in the nitrite-amended sample is due to nitrite itself.

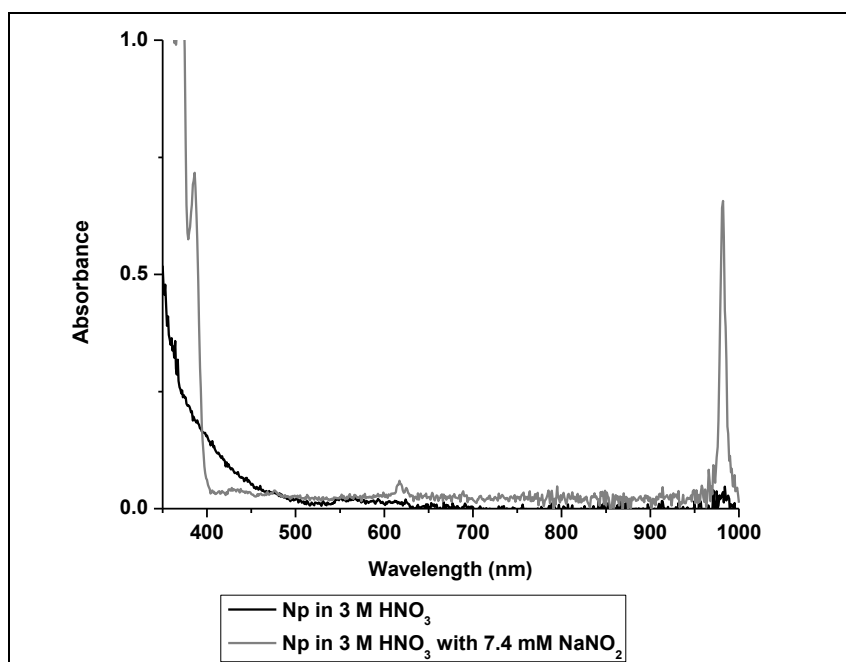


Figure 5-4 UV-Vis absorption spectra of Np species. Black- Np dissolved in 3M nitric acid showing mainly Np(VI) from 350-450 nm. Gray- Np and 0.1 M  $\text{NaNO}_2$  dissolved in 3 M nitric acid showing mainly Np(V) at 980 nm. (\*Reprinted with permission).

The extraction efficiencies of Np at various nitric acid concentrations in the presence of sodium nitrite are shown in Figure 5-5. In the absence of nitrite, Np(VI) was about 20% extracted by  $\text{sc-CO}_2$  containing 1 mol% TBP at 1 M  $\text{HNO}_3$ . Its extraction was less efficient in the presence of sodium nitrite, and also OA and AHA, also shown in Figure 5-5. It can be seen that the effect of reducing and complexing agents are again less effective at

the higher nitric acid concentrations, due to the reactions shown in eqs. 4, 5, and 9. To ensure that the Np is not co-extracted with U the extraction must be performed at  $\leq 1$  M nitric acid concentration.

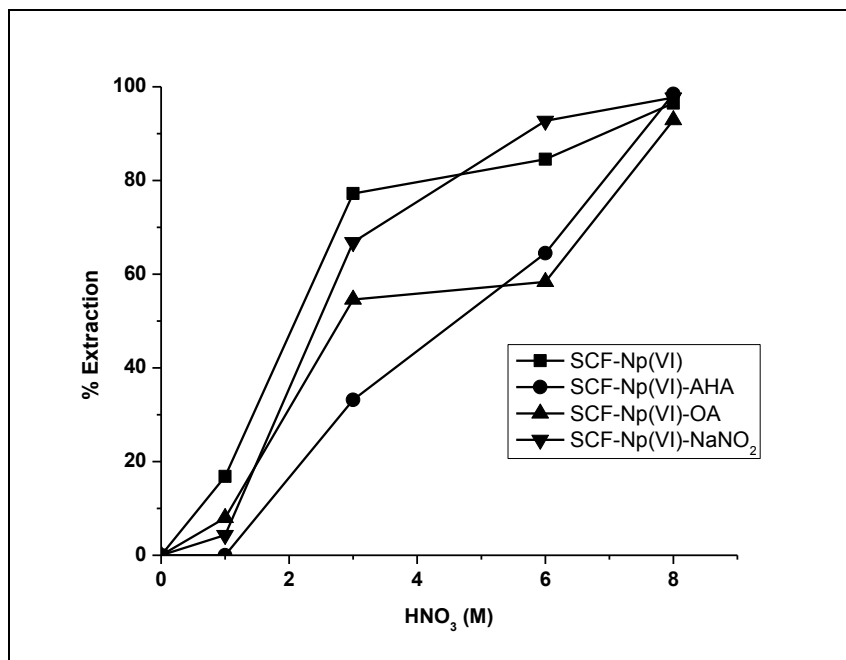


Figure 5-5 Extraction of nominally Np(VI) from nitric acid solutions into sc-CO<sub>2</sub> phase containing 1 mol % TBP in the presence and absence of reducing and/or complexing agents. AHA is acetohydroxamic acid, OA is oxalic acid. The lines connecting the data points are meant merely to guide the eye. (\*Reprinted with permission).

Table 5-2 shows the extraction efficiencies for a mixture of U(VI) and initially Np(VI) in 1 M nitric acid using 1 mol % TBP modified sc-CO<sub>2</sub> in the presence of sodium nitrite. The results indicate the successful separation of U(VI) from Np due to reduction of the oxidation state of Np to inextractable Np(V).

Table 5-2 Extraction efficiency of U(VI) and Np(VI) in the absence and presence of 0.1 M  $\text{NO}_2^-$  in 1 M nitric acid. NE = no extraction. (\*Reprinted with permission).

1M $\text{HNO}_3$	%U(VI) extraction	%Np(VI) extraction
U/Np untreated	93.3 $\pm$ 0.5	13.4 $\pm$ 1.2
U/Np + $\text{NO}_2^-$	92.4 $\pm$ 0.5	NE

#### 5.3.4 sc-CO<sub>2</sub> extraction and separation process

Based on the results given in the previous sections, it is of interest to extract U(VI) and Pu(IV) and then separate them from each other. The schematic of the sc-CO<sub>2</sub> extraction and separation system is shown in Figure 5-6. The figure is similar to what has been shown in section 5.2.2, except two stripping columns are added to selectively isolate certain actinides. The first stripping column contains 0.1 M OA in 1 M  $\text{HNO}_3$  to remove Np(VI) and Pu(IV) from the sc-CO<sub>2</sub> phase and the second stripping column contains H<sub>2</sub>O to remove U(VI) from the sc-CO<sub>2</sub> phase.

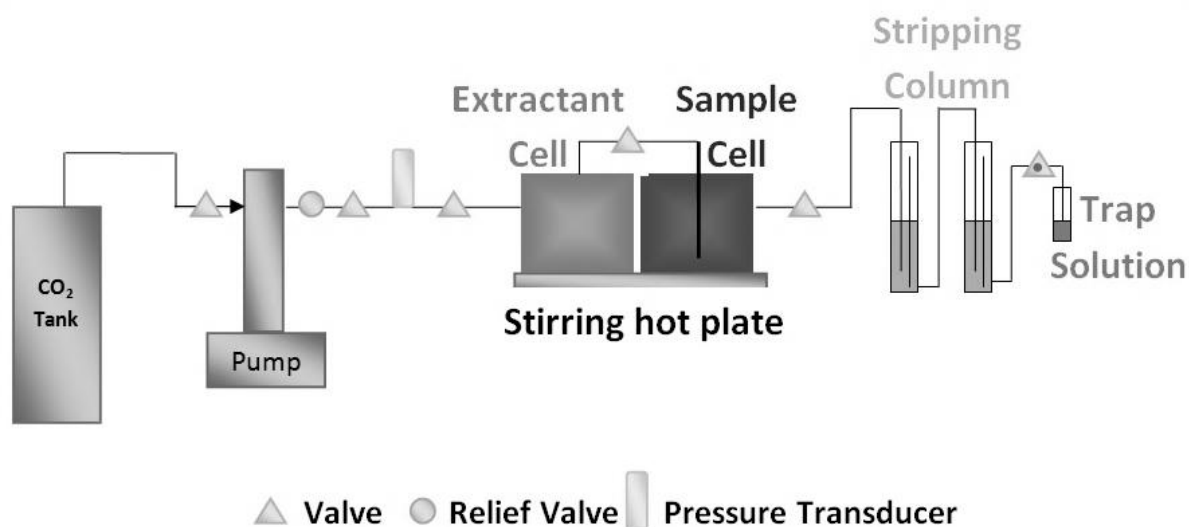


Figure 5-6 sc-CO<sub>2</sub> schematic containing two stripping columns in addition to an extractant and sample cell.

Table 5-3 shows the extraction efficiencies for the Ln(III) series, U(VI), Np(VI), Pu(IV), and Am(III) in 1 M nitric acid using 1 mol % TBP modified sc-CO<sub>2</sub>. The first row of the table (row A-1) shows the extraction efficiencies of the metals extracted from 1 M HNO<sub>3</sub>. Trivalent species do not extract under the conditions used in this sc-CO<sub>2</sub> extraction, thus negligible amounts of the Ln(III) series and Am(III) are extracted. The extraction efficiencies of U(VI), Np(VI), and Pu(IV) were 93, 16, and 87 %, respectively. These results are expected based the sc-CO<sub>2</sub> extraction efficiencies reported in Figure 5-2 b. The U(VI), Np(VI), and Pu(IV) in the sc-CO<sub>2</sub> phase are bubbled in a stripping column filled with 0.1 M oxalic acid in 1 M HNO<sub>3</sub>. Oxalic acid is capable of complexing with tetravalent metal species and reducing the oxidation state of Np(VI) to Np(V) to suppress its extractability. Row A-2 in Table 5-3 show the % stripped by the stripping column containing OA. The stripping column proved to be effective in removing 35 and 47% of Np(VI) and Pu(IV) from the sc-CO<sub>2</sub>; however 24%

of U(VI) was also stripped from the sc-CO<sub>2</sub>. The loss in U(VI) was not expected based on the results in section 5.3.3.

Table 5-3 The percent extraction of uranium, neptunium, plutonium, americium, and the lanthanide series from 1 M nitric acid solution by sc-CO<sub>2</sub> modified with 1 % TBP at 40°C and 200 atm. Lanthanide series: La, Ce, Pr, Nd, Sm, Eu, Gd, Tb, Dy, Ho, Tm, Yb, and Lu.

	Ln(III) series*	U(VI)	Np(VI)	Pu(IV)	Am(III)
A-1	1.81	92.8 ± 0.765	15.9 ± 2.15	87.1	2.85
A-2	ND	24.2 ± 3.12	35.1 ± 8.35	46.8 ± 2.95	ND
*Average Ln series value; ND- Not Detected; NA- Not Applicable					
A-1. % Extraction from 1 M HNO <sub>3</sub> solution					
A-2. % Stripped by 0.1 M Oxalic Acid 1 M HNO <sub>3</sub> aqueous solution					

Generally Np is found in several waste streams in the PUREX process, so in this sc-CO<sub>2</sub> separation method it is favorable to suppress the extractability of Np(VI) upfront to eliminate efforts of removing Np from other waste streams. Table 5-4 shows the extraction efficiencies of the mixed Ln(III) and Ac(VI/IV) in 1 M HNO<sub>3</sub> solution with 0.1 M NO<sub>2</sub><sup>-</sup>. In row B-1 from Table 5-4, NO<sub>2</sub><sup>-</sup> was added to reduce Np(VI) to Np(V), but does not affect the extractability of U(VI) and Pu(IV). It was found, U(VI) and Pu(IV) had an extraction yield of greater than 82.6 % and Np(VI), Ln(III), and Am(III) were not detected. Only U(VI) and Pu(IV) proceeded to the oxalic acid stripping column (row B-2) where 24.3 and 43.2 % of U(VI) and Pu(IV) was stripped from the sc-CO<sub>2</sub>, respectively. The remaining amount of U(VI) and Pu(IV) were then carried to the water stripping column (B-3), where about 52.6 % of U(VI) and about 1.89 % of Pu(IV) are stripped from the sc-CO<sub>2</sub> phase.

Table 5-4 The percent extraction of uranium, neptunium, plutonium, americium, and the lanthanide series from 1 M nitric acid solution with 0.1 M sodium nitrite by sc-CO<sub>2</sub> modified with 1 % TBP at 40°C and 200 atm. Lanthanide series: La, Ce, Pr, Nd, Sm, Eu, Gd, Tb, Dy, Ho, Tm, Yb, and Lu.

	Ln(III) series*	U(VI)	Np(VI)	Pu(IV)	Am(III)
B-1	ND	89.1 ± 2.48	ND	82.6 ± 0.634	ND
B-2	NA	24.3 ± 1.55	NA	43.2 ± 8.01	NA
B-3	NA	52.6 ± 16.1	NA	1.89	NA
*Average Ln series value; ND- Not Detected; NA- Not Applicable B-1. % Extraction from 0.1 M Sodium Nitrite in 1 M HNO <sub>3</sub> aqueous solution B-2. % Stripped by 0.1 M Oxalic Acid in 1 M HNO <sub>3</sub> aqueous solution B-3. % Stripped by H <sub>2</sub> O					

Although we did not observe complete separation, we are optimistic if more stripping columns were added or longer stripping columns were included to give more contact time between the sc-CO<sub>2</sub> and stripping solutions, complete separation would be accomplished.

#### 5.4 Conclusion and future studies

These results indicate that U(VI) was readily partitioned from Np(VI), Pu(IV), and Am(III) by conducting sc-CO<sub>2</sub> extraction at 20 MPa and 40°C from acidic aqueous solutions using TBP, with the appropriate reducing and/or complexing agents. The extraction of U(VI) was unaffected by the presence of AHA, OA or sodium nitrite. At nitric acid concentrations of less than 3 M, Pu was not well extracted in the presence of AHA or OA. Neptunium extraction was suppressed at nitric acid concentrations below 1 M in the presence of AHA,

OA or sodium nitrite allowing for the selective extraction of U(VI). These results for sc-CO<sub>2</sub> extraction are as expected based upon analogy to actinide partitioning in liquid/liquid TBP extraction.

This study has also demonstrated the feasibility of using the more environmentally friendly solvent sc-CO<sub>2</sub> to extract and separate uranium from neptunium, plutonium, americium, and the lanthanide series by modifying sc-CO<sub>2</sub> with 1 % mole fraction of TBP and the use of the complexing agent oxalic acid and reducing agent sodium nitrite. In continued work, we will improve the scheme on the laboratory scale. Such a supercritical fluid-based dissolution and separation technology may be a more efficient and environmentally sustainable technology for treating nuclear wastes and for recycling uranium from used fuel than the conventional liquid-liquid extraction processes.

## 5.5 Acknowledgement

This work is supported by INL-LDRD Program under Idaho Operations Contract DE-AC07-05ID14517.

## 5.6 References

1. M. J. Carrott, B. E. Waller, N. G. Smart and C. M. Wai, *Chem. Comm.*, 1998, 373–374.
2. Y. Meguro, S. Iso, H. Takeishi and Z. Yoshida, *Radiochim. Acta*, 1996, **75**, 185–191.
3. S. Iso, S. Uno, Y. Meguro, T. Sasaki and Z. Yoshida, *Progress Nucl. Energy*, 2000, **37**, 423–428.
4. Y. Meguro, S. Ito, and Z. Yoshida, *Anal. Chem.*, 1998, **70**, 1262–1267.

5. C. M. Wai, Y.-J. Liao, W. Liao, G. Tian, R. S. Addleman, D. Quach, and S. P. Pasilis, *Dalton Trans.*, 2011, **40**, 5039–5045.
6. C. M. Wai and B. Waller, *Ind. Eng. Chem. Res.*, 2000, **39**, 4837–4841.
7. A. Rao, P. Kumar, and K. L. Ramakumar, *Radiochim. Acta*, 2008, **96**, 787–798.
8. L. T. K. Dung, T. Imai, O. Tomioka, M. Nakashima, and Y. Meguro, *Anal. Sci.*, 2006, **22**, 1425–1430.
9. T. Shimada, S. Oguma, K. Sawada, Y. Enokida, and I. Yamamoto, *Anal. Sci.*, 2006, **22**, 1387–1391.
10. S. S. Koegler, in *Nuclear energy and the environment*, ed. C. M. Wai and B. J. Mincher, ACS Symposium Series 1046, Washington DC, USA, 2010, Ch. 6.
11. L. Zhu, W. Duan, J. Xu and Y. Zhu, *J. Haz. Mat.* 2012, **241–242**, 456–462.
12. W. Duan, L. Zhu and Y. Zhu, *Progress Nucl. Energy*, 2011, **53**, 664–667.
13. B. Kumar, M. Sampeth, S. Kumar, D. Sivakumar, U.K. Mudali and R. Natarajan, *J. Radioanal. Nucl. Chem.*, 2011, **289**, 861–864.
14. Y. Lin, N. G. Smart, and C. M. Wai, *Environ. Sci. Technol.*, 1995, **29**, 2706–2711.
15. S. Iso, S. Uno, Y. Meguro, T. Sasaki, and Z. Yoshida, *Prog. Nucl. Energy*, 2000, **37**, 423–428.
16. T. I. Trofimov, M. D. Samsonov, Y. M. Kulyako and B. F. Myasoedov, *C. R. Chimie*, 2004, **7**, 1209–1213.
17. A. Rao, N. V. Rathod, V. V. Raut, and K. L. Ramakumar, *Sep. Sci. Technol.*, 2013, **48**, 644–651.
18. Y. Meguro, S. Iso, T. Sasaki, and Z. Yoshida, *Anal. Chem.*, 1998, **70**, 774–779.
19. K. L. Toews, N. G. Smart, and C. M. Wai, *Radiochim. Acta*, 1996, **75**, 179–184.
20. N. M. Rice, H. M. N. H. Irving, and M. A. Leonard, *Pur. Appl. Chem.* 1993, **65**, 2373–2396.
21. W. W. Schulz, L. L. Burger and J. D. Navratil, *Science and technology of tributyl phosphate Volume III: Applications of tributyl phosphate in nuclear fuel reprocessing*, CRC Press, Boca Raton, FL, USA, 1990.



22. Y. Enokida, O. Tomioka, S. Lee, A. Rustenholtz, and C. M. Wai, *Ind. Eng. Chem. Res.* 2003, **42**, 5037–5041.
23. R. Kumar, N. Sivaraman, K. Sujatha, T. G. Srinivasan, P. R. Vasudeva Rao, *Radiochim. Acta*, 2007, **95**, 577–584.
24. B. J. Mincher, R. V. Fox, R. G. G. Holmes, R. A. Robbins, C. Boardman, *Radiochim. Acta*, 2001, **89**, 613–617.
25. R. J. Taylor, I. May, A. L. Wallwork, I. S. Denniss, N. J. Hill, B. Ya. Galkin, B. Ya. Zilberman and Yu. S. Fedorov, *J. Alloy Comp.*, 1998, **271–273**, 534–537.
26. Y. Ban, T. Asakura and Y. Morita, *J. Radioanal. Nucl. Chem.*, 2009, **279**, 423–429.
27. Y. Ban, A. Toshihide and Y. Morita, *Radiochim. Acta*, 2004, **92**, 883–887.
28. V. S. Koltunov, S. M. Baranov and M. F. Tikhonov, *Radiochem.*, 2002, **44**, 248–252.
29. V.S. Koltunov, K. M. Frolov and Yu. V. Isaev, *Radiochem.*, 2002, **44**, 121–126.
30. V. S. Koltunov, V. I. Marchenko and O. A. Savilova, *Radiochem.*, 2001, **43**, 338–341.
31. V. S. Koltunov, R. J. Taylor, S. M. Baranov, E. A. Mezhov, V. G. Pastuschak and I. May, *Radiochim. Act.*, 2000, **88**, 65–70.
32. A. Zhang, J. Hu, X. Zhang and F. Wang, *J. Radioanal. Nucl. Chem.*, 2002, **253**, 107–113.
33. I. May, R. J. Taylor, I. S. Denniss, G. Brown, A. L. Wallwork, N. J. Hill, J. M. Rawson and R. Less, *J. Alloy. Comp.*, 1998, **275–277**, 769–772.
34. A. Barocas, F. Baroncelli, G. B. Biondi and G. Grossi, *J. Inorg. Nucl. Chem.* 1966, **28**, 2961–2967.
35. F. Baroncelli and G. Grossi, *J. Inorg. Nucl. Chem.*, 1965. **27**, 1085–1092.
36. B. Chatterjee, *Coord. Chem. Rev.*, 1978. **26**, 281–303.
37. N. K. Shastri and E. S. Amis, *Inorg. Chem.*, 1969, **8**, 2487–2489.
38. S. V. Bagawde, V. V. Ramakrishna and S. K. Patil, *J. Inorg. Nucl. Chem.*, 1976, **38**, 1669–1672.
39. T. H. Siddall and E. K. Dukes, *J. Am. Chem. Soc.*, 1959, **81**, 790–794.
40. A. Paulenova, *Plutonium Chemistry in the UREX + Separation Processes*, US DOE Report DE-FC07-05ID14652, Oregon State University, 2011.

41. M. Kubota, *J. Radioanal. Chem.*, 1982, **75**, 39–49.
42. W. Hummel, G. Anderegg, L. Rao, I. Puigdomenech and O. Tochiyama in *Chemical Thermodynamics*, Vol. 9., ed.F.J. Mompean, Elsevier, Boston, MA, USA, 2005.
43. J. M. Cleveland, *The Chemistry of Plutonium*. American Nuclear Society, LaGrange, IL, USA, 1979.
44. R. E. Connick, in *The Actinide Elements*, ed. G.T. Seaborg and J. J. Katz, McGraw Hill, New York, NY, USA, 1954.
45. Z. J. Yoshida, G. Stephen, T . Kimura, and J. R.Krsul, in *The Chemistry of the Actinide and Transactinide Elements*, Springer:, Netherlands. 2010.
46. B. J. Mincher, M. Precek, G. Elias, S. P. Mezyk and A. Paulenova, *Radiochim. Acta*, 2013, **101**, 259–266.

## Chapter 6

### Conclusions

Non-traditional solvents are desirable in the development of new recycling methods for used nuclear fuel. Room temperature ionic liquids (RTILs) are a promising alternative solvent due to their low volatility and ability to mitigate the volume of toxic waste produced. In this work, the coordination environment of uranyl dissolved in the RTIL, 1-butyl-3-methylimidazolium bis(trifluoromethylsulfonyl)imide ( $[\text{C}_4\text{MIM}][\text{Tf}_2\text{N}]$ ) containing either tetrabutylammonium nitrate (TBAN), nitric acid, or TBAN and tri-n-butyl phosphate (TBP) was characterized using attenuated total reflection-Fourier transform infrared spectroscopy (ATR-FTIR).  $\nu_{\text{as}}(\text{UO}_2^{2+})$  for uranyl bis(trifluoromethylsulfonyl)imide was found to be at  $968\text{ cm}^{-1}$ , while the species  $\text{UO}_2(\text{NO}_3)_2$  and  $\text{UO}_2(\text{NO}_3)_3^-$  were detected in solutions containing TBAN at  $\nu_{\text{as}}(\text{UO}_2^{2+})$  950 and  $945\text{ cm}^{-1}$ , respectively. When nitric acid was used as the nitrate source only the dinitrato complex was detected, possibly due to high water content. The  $\text{UO}_2(\text{NO}_3)^+$  species was not detected under the conditions used in this study. The complex  $\text{UO}_2(\text{NO}_3)_2(\text{TBP})_2$  was formed when the total TBP concentration added to uranyl nitrate was 0.2 M or higher. The  $\nu_{\text{as}}(\text{UO}_2^{2+})$  mode appeared at  $942\text{ cm}^{-1}$ .

Tristructural isotopic (TRISO) fuel particles are used in very high temperature reactors (VHTR), which are being proposed for future deployment. Thus, development of recycling techniques of TRISO fuels is desired. In this study, TRISO fuel particles were exposed to 691 and 1041 kGy of gamma radiation and sc-CO<sub>2</sub> extraction was performed on crushed samples ( $x < 60$  mesh) to give an increase from  $67 \pm 2\%$  to  $98 \pm 1\%$  and  $99 \pm 1\%$ ,

respectively. This phenomenon may be due to the radiation defects produced in the uranium carbide crystal structure, which allows for higher diffusion of the  $\text{TBP}(\text{HNO}_3)_{1.8}(\text{H}_2\text{O})_{0.6}$  in  $\text{sc-CO}_2$ . Also, ultrasound studies were used to assist the cracking of TRISO fuel particles. The TRISO fuel particle surface was examined by scanning electron microscopy (SEM). The surface was found to be penetrated by cavitation in liquid  $\text{CO}_2$ ; however, crevices were not observed. The pretreatment of the TRISO fuel with HF assisted cavitation in liquid  $\text{CO}_2$ , but was unsuccessful in penetrating the silicon carbide layer.

The feasibility of separating U(VI) from nitric acid solutions of mixed actinides using TBP-modified  $\text{sc-CO}_2$  was investigated. The actinides U(VI), Np(VI), Pu(IV), and Am(III) were extracted into  $\text{sc-CO}_2$  modified with TBP from a range of nitric acid concentrations, in the absence of, or in the presence of, a number of traditional reducing and/or complexing agents to demonstrate the separation of these metals from U(VI) under  $\text{sc-CO}_2$  conditions. The separation of U(VI) from Pu(IV) using  $\text{sc-CO}_2$  was successful at nitric acid concentrations of less than 3 M in the presence of acetohydroxamic acid (AHA) or oxalic acid (OA) to mitigate Pu(IV) extraction, and the separation of U(VI) from Np(VI) was successful at nitric acid concentrations of less than 1 M in the presence of AHA, OA, or sodium nitrite to mitigate Np(VI) extraction. Americium was not well extracted under any condition studied. In addition the  $\text{sc-CO}_2$  extraction and separation of U(VI) from Np(VI), Pu(IV), Am(III), and the lanthanide series by using 1 % mole fraction TBP, sodium nitrite, and oxalic acid from 1 M  $\text{HNO}_3$  was presented. The results demonstrated the possibility of using  $\text{sc-CO}_2$  as a solvent to develop an alternative separation technique to the PUREX process for recycling used nuclear fuel.

The results found in this dissertation demonstrate how effective and efficient the non-traditional solvents sc-CO<sub>2</sub> and RTIL are over traditional solvents for nuclear waste management. Although the demonstration of cracking TRISO fuel particles was not successful, the data still provides a good beginning to the following proposed development of a green recycling technique for nuclear waste management. The envisioned sc-CO<sub>2</sub> extraction and separation of used nuclear fuel method is summarized in Figure 6-1. Used fuel removed from storage can be placed in an RTIL inside a pressure vessel. The complex TBP(HNO<sub>3</sub>)<sub>1.8</sub>(H<sub>2</sub>O)<sub>0.6</sub> modified with sc-CO<sub>2</sub> can be used for the dissolution and extraction of actinide, lanthanide, and fission products. The entire recycling process of UNF can be contained within a closed system. Actinides, lanthanides, and fission products can be extracted efficiently and travel through different stripping columns. Depending on the desired product, the stripping column can contain a specific solution to isolate the desired product. Each column can contain an aqueous solution with varying concentrations of nitric acid and/or a reducing and/or complexing agent. Overall U(VI) can be isolated from all other species or kept together with Pu(IV) like in the PUREX process and the remaining actinides and lanthanides can be isolated in their respective column as well. The sc-CO<sub>2</sub> can be recycled to the beginning of the process for reuse.

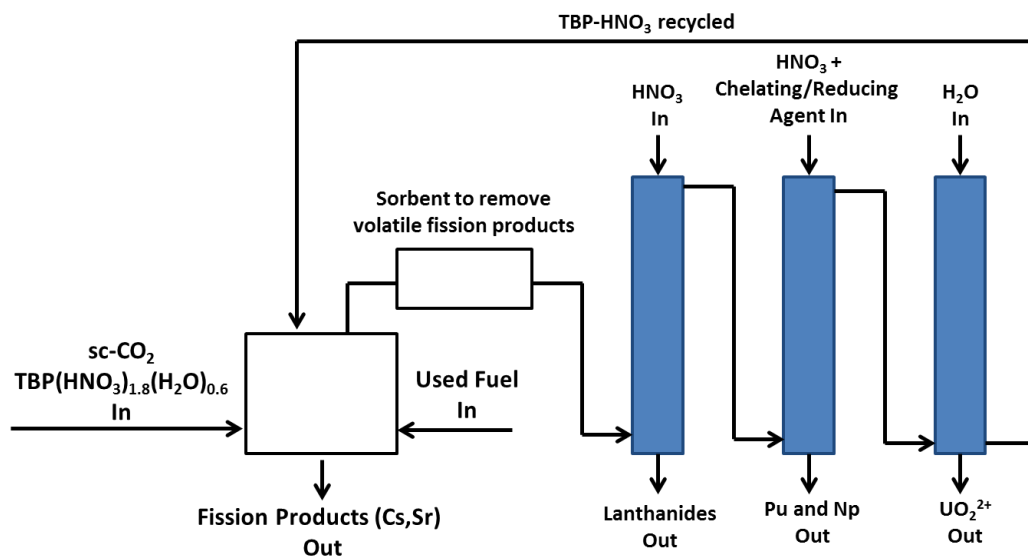


Figure 6-1 Schematic diagram illustrating the concept of recycling uranium from used fuel by using sc-CO<sub>2</sub> and counter-current stripping columns.

**Appendix A**  
**Copyright Permission Letter**

Dear Donna Quach,

<b>About the Wiley-VCH book</b>	
ISBN	3-527-30317-0
Author / Editor	Karl Heinrich Lieser
Full Title of Book	Nuclear and Radiochemistry Fundamentals and Applications
Chapters Requested (please include page numbers)	Chapter 8 and 11
Year of Publication	2001
Figure and Page Reference	figure 8.13 (pg. 152) and 11.5(208); table 11.9 (pg. 225)
Are you the original author of the requested material?	yes
<b>Where would you like to include our material?</b>	
<b>About Your Publication</b>	
Author / Editor	Donna Baek
Title of Publication	UTILIZING SUPERCRITICAL CO <sub>2</sub> AND IONIC LIQUIDS FOR THE EXTRACTION OF ACTINIDES AND LANTHANIDES: APPLICATIONS OF NON-CONVENTIONAL SOLVENTS FOR NUCLEAR WASTE MANAGEMENT
Rights Required (eg. Print/ Electronic/ Translation, etc.)	print/ electronic
Publisher	ProQuest
Publication Date	unknown
Medium (e.g. Book/Journal, Handout, CD Rom, Internet, etc.)	dissertation (book)
Print Run (hard back / paper back)	hard back
If Making Copies Please Include the Number of Copies You Wish to Make	2
Retail Price	unknown
Web address material will be posted on	<a href="http://ida.lib.uidaho.edu:2432/pqdtft/advanced?accountid=14551">http://ida.lib.uidaho.edu:2432/pqdtft/advanced?accountid=14551</a>
Is the website password-protected?	no
<b>Tell us how to get in touch with you (Please note that this will be where your invoice and/or permission will be addressed to. We are unable to send documents to more than one address):</b>	
<b>Please provide your full address details:</b>	
Name	Donna Baek
Salutation	
Department	
Job title	
Organisation	
Street	1065 Caswell Ave W
Town	Twin Falls
State / Province	ID
Zip / Postal Code	83301
Country	USA
Telephone	208-316-2758
Fax	
Email	<a href="mailto:dquach@vandals.uidaho.edu">dquach@vandals.uidaho.edu</a>

**We hereby grant permission for the requested use expected that due credit is given to the original source.**



**ELSEVIER LICENSE  
TERMS AND CONDITIONS**

Jun 05, 2014

This is a License Agreement between Donna Baek ("You") and Elsevier ("Elsevier") provided by Copyright Clearance Center ("CCC"). The license consists of your order details, the terms and conditions provided by Elsevier, and the payment terms and conditions.

**All payments must be made in full to CCC. For payment instructions, please see information listed at the bottom of this form.**

Supplier	Elsevier Limited The Boulevard, Langford Lane Kidlington, Oxford, OX5 1GB, UK
Registered Company Number	1982084
Customer name	Donna Baek
Customer address	1065 Caswell Ave W TWIN FALLS, ID 83301
License number	3402590080468
License date	Jun 05, 2014
Licensed content publisher	Elsevier
Licensed content publication	Journal of Inorganic and Nuclear Chemistry
Licensed content title	Distribution ratios and empirical equations for the extraction of elements in PUREX high level waste solution: I:TBP
Licensed content author	I. Svantesson, I. Hagström, G. Persson, J.O. Liljenzin
Licensed content date	1979
Licensed content volume number	41
Licensed content issue number	3
Number of pages	7
Start Page	383
End Page	389
Type of Use	reuse in a thesis/dissertation
Intended publisher of new work	other
Portion	figures/tables/illustrations
Number of figures/tables /illustrations	1
Format	both print and electronic
Are you the author of this Elsevier article?	No
Will you be translating?	No
Title of your thesis/dissertation	UTILIZING SUPERCRITICAL CO <sub>2</sub> AND IONIC LIQUIDS FOR THE EXTRACTION OF ACTINIDES AND LANTHANIDES: APPLICATIONS OF NON-CONVENTIONAL SOLVENTS FOR NUCLEAR WASTE MANAGEMENT
Expected completion date	Aug 2014
Estimated size (number of pages)	160
Elsevier VAT number	GB 494 6272 12
Permissions price	0.00 USD
VAT/Local Sales Tax	0.00 USD / 0.00 GBP
Total	0.00 USD

**ELSEVIER LICENSE  
TERMS AND CONDITIONS**

Jun 05, 2014

This is a License Agreement between Donna Baek ("You") and Elsevier ("Elsevier") provided by Copyright Clearance Center ("CCC"). The license consists of your order details, the terms and conditions provided by Elsevier, and the payment terms and conditions.

**All payments must be made in full to CCC. For payment instructions, please see information listed at the bottom of this form.**

Supplier	Elsevier Limited The Boulevard, Langford Lane Kidlington, Oxford, OX5 1GB, UK
Registered Company Number	1982084
Customer name	Donna Baek
Customer address	1065 Caswell Ave W TWIN FALLS, ID 83301
License number	3402581400754
License date	Jun 05, 2014
Licensed content publisher	Elsevier
Licensed content publication	Journal of Inorganic and Nuclear Chemistry
Licensed content title	Tri- <i>n</i> -butyl phosphate as an extracting solvent for inorganic nitrates—V: Further results for the tetra- and hexavalent actinide nitrates
Licensed content author	K. Alcock, G.F. Best, E. Hesford, H.A.C. McKay
Licensed content date	July 1958
Licensed content volume number	6
Licensed content issue number	4
Number of pages	6
Start Page	328
End Page	333
Type of Use	reuse in a thesis/dissertation
Portion	figures/tables/illustrations
Number of figures/tables /illustrations	1
Format	both print and electronic
Are you the author of this Elsevier article?	No
Will you be translating?	No
Title of your thesis/dissertation	UTILIZING SUPERCRITICAL CO <sub>2</sub> AND IONIC LIQUIDS FOR THE EXTRACTION OF ACTINIDES AND LANTHANIDES: APPLICATIONS OF NON-CONVENTIONAL SOLVENTS FOR NUCLEAR WASTE MANAGEMENT
Expected completion date	Aug 2014
Estimated size (number of pages)	160
Elsevier VAT number	GB 494 6272 12
Permissions price	0.00 USD
VAT/Local Sales Tax	0.00 USD / 0.00 GBP
Total	0.00 USD



[Creative Commons](#)

## Creative Commons License Deed

---

**Attribution-NonCommercial-NoDerivs 3.0 Unported (CC BY-NC-ND 3.0)**

This is a human-readable summary of (and not a substitute for) the [license](#).  
[Disclaimer](#)

**You are free to:**



**Share** — copy and redistribute the material in any medium or format

The licensor cannot revoke these freedoms as long as you follow the license terms.

**Under the following terms:**



**Attribution** — You must give [appropriate credit](#), provide a link to the license, and [indicate if changes were made](#). You may do so in any reasonable manner, but not in any way that suggests the licensor endorses you or your use.



**NonCommercial** — You may not use the material for [commercial purposes](#).



**NoDerivatives** — If you [remix, transform, or build upon](#) the material, you may not distribute the modified material.

**No additional restrictions** — You may not apply legal terms or [technological measures](#) that legally restrict others from doing anything the license permits.

**Notices:**

You do not have to comply with the license for elements of the material in the public domain or where your use is permitted by an applicable [exception or limitation](#).

No warranties are given. The license may not give you all of the permissions necessary for your intended use. For example, other rights such as [publicity, privacy, or moral rights](#) may limit how you use the material.

The applicable mediation rules will be designated in the copyright notice published with the work, or if none then in the request for mediation. Unless otherwise designated in a copyright notice attached to the work, the UNCITRAL Arbitration Rules apply to any arbitration.

[More info.](#)

You may also use a license listed as compatible at <https://creativecommons.org/compatiblelicenses>

[More info.](#)



RightsLink®

[Home](#)[Account Info](#)[Help](#)ACS Publications  
MOST TRUSTED. MOST CITED. MOST READ.

**Title:** Characterization of Uranyl(VI) Nitrate Complexes in a Room Temperature Ionic Liquid Using Attenuated Total Reflection-Fourier Transform Infrared Spectrometry

Logged in as:  
Donna Baek  
Account #:  
3000798409

[LOGOUT](#)

**Author:** Donna L. Quach, Chien M. Wai, and Sofie P. Pasilis

**Publication:** Inorganic Chemistry

**Publisher:** American Chemical Society

**Date:** Sep 1, 2010

Copyright © 2010, American Chemical Society

### PERMISSION/LICENSE IS GRANTED FOR YOUR ORDER AT NO CHARGE

This type of permission/license, instead of the standard Terms & Conditions, is sent to you because no fee is being charged for your order. Please note the following:

- Permission is granted for your request in both print and electronic formats, and translations.
- If figures and/or tables were requested, they may be adapted or used in part.
- Please print this page for your records and send a copy of it to your publisher/graduate school.
- Appropriate credit for the requested material should be given as follows: "Reprinted (adapted) with permission from (COMPLETE REFERENCE CITATION). Copyright (YEAR) American Chemical Society." Insert appropriate information in place of the capitalized words.
- One-time permission is granted only for the use specified in your request. No additional uses are granted (such as derivative works or other editions). For any other uses, please submit a new request.

[BACK](#)[CLOSE WINDOW](#)

**ELSEVIER LICENSE  
TERMS AND CONDITIONS**

Jun 27, 2014

This is a License Agreement between Donna Baek ("You") and Elsevier ("Elsevier") provided by Copyright Clearance Center ("CCC"). The license consists of your order details, the terms and conditions provided by Elsevier, and the payment terms and conditions.

**All payments must be made in full to CCC. For payment instructions, please see information listed at the bottom of this form.**

Supplier	Elsevier Limited The Boulevard, Langford Lane Kidlington, Oxford, OX5 1GB, UK
Registered Company Number	1982084
Customer name	Donna Baek
Customer address	1065 Caswell Ave W TWIN FALLS, ID 83301
License number	3417240390934
License date	Jun 27, 2014
Licensed content publisher	Elsevier
Licensed content publication	Journal of Inorganic and Nuclear Chemistry
Licensed content title	The trinitratouranyl ion in organic solvents
Licensed content author	Louis Kaplan, R.A. Hildebrandt, Milton Ader
Licensed content date	March 1956
Licensed content volume number	2
Licensed content issue number	3
Number of pages	11
Start Page	153
End Page	163
Type of Use	reuse in a thesis/dissertation
Intended publisher of new work	other
Portion	figures/tables/illustrations
Number of figures/tables /illustrations	1
Format	both print and electronic
Are you the author of this Elsevier article?	No
Will you be translating?	No
Title of your thesis/dissertation	UTILIZING SUPERCRITICAL CO <sub>2</sub> AND IONIC LIQUIDS FOR THE EXTRACTION OF ACTINIDES AND LANTHANIDES: APPLICATIONS OF NON-CONVENTIONAL SOLVENTS FOR NUCLEAR WASTE MANAGEMENT
Expected completion date	Aug 2014
Estimated size (number of pages)	160
Elsevier VAT number	GB 494 6272 12
Permissions price	0.00 USD
VAT/Local Sales Tax	0.00 USD / 0.00 GBP
Total	0.00 USD

Dear Donna Quach

<b>About the Wiley-VCH book</b>	
ISBN	978-3-527-41201-3
Author / Editor	K. Linga Murty and Indrajit Charit
Full Title of Book	An Introduction to Nuclear Materials: Fundamentals and Applications
Chapters Requested (please include page numbers)	Chapter 2 (43-110)
Year of Publication	2013
Figure and Page Reference	Figure 2.25 (pg. 70)
Are you the original author of the requested material?	No
<b>Where would you like to include our material?</b>	
<b>About Your Publication</b>	
Author / Editor	Donna Baek
Title of Publication	UTILIZING SUPERCRITICAL CO <sub>2</sub> AND IONIC LIQUIDS FOR THE EXTRACTION OF ACTINIDES AND LANTHANIDES: APPLICATIONS OF NON-CONVENTIONAL SOLVENTS FOR NUCLEAR WASTE MANAGEMENT
Rights Required (eg. Print/ Electronic/ Translation, etc.)	Print/ Electronic
Publisher	ProQuest
Publication Date	unknown
Medium (e.g. Book/Journal, Handout, CD Rom, Internet, etc.)	Dissertation (Book)
Print Run (hard back / paper back)	hard back
If Making Copies Please Include the Number of Copies You Wish to Make	2
Retail Price	unknown
Web address material will be posted on	<a href="http://ida.lib.uidaho.edu:2432/pqdtft/advanced?accountid=14551">http://ida.lib.uidaho.edu:2432/pqdtft/advanced?accountid=14551</a>
Is the website password-protected?	no
<b>Tell us how to get in touch with you (Please note that this will be where your invoice and/or permission will be addressed to. We are unable to send documents to more than one address):</b>	
<b>Please provide your full address details:</b>	
Name	Donna Baek
Salutation	
Department	
Job title	
Organisation	
Street	1065 Caswell Ave W
Town	Twin Falls
State / Province	ID
Zip / Postal Code	83301
Country	USA
Telephone	208-316-2758
Fax	
Email	<a href="mailto:dquach@vandals.uidaho.edu">dquach@vandals.uidaho.edu</a>

**We hereby grant permission for the requested use expected that due credit is given to the original source.**

**ELSEVIER LICENSE  
TERMS AND CONDITIONS**

Jun 05, 2014

This is a License Agreement between Donna Baek ("You") and Elsevier ("Elsevier") provided by Copyright Clearance Center ("CCC"). The license consists of your order details, the terms and conditions provided by Elsevier, and the payment terms and conditions.

**All payments must be made in full to CCC. For payment instructions, please see information listed at the bottom of this form.**

Supplier	Elsevier Limited The Boulevard, Langford Lane Kidlington, Oxford, OX5 1GB, UK
Registered Company Number	1982084
Customer name	Donna Baek
Customer address	1065 Caswell Ave W TWIN FALLS, ID 83301
License number	3402590568395
License date	Jun 05, 2014
Licensed content publisher	Elsevier
Licensed content publication	Journal of Hazardous Materials
Licensed content title	Supercritical fluid extraction and separation of uranium from other actinides
Licensed content author	Donna L. Quach, Bruce J. Mincher, Chien M. Wai
Licensed content date	15 June 2014
Licensed content volume number	274
Licensed content issue number	None
Number of pages	7
Start Page	360
End Page	366
Type of Use	reuse in a thesis/dissertation
Intended publisher of new work	other
Portion	full article
Format	both print and electronic
Are you the author of this Elsevier article?	Yes
Will you be translating?	No
Title of your thesis/dissertation	UTILIZING SUPERCRITICAL CO <sub>2</sub> AND IONIC LIQUIDS FOR THE EXTRACTION OF ACTINIDES AND LANTHANIDES: APPLICATIONS OF NON-CONVENTIONAL SOLVENTS FOR NUCLEAR WASTE MANAGEMENT
Expected completion date	Aug 2014
Estimated size (number of pages)	160
Elsevier VAT number	GB 494 6272 12
Permissions price	0.00 USD
VAT/Local Sales Tax	0.00 USD / 0.00 GBP
Total	0.00 USD